5-1998

Synthesis of Novel Amino Acids and 310- And Alpha-Helical Alpha, Alpha-Disubstituted Amino Acid Rich Antimicrobial Peptides

Thomas Scott Yokum
Louisiana State University and Agricultural and Mechanical College

SYNTHESIS OF NOVEL AMINO ACIDS AND 3_{10}- AND ALPHA-HELICAL ALPHA, ALPHA-DISUBSTITUTED AMINO ACID RICH ANTIMICROBIAL PEPTIDES

A Dissertation

Submitted to the Graduate Faculty of the
Louisiana State University and
Agricultural and Mechanical College
in partial fulfillment of the
requirements for the degree of
Doctor of Philosophy

in

The Department of Chemistry

by
Thomas Scott Yokum
B.S., Marietta College, 1992
May, 1998

MANUSCRIPT THESES

Unpublished theses submitted for the Master's and Doctor's Degrees and deposited in the Louisiana State University Libraries are available for inspection. Use of any thesis is limited by the rights of the author. Bibliographical references may be noted, but passages may not be copied unless the author has given permission. Credit must be given in subsequent written or published work.

A library which borrows this thesis for use by its clientele is expected to make sure that the borrower is aware of the above restrictions.

LOUISIANA STATE UNIVERSITY LIBRARIES

Acknowledgments

I would like to thank my major professor Dr. Mark McLaughlin for his invaluable guidance and support during my tenure at LSU. He has always given me the freedom to develop my own ideas. I would also like to thank Dr. Robert Hammer for his significant contributions to my graduate studies.

A major amount of thanks must be given to Martha Juban for help with peptide synthesis and purification, to Dr. Phil Elzer for biological studies, to Dr. Tracy McCarley for mass specs, and to Dr. Frank Fronczek for crystal structure determinations. In addition, I would like to thank Dr. Mary Barkley for her support.

I also greatly appreciate the contributions of many former and current students in laboratory work and manuscript publications including: Ted Gauthier, Matt Bursavich, Pari Tungaturthi, Sarah Piha-Paul, Chris Wysong, and Guillermo Morales.

Finally, I would like to thank all of my committee members: Dr. Mark McLaughlin, Dr. Robert Hammer, Dr. Robert Strongin, Dr. Nikolaus Fischer, and Dr. Roger Laine.

Table of Contents

Acknowledgments ii

List of Tables vi

List of Figures vii

List of Abbreviations x

Abstract xv

Chapter 1 Introduction 1
- 1.1 Introduction 1
- 1.2 Peptide Secondary Structure 1
- 1.3 Amphipathic α-Helix 5
- 1.4 Antimicrobial Peptides 7
  - 1.4.1 Melittin 8
  - 1.4.2 Cecropin A 8
  - 1.4.3 Magainin 2 11
  - 1.4.4 Mechanism of Action of Antimicrobial Peptides 13
  - 1.4.5 Structure-Activity Relationships of Antimicrobial Peptides 14
- 1.5 Synthesis of Short, Helical Peptides 16
  - 1.5.1 α-Aminoisobutyric Acid 17
  - 1.5.2 Other α,α-Disubstituted Amino Acids 18
  - 1.5.3 Incorporation of α,α-Disubstituted Amino Acids Into Peptides 23
- 1.6 Amino Acid Synthesis 28
- 1.7 Secondary Structures Promoted by α,α-Disubstituted Amino Acids 41
- 1.8 Characterization of Peptides Rich in α,α-Disubstituted Amino Acids 46
- 1.9 References 50

Chapter 2 Antimicrobial α,α-Dialkylated Amino Acid Rich Peptides With *In Vivo* Activity Against an Intracellular Pathogen 57
- 2.1 Introduction 57
- 2.2 Results 60
- 2.3 Discussion 77

2.4 Conclusions 85
2.5 Experimental 86
2.5.1 Peptide Synthesis 86
2.5.2 Amino Acid Analysis 88
2.5.3 N^1-*tert*-butyloxycarbonyl-4-(amino-(9-fluorenylmethyloxycarbonyl))-piperidine-4-carboxylic acid ... 88
2.5.4 N^1-*tert*-butyloxycarbonyl-4-(amino-(9-fluorenylmethyloxycarbonyl))-piperidine-4-carboxylic acid fluoride 90
2.5.5 General Acid Fluoride Synthesis 91
2.5.6 Circular Dichroism 92
2.5.7 MIC Assays 93
2.5.8 Enzymatic Stability Assays 93
2.5.9 *In Vivo B. abortus* Studies 94
2.5.10 Macrophage Assays 95
2.5.11 Direct Bacterial Effects on *B. abortus* 96
2.5.12 Statisitics 97
2.5.13 Biological Containment and Animal Use 97
2.6 References 97

Chapter 3 Synthesis of a Series of Polar, Orthogonally Protected, α,α-Disubstituted Amino Acids 103
3.1 Introduction 103
3.2 Results and Discussion 105
3.3 Conclusions 110
3.4 Experimental 111
3.4.1 N^4-*tert*-butyloxycarbonyl-N^4-ethyl-N^1-(9-fluorenylmethyloxycarbonyl)-1,4-bis-aminocyclohexane-1-carboxylic acid 111
3.4.2 N^4-butyl-N^4-*tert*-butyloxycarbonyl-N^1-9-fluorenylmethyloxycarbonyl-1,4-bis-aminocyclohexane-1-carboxylic acid 116
3.4.3 N^4-benzyl-N^4-*tert*-butyloxycarbonyl-N^1-(9-fluorenylmethyloxycarbonyl)-1,4-bis-aminocyclohexane-1-carboxylic acid 121
3.4.4 N^4-*tert*-butyloxycarbonyl-N^1-(9-fluorenylmethyloxycarbonyl)-N^4-(2-naphthylmethyl)-1,4-bis-aminocyclohexane-1-carboxylic acid 126
3.5 References 131

Chapter 4 Solvent Effects on the 3_{10}-/α-Helix Equilibrium in Short Amphipathic Peptides Rich in α,α- Disubstituted Amino Acids 133
4.1 Introduction 133
4.2 Results 138
4.3 Discussion 148
4.4 Conclusions 155
4.5 Experimental 156
4.5.1 Peptide Synthesis 156
4.5.2 Acid Fluoride Synthesis 157
4.5.3 Circular Dichroism 158
4.6 References 159

Chapter 5 Benz[*f*]tryptophan, a Bathochromic Analog of Tryptophan, Synthesis of its N^{α}-Boc Derivative 164
5.1 Introduction 164
5.2 Results and Discussion 167
5.3 Conclusions 173
5.4 Experimental 174
5.4.1 *N,N*-(bis-2-propenyl)-2-amino-3-bromonaphthalene 174
5.4.2 *rac. N*-(2-propenyl)-3-(2-ethanal)-benz[*f*]indoline 175
5.4.3 *rac. N*-(2-propenyl)-3-(methano-2,4-diaza-3,5-cyclopentanedione)-benz[*f*]indoline 176
5.4.4 *rac. N*-(2-propenyl)-3-(methano-2,4-diaza-2,4-bis-*tert*-butyloxycarbonyl-3,5-cyclopentanedione)-benz[*f*]indoline 177
5.4.5 *rac.* 3-(methano-2,4-diaza-2,4-bis-*tert*-butyloxycarbonyl-3,5-cyclopentanedione)-benz[*f*]indoline 179
5.4.6 *rac.* 3-(methano-2,4-diaza-2,4-bis-*tert*-butyloxycarbonyl-3,5-cyclopentanedione)-benz[*f*]indole 180
5.4.7 *rac.* N^{α}-*tert*-butyloxycarbonyl-benz[*f*]tryptophan 181
5.5 References 182

Chapter 6 Summary and Future Studies 185
6.1 Summary and Future Studies 185
6.2 References 191

Appendix: Letters of Permission 193

Vita 202

List of Tables

Table 1.1 Factors determining helix preference in Aib rich peptides 43

Table 2.1 Sequences of peptides **2.1-2.12** 63

Table 2.2 Sequences of peptides **2.13-2.24** 64

Table 2.3 Peptide antibacterial activity and percent helicity 65

Table 2.4 Indirect *in vivo* peptide activity against *Brucella abortus* in BALB/c mice of peptides **2.1-2.12** 72

Table 2.5 Indirect *in vivo* peptide activity against *Brucella abortus* in BALB/c mice of peptides **2.13-2.24** 73

Table 2.6 Normal macrophage survival versus peptide concentration 75

Table 2.7 *In vitro* peptide toxicity against normal and infected murine macrophages 76

Table 4.1 CD data and derived structural parameters for Pi-10 146

Table 4.2 CD data and derived structural parameters for Ipi-10 146

Table 4.3 CD data and derived structural parameters for Sb-10 147

List of Figures

Figure 1.1 Hydrogen bonding patterns of parallel and antiparallel β-sheets.....2

Figure 1.2 Hydrogen bonding patterns of the α-helix and the 3_{10}-helix 4

Figure 1.3 Helical wheel representation of an amphipathic α-helix 6

Figure 1.4 Sequence and helical wheel representation of Melittin 9

Figure 1.5 Sequence of Cecropin A and helical wheel representation of Cecropin A helix region 5-21 10

Figure 1.6 Helical wheel representation of Cecropin A helix 2 region 25-37....11

Figure 1.7 Sequence and helical wheel representation of Magainin 2 12

Figure 1.8 Structure of α-Aminoisobutyric acid 17

Figure 1.9 Torsional angles of the peptide backbone 18

Figure 1.10 Representative acyclic, symmetrical, non-polar ααAAs 19

Figure 1.11 Representative cyclic, non-polar ααAAs 20

Figure 1.12 Methylated derivatives of proteinogenic amino acids 21

Figure 1.13 Representative polar ααAAs.....22

Figure 1.14 Traditional amino acid coupling reagents/additive 24

Figure 1.15 Alternate reagents for ααAA couplings.....25

Figure 1.16 Current reagents used for ααAA couplings 27

Figure 1.17 Amino acid synthesis via amino introduction on an α-halo carboxylic acid 29

Figure 1.18 Amino acid synthesis via rearrangements.....30

Figure 1.19 Amino acids synthesis via reductive amination 31

Figure 1.20 Strecker and Bucherer-Bergs Syntheses 32

Figure 1.21 Amino acid synthesis via asymmetric hydrogenation 33

Figure 1.22 Amino acid synthesis with an achiral glycine template 34

Figure 1.23 Amino acid synthesis using Schöllkopf's template 36

Figure 1.24 Amino acid synthesis using Seebach's template 37

Figure 1.25 Amino acid synthesis using William's template 39

Figure 1.26 Amino acid synthesis using Meyer's template 40

Figure 1.27 Equation for the determination of R values 48

Figure 1.28 Donor/Acceptor system positioning in 3_{10}- and α-helices 49

Figure 2.1 Structures of Aib, Ch, and Api amino acids 61

Figure 2.2 CD spectra of Ai-11 and Ai-14 in SDS 66

Figure 2.3 CD spectra of Ch-10 and Ch-13 in SDS 67

Figure 2.4 CD spectra of Pi-10 and Pi-10-ac in SDS 68

Figure 2.5 CD spectra of Ipi-10 and Ipi-10-ac in SDS 69

Figure 3.1 General structure of α,α-disubstituted amino acids 104

Figure 3.2 General structure of the target amino acids 105

Figure 3.3 Synthesis of ketones **3.6 a-d** 107

Figure 3.4 Synthesis of amino acids **3.9 a-d** 108

Figure 3.5 Synthesis of protected amino acids **3.10 a-d** 110

Figure 4.1 Structure of Aib 134

Figure 4.2 The α- and 3_{10}-helical wheel diagrams and sequence of Pi-10 135

Figure 4.3 The α- and 3_{10}-helical wheel diagrams and sequence of Ipi-10 136

Figure 4.4 The α- and 3_{10}-helical wheel diagrams and sequence of Sb-10 137

Figure 4.5 Structure of Api 140

Figure 4.6 CD spectra of Pi-10,Ipi-10, and Sb-10 in SDS 141

Figure 4.7 CD spectra of Pi-10 in 1:1 CH_3CN-H_2O, 9:1 CH_3CN-H_2O, and 9:1 CH_3CN-TFE 142

Figure 4.8 CD spectra of Ipi-10 in 1:1 CH_3CN-H_2O, 9:1 CH_3CN-H_2O, and 9:1 CH_3CN-TFE 143

Figure 4.9 CD spectra of Sb-10 in 1:1 CH_3CN-H_2O, 9:1 CH_3CN-H_2O, and 9:1 CH_3CN-TFE 144

Figure 4.10 CD spectra of Sb-10 with 0.1 M TMAT in 9:1 CH_3CN-TFE,0.01 M TMAT in 9:1 CH_3CN-TFE,0.01 M TMAT in 9:1 CH_3CN-TFE, and 9:1 CH_3CN-TFE 145

Figure 5.1 Structure of N^{α}-*tert*-butyloxycarbonyl-benz[*f*]tryptophan 166

Figure 5.2 Structures of benz[*g*]tryptophan and benz[*e*]tryptophan 167

Figure 5.3 Synthesis of indoline **5.7** 168

Figure 5.4 Synthesis of indole **5.10** 170

Figure 5.5 Synthesis of N^{α}-*tert*-butyloxycarbonyl-benz[*f*]tryptophan 172

List of Abbreviations

ααAA	α,α-disubstituted amino acid
Ac_3c	1-Aminocyclopropane carboxylic acid
Ac_4c	1-Aminocyclobutane carboxylic acid
Ac_5c	1-Aminocyclopentane carboxylic acid
Ac_6c	1-Aminocyclohexane carboxylic acid
Ac_7c	1-Aminocycloheptane carboxylic acid
Ac_8c	1-Aminocyclooctane carboxylic acid
Aib	α-Aminoisobutyric acid
Api	4-Aminopiperidine-4-carboxylic acid
ATCC	American Type Culture Collection
bm	Broad Multiplet
Boc	*tert*-Butyloxycarbonyl
BOP	Benzotriazolyloxy-tris(dimethylamino)phophonium hexafluorophosphate (BOP)
bs	Broad Singlet
BSA	Bis-trimethylsilylamide
calcd	Calculated
CD	Circular Dichroism
cfu	Colony Forming Unit
Ch	1-Aminocyclohexane carboxylic acid

cm	Centimeter
COSY	*J*-Correlated Spectroscopy
d	Doublet
$Db^{n}g$	Di-*n*-butylglycine
$Db_{z}g$	Dibenzylglycine
DBU	1,8-Diazobicyclo[4.5.0]undec-7-ene
DCC	Dicyclohexyl Carbodiimide
DCE	1,2-Dichloroethane
dd	Doublet of Doublets
DDQ	2,3-dichloro-5,6-dicyano-1,4-benzoquinone
deg	degree
Deg	Diethylglycine
DIC	Diisopropyl Carbodiimide
DIEA	Diisopropylethylamine
DMAP	4-Dimehtylaminopyridine
DMF	*N,N*-dimethylformamide
DMSO	Dimethylsulfoxide
$Dp^{n}g$	Di-*n*-propylglycine
$D\phi g$	Diphenylglycine
ee	Enantiomeric Excess
Et_3N	Triethylamine

Et_2O	Diethyl Ether
EtOAc	Ethyl Acetate
FCS	Fetal Calf Serum
Fmoc	9-Fluorenylmethyloxycarbonyl
GC	Gas Chromatography
HATU	*N*-[[(dimethylamino)-1*H*-1,2,3-triazolo[4,5-b]pyrindin-1-yl]methylene]-*N*-methylmethanaminium hexafluorophosphate *N*-oxide
HBTU	*O*-benzotriazolyl-*N,N,N',N'*-tetramethyluronium hexafluorophosphate
HOAt	1-Hydroxy-7-azabenzotriazole
HOBt	1-Hydroxybenzotriazole
HPLC	High Performance Liquid Chromatography
HRMS	High Resolution Mass Spectrometry
m	Multiplet
MALDI	Matrix Assisted Laser Desorption Ionization
αMeLeu	α-Methylleucine
αMePhe	α-Methylphenylalanine
αMeTrp	α-Methyltryptophan
αMeVal	α-Methylvaline
MHz	Megahertz
MIC	Minimum Inhibitory Concentration
mL	Milliliter
mmol	Millimole

MS	Mass Spectrometry
NCA	*N*-carboxyanhyride
NMR	Nuclear Magnetic Resonance
NOE	Nuclear Overhauser Effect
NOESY	Nuclear Overhauser Effect Spectroscopy
PAL	Peptide Amide Linker
PBS	Phosphate Buffered Saline
PEG	Polyethylene glycol
PS	Polystyrene
PyAOP	7-Azabenzotriazole-1-yloxytris(pyrrolindino)phosphonium hexafluorophosphate
s	Singlet
SAR	Structure-Activity Relationship
SDS	Sodium Dodecyl Sulfate
SPPS	Solid-Phase Peptide Synthesis
t	Triplet
TBME	*tert*-Butylmethyl ether
TFA	Trifluoroacetic Acid
TFE	Trifluoroethanol
TFFH	Tetramethylfluoroformamidinium Hexafluorophosphate
THF	Tetrahydrofuran
TLC	Thin Layer Chromatography

TMAT	Tetramethylammonium trifluoroacetate
TMS-Cl	Trimethylsilyl chloride
TOCSY	Total Correlation Spectroscopy

Abstract

Amphipathic peptides rich in α,α-disubstituted amino acids (ααAAs) were synthesized and examined for antimicrobial activity and helix preference in various solvent systems. Also, a series of polar, ααAAs were synthesized for incorporation into helical peptides and a red-shifted tryptophan analog was synthesized as a fluorescent probe.

A series of short, amphipathic, 3_{10}- and α-helical peptides containing 50 to 80 percent ααAAs was synthesized. Various combinations of 1-aminocyclohexane-1-carboxylic acid, α-aminoisobutyric acid, and 4-aminopiperidine-4-carboxylic acid were incorporated using preformed acid fluorides. *In vitro* testing revealed that most of these peptides show direct antibacterial activity against *E. coli* and *S. aureus* while none exhibited direct activity against *B. abortus*. However, many of the peptides significantly reduced *B. abortus* loads in chronically infected BALB/c mice.

A series of orthogonally protected, polar, ααAAs was synthesized. A variety of amines were introduced onto 1,4-cyclohexanedione monoethylene ketal via reductive amination. Ketal removal and amino protection with *tert*-butyloxycarbonyl was followed by hydantoin formation via a Bucherer-Bergs reaction. The hydantoin was activated and then hydrolyzed using mild base and the resulting α-amino was protected with 9-fluorenylmethyloxycarbonyl to yield the desired amino acid.

An amphipathic α-helical peptide, an amphipathic 3_{10}-helical peptide, and an amphipathic 3_{10}-helical peptide containing two salt-bridges were studied for their helix preference via circular dichroism in organic and aqueous-organic solvent mixtures. The α-helical peptide displayed the designed structure in all solvents studied. Both 3_{10}-helical peptides exhibited a transition from a 3_{10}-helix to an α-helix as the percent water is increased.

N^{α}-Boc-benz[*f*]tryptophan, a red-shifted tryptophan analog, was synthesized in seven steps from 3-bromo-2-aminonaphthalene. Alkylation of the starting material, anionic cyclization, hydantoin formation, hydantoin activation, indoline deprotection, and dehydrogenation yielded the activated hydantoin of benz[*f*]tryptophan. Mild hydrolysis of the hydantoin gave the *tert*-butyloxycarbonyl protected amino acid.

The work presented focuses on synthesis of helical peptides for antimicrobial and structural studies and amino acids for the synthesis and characterization of these peptides.

Chapter 1

Introduction

1.1 Introduction

Amino acid and peptide chemistry is an extremely vast field of investigation. A myriad of important contributions have been made to the field which are too extensive for thorough review. This chapter focuses on recent work by our group and countless others on peptide secondary structure, antimicrobial peptides, amino acid synthesis, and peptide characterization. The review in Chapter 1 puts in perspective the original research presented in Chapters 2-5.

1.2 Peptide Secondary Structure

Peptides and proteins have the ability to fold into different types of structures which are primarily stabilized by hydrogen bonds and can be further stabilized by hydrophobic, electrostatic, and steric interactions.[1.1-1.3] Helices and turns rely on intramolecular hydrogen bonds in continuous segments of the polypeptide chain for structural stability. β-Sheets form through either inter or intramolecular hydrogen bonds between peptide segments. Secondary structures which do not appear in the above structures are classified as random coil. The random coil has no regular repeating, structure (no consistent pattern of ϕ, ψ angles) in significant stretches of the peptide chain, but the structure is reproducibly formed in each peptide chain.[1.1] The β-sheet structure results from two or more β-strands forming interchain hydrogen bonds.[1.1-1.3] Two forms of the β-sheet are known: the antiparallel β-sheet

and the parallel β-sheet.[1.1-1.3] The N → C sequence of both participating strands occurs in the same direction in the parallel β-sheet, while the N → C sequence is opposite in the participating β-strands of the antiparallel β-sheet. The β-strands forming the β-sheet structures are in almost a fully extended conformation with hydrogen bonds occurring between every other carbonyl oxygen and amide proton in the opposing strands. The hydrogen bonding patterns of the two forms are shown in Figure 1.1.

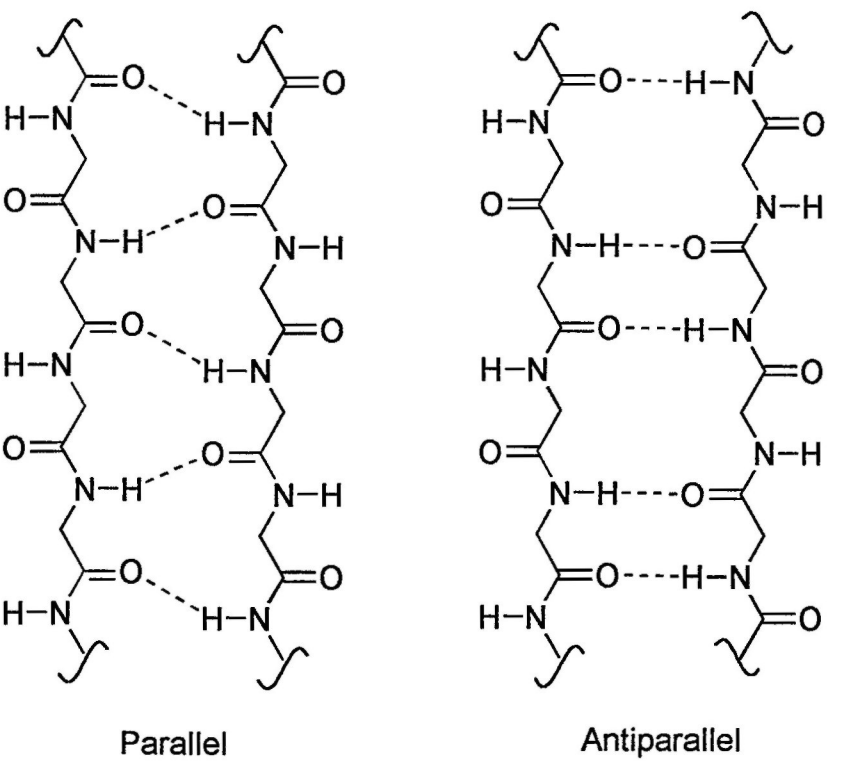

Figure 1.1. Hydrogen bonding patterns of parallel and antiparallel β-sheets.

Turns are types of secondary structures which rely on an intramolecular hydrogen bond to facilitate a directional change in a peptide chain.[1.2-1.3] α-Helices and β-sheets can be folded back onto themselves by the incorporation of a turn. Turns are classified by the number of residues contained in the structure. β-Turns contain four residues and a hydrogen bond between the carbonyl of the *i* residue and the amide proton of the *i* + 3 residue while the γ-turns contain three residues and a hydrogen bond between the *i* and the *i* + 2 residues.[1.3] The types of turns are defined by the possible conformations of the *i* + 1 residue in the γ-turn and the *i* + 1 and *i* + 2 torsional angles in the β-turns.[1.3] Notably, the type III β-turn structure has torsional angles and bonding patterns identical to the 3_{10}-helix.[1.3]

The helix is one of the most common secondary structures found in proteins.[1.2,1.3] The helix is stabilized by intrachain hydrogen bonds that are near parallel to the helix axis between carbonyl oxygens and amide hydrogens.[1.1-1.3] The carbonyls, which point downward toward the C-terminus, hydrogen bond to the amide protons which are directed upward toward the N-terminus. The helix may acquire additional stabilization through side chain interactions. Additional hydrogen bonds, salt bridges, hydrophobic interactions, and steric constraints are the most prevalent mechanisms of auxiliary peptide helix stabilization.

Multiple forms of helices are known, but the right-handed α-helix is the most predominant helix found in nature.[1.1-1.3] The right-handed helix is promoted by L

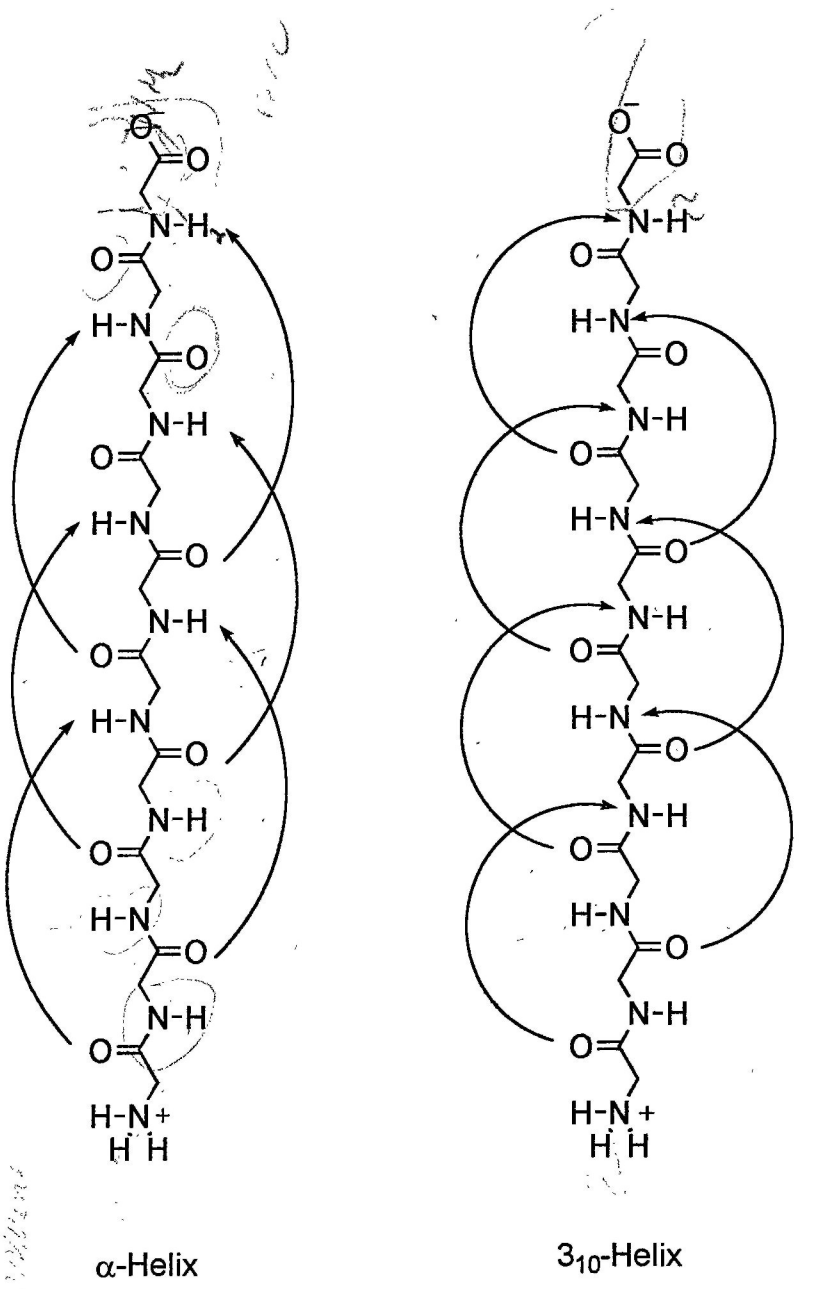

Figure 1.2. Hydrogen bonding patterns of the α-helix and the 3_{10}-helix.

amino acids, while D-amino acids propagate the less common left-handed helix. In the α-helix, the amide proton of the *i* residue hydrogen bonds to the carbonyl of the *i* + 4 residue forming a 13-membered ring (Figure 1.2).[1.2] There are 3.6 residues per turn and a pitch of 1.56 Å per residue in the α-helix.[1.1-1.3] The α-helix is also known as a 3.6_{13}-helix with 3.6 arising from the residues per turn, and 13 being the number of atoms in the hydrogen bonding pattern.

The 3_{10}-helix, though not as common as the α-helix, comprises approximately 10% of all recognized helical structures found in proteins.[1.4,1.5] The amide proton of the *i* residue hydrogen bonds to the carbonyl oxygen of the *i* + 3 residue in the 3_{10}-helix (Figure 1.26).[1.3] The 3_{10}-helix hydrogen bonding pattern forms a 10-membered ring with three residues per turn.[1.3] The 3_{10}-helix is a "tighter", longer helix (1.94 Å per residue) as compared to the α-helix.[1.4]

The α-helix and the 3_{10}-helix are the most recognized forms of helices, but other helical conformations are possible. Helices have been observed for specific homopolymers such as the poly-proline type I and II helices and the poly-glycine type I and II helices.[1.67] The π-helix, which contains a *i* to *i* + 5 hydrogen bonding pattern, has been theorized but not yet observed in proteins.[1.2]

1.3 Amphipathic α-Helix

The amphipathic α-helix is a structural feature commonly found in biologically active peptides and proteins.[1.6] This ubiquitous structure is important in peptide and protein interactions with lipids.[1.7] The amphipathic α-helix also facilitates protein

folding and promotes protein recognition processes.[1.6] Peptides containing an amphipathic α-helix have a tendency to self-associate into defined aggregates with the hydrophobic regions interacting.[1.1] The helices may interact in a similar fashion within proteins to sequester hydrophobic regions and expose polar regions to polar media. Also, the majority of naturally occurring antimicrobial peptides contain an amphipathic α-helix as the primary structural motif.[1.8]

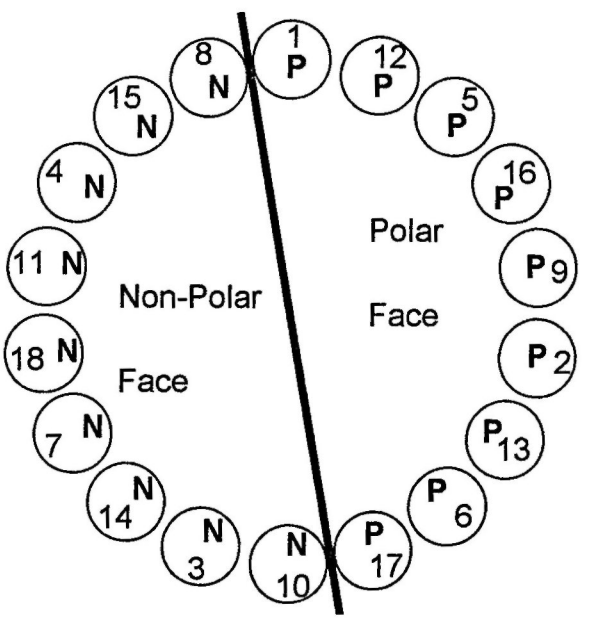

Figure 1.3 Helical wheel representation of an amphipathic α-helix.

Amphipathic α-helices contain a hydrophobic, or non-polar, face and a hydrophilic, or polar, face of the peptide helix. The Schiffer-Edmunson helical wheel diagram provides a two-dimensional representation of the α-helix.[1.9] The helical wheel is displayed as if looking down the helix axis from the C-terminus to the N-terminus. The amphipathic α-helix is shown in Figure 1.3 with P representing polar residues, comprising the hydrophilic face, and N representing non-polar residues, comprising the hydrophobic face.

1.4 Antimicrobial Peptides

Antimicrobial peptides are isolated from a variety of different organisms such as insects, mammals, amphibians, bacteria, and plants.[1.10] With few exceptions, antimicrobial peptides contain many structural similarities even though their sequences often vary greatly. Antimicrobial peptides are generally unstructured in aqueous media, but the peptides, or at least a significant portion of the peptides, adopt an amphipathic α-helical structure in membranes or membrane-like environments.[1.11-1.13] Antimicrobial peptides are frequently less than 40 residues in length and contain approximately equal numbers of polar and non-polar amino acids.[1.11,1.14] Cationic residues are more prevalent than anionic residues on the polar face, which gives rise to an overall positive charge at physiological pH.[1.14] The size of the polar face varies by peptide, but it rarely exceeds 180°.[1.11] Extensive structural and biological studies have been performed on three well known classes of antimicrobial peptides: melittin, magainins, and cecropins.[1.11,1.15]

1.4.1 Melittin

Melittin, a 26 residue antimicrobial peptide with a C-terminal amide, is isolated from the venom of the honey bee, *Apis mellifera*.[1.15] It contains an overall +6 charge with a highly basic C-terminus and a mostly hydrophobic N-terminus (Figure 1.4).[1.15] Melittin is relatively unstructured in aqueous solution at low peptide concentrations, but increased peptide concentrations, high salt, or membrane-like environments cause it to adopt an amphipathic α-helical structure.[1.11] At the higher peptide concentrations, melittin forms a tetrameric species which is driven by the formation of a hydrophobic core.[1.11,1.15]

The structure of melittin is very α-helical except for the 120° bend at residues 11 and 12 which results in the overall helix-bend-helix structure.[1.11] The hydrophilic face of melittin is narrow with an extensive hydrophobic face relative to other antimicrobial peptides. Melittin exhibits broad spectrum antimicrobial activity with minimum inhibitory concentrations (MICs) in the μM range.[1.14] This antimicrobial peptide exhibits a high degree of hemolysis which limits its effectiveness as a drug due to the poor therapeutic index.[1.11]

1.4.2 Cecropin A

Cecropin A is a 37 residue antimicrobial peptide containing a C-terminal amide. It is isolated from the North American silk moth, *Hyalophora cecropia*.[1.11] Cecropin A is a member of the cecropin class of antimicrobial peptides, which

includes similar peptides isolated from the cecropia moth, other insects, and pig intestine.[1.16]

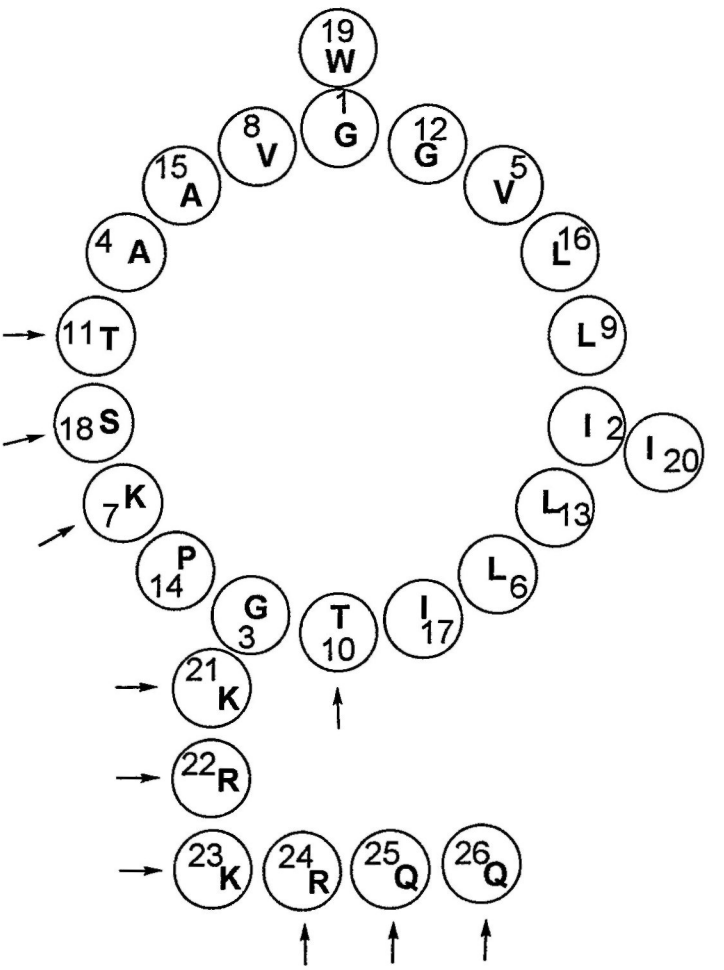

GIGAVLKVLTTGLPALISWIKRKRQQ-NH_2

Figure 1.4. Sequence and helical wheel representation of Melittin. Polar residues are indicated by arrows.

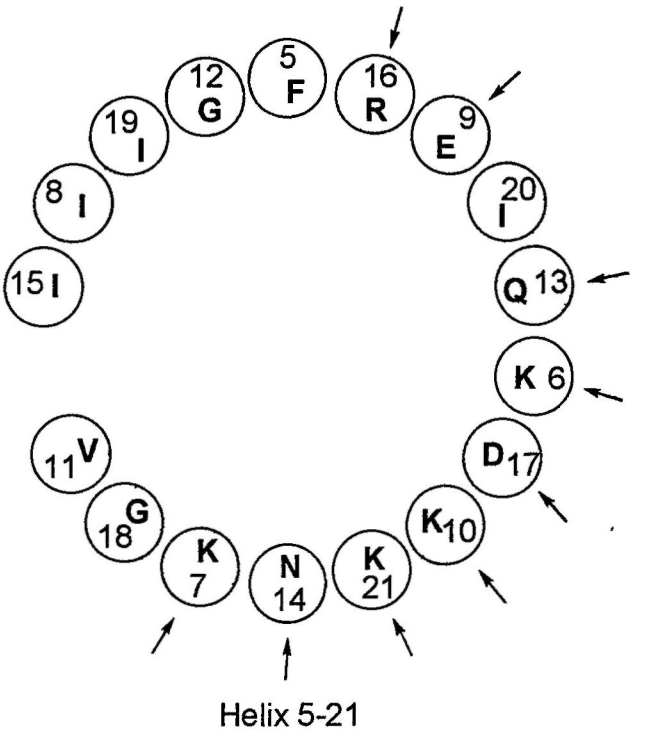

KWKLFKKIEKVGQNIRDGIIKAGPAVAVVGQATQIAK-NH_2

Figure 1.5. Sequence of Cecropin A and helical wheel representation of Cecropin A helix region 5-21. Polar residues are indicated by arrows.

Cecropin A, like melittin, adopts a helix-bend-helix structure in membrane-like environments and aggregate formation is also seen in these media.[1.13,1.16] The helix 1 region (residues 5-21) forms an amphipathic α-helix, the helix 2 region (residues 25-37) is largely hydrophobic, and the 70°-100° bend is formed by residues 23 and 24 (Figures 1.5 and 1.6).[1.16]

Cecropin A possesses excellent antimicrobial activity against representative Gram-negative bacteria and moderate activity against representative Gram-positive bacteria.[1.11,1.16] The cecropins demonstrate no hemolysis at concentrations at which they have potent antimicrobial activity.[1.11]

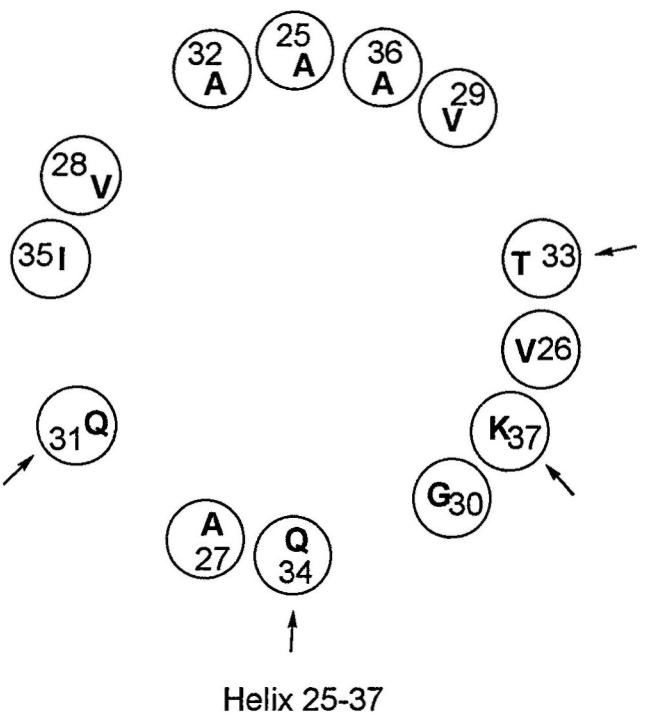

Figure 1.6. Helical wheel representation of Cecropin A helix 2 region 25-37. Polar residues are indicated by arrows.

1.4.3 Magainin 2

Magainin 2, isolated from the skin of the frog, *Xenopus laevis*, is a 23 residue antimicrobial peptide (Figure 1.7).[1.17] Other magainins and related antimicrobial peptides have also been isolated from the skin of *Xenopus laevis*.[1.17]

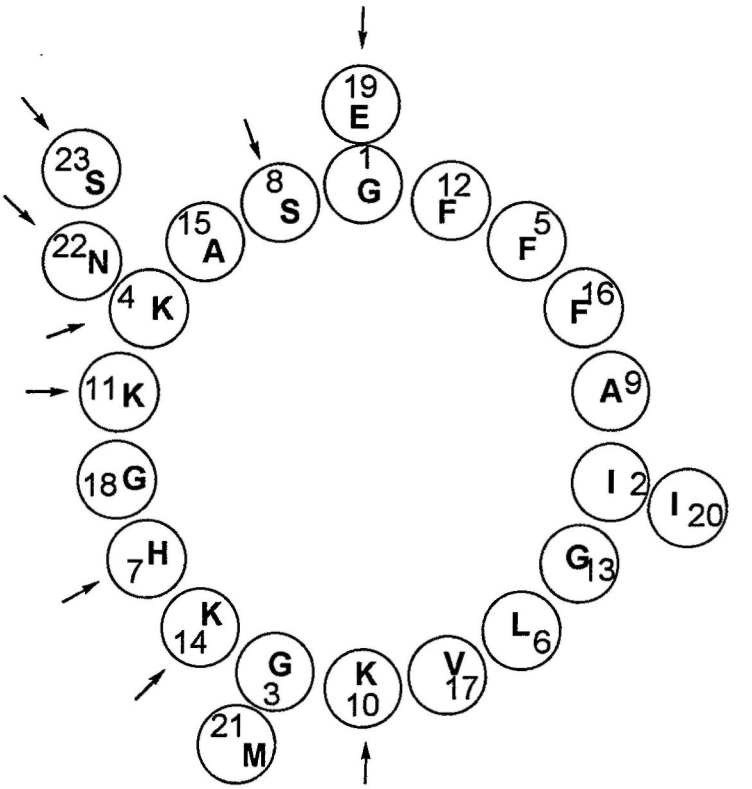

GIGKFLHSAKKFGKAFVGEIMNS

Figure 1.7. Sequence and helical wheel representation of Magainin 2. Polar residues are indicated by arrows.

Magainin 2 is relatively unstructured in aqueous solution, existing mostly as a random coil.[1.12] Upon exposure to membrane like environments, it adopts an amphipathic α-helical structure and has also been shown to form aggregates in this media.[1.12] Magainin 2 exhibits broad spectrum antimicrobial activities and is non-hemolytic at concentrations used for effective antimicrobial activity.[1.18]

1.4.4 Mechanism of Action of Antimicrobial Peptides

The outer bacterial phospholipid bilayer is the target of antimicrobial peptides.[1.19] However, the exact mechanism of action of antimicrobial peptides is not yet fully understood. The initial interaction between the peptide and bacteria is an electrostatic attraction.[1.19] The negatively charged outer bacterial phospholipid bilayer attracts the cationic peptide, which adopts an amphipathic α-helical conformation and inserts into the membrane.[1.19] Two mechanisms of antimicrobial peptides action on membranes are generally proposed: the raft model and the pore model. The amphipathic α-helical peptide lies parallel to the cell surface, in the raft model, where the hydrophobic face interacts with the cell surface and the hydrophilic face of the peptide is exposed to the extracellular aqueous media.[1.19] In the pore model, the peptides lie perpendicular to the cell membrane surfaces. The peptides insert either as monomers or as preformed aggregates to form a pore with the hydrophobic faces on the outside interacting with the phospholipids and the hydrophilic face comprising the interior of the pore.[1.19]

Some peptides demonstrate excellent selectivity for the destruction of bacterial cells over mammalian cells. The exact mechanism for selectivity is not definite, but it has been ascribed to differences in the membranes of bacterial and mammalian cells. The outer leaflets of mammalian cell membranes are zwitterionic, essentially neutral, and bacterial membranes are partially negatively charged. Therefore, the bacterial membranes may selectively attract the positively charged

peptides.[1.20] Cholesterol present in the mammalian membranes has been proposed to inhibit cell disruption by the antimicrobial peptides.[1.18] The membrane potential differences between bacterial and mammalian cells has also been suggested as a mechanism of selectivity.[1.21]

1.4.5 Structure-Activity Relationships of Antimicrobial Peptides

Analogs of naturally occurring antimicrobial peptides have been synthesized to probe the structure-function activities of the peptides.[1.11,1.16,1.21] Numerous analogs were prepared with residue deletions to examine whether specific residues were required for activity.[1.11,1.16,1.21] The deletion sequences were slightly less active, but were not single residue specific.[1.11,1.16,1.21] To explore the importance of cationic amino acids, the polar residues were replaced by non-polar or anionic amino acids.[1.11] It was determined that positively charged amino acids are required for activity. Anionic replacements have overall significantly lower the activity.[1.11]

Our group and others studied whether the amphipathic α-helix, a common structural motif in antimicrobial peptides; is a prerequisite for antimicrobial activity.[1.11,1.14,1.16,1.23] No activity was observed for peptides devoid of the amphipathic α-helix, while peptides containing solely the amphipathic α-helix displayed antimicrobial activity.[1.11,1.14] Also, increased activity was observed with the addition of helix promoting residues in the helical portions of the native peptides.[1.11,1.16] Various combinations of helical segments of cecropin A and melittin were synthesized resulting in shorter (~ 14 residues), helical peptides.[1.23]

The hybrids were active against bacteria and showed no hemolysis of red blood cells.[1.23]

Sequence homology is not required for antimicrobial activity which is exemplified by the scores of distinct peptides exhibiting biological activity.[1.11,1.16] However, this provides little information regarding a specific binding or chiral recognition mechanism. The all D-analogs of melittin, cecropin, and magainin were synthesized and tested for antimicrobial activity to examine the role of chiral recognition in antimicrobial activity.[1.24,1.25] The analogs showed antimicrobial activities identical to those of their L-counterparts, thus indicating that no chiral recognition is involved in antimicrobial peptide mechanism of action.[1.24,1.25]

De novo peptides have been designed and synthesized to further examine the structure-activity relationships (SAR) of antimicrobial peptides.[1.10,1.14,1.19,1.26] It is widely accepted that the amphipathic α-helix is the only structural motif required for antimicrobial activity. Short peptides (10-16 residues) containing only the amphipathic α-helix have shown essentially the same antimicrobial activities as longer peptides and have demonstrated a higher degree of selectivity of bacterial killing over red blood cells.[1.14,1.19,1.26] These findings cast doubt on the theory of pore-formation because the peptides are not long enough to span the membrane, but do not eliminate the possibility of pore formation because dimerization is possible.[1.19,1.26]

Hydrophobic interactions have been reported to play a major role in the lysis of red blood cells. Strong hydrophobic interactions (i.e. incorporation of highly

hydrophobic residues or extensive hydrophobic faces, 300° or more) increase hemolytic activity of antimicrobial peptides.[1.26] Another study, by our group, on a series of designed amphipathic α-helical peptides disclosed a direct correlation between helicity and bioactivity.[1.14] The correlation revealed that increased peptide helicity was accompanied by increased biological activity.

The vast number of SAR studies reported on antimicrobial peptides yield important information for the development of an effective antimicrobial drug. An important finding is that sequence homology and chiral interactions are not required for biological activity which allows a variety of amino acids to be incorporated to serve specific functions.[1.24,1.25] Two other significant findings were that short peptides showed excellent selectivity and that biological activity was directly proportional to the helicity of the peptides.[1.14,1.19,1.23,1.26] Considering the above and other findings, short, highly helical peptides have the potential to be very active and selective antimicrobial agents.

1.5 Synthesis of Short, Helical Peptides

The synthesis of short, helical peptides requires the incorporation of amino acids which strongly promote helical structures. Several systematic studies have examined the helix promoting ability of the proteinogenic amino acids.[1.27-1.29] The first studies determined the frequency of amino acids occurring in helical regions of proteins and peptides.[1.27] Later studies investigated the effects of incorporating each proteinogenic amino acid into a host peptide on the helicity of the resulting peptide.

The studies generally found residues like Ala, Leu, and Lys were helix promoters and Pro and Gly were helix breakers.[1.28,1.29] Even though some proteinogenic amino acids promote helicity, they do not promote helicity to the extent required for the synthesis of very short and helical peptides.

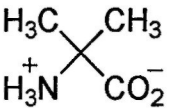

Figure 1.8. Structure of α-Aminoisobutyric acid.

1.5.1 α-Aminoisobutyric Acid

α-Aminoisobutyric acid (Aib) (Figure 1.8) was first postulated to be a strong helix promoter upon its discovery in the channel-forming peptide, alamethicin. Alamethicin was found to be more helical than would have been predicted by the helix forming propensities of the proteinogenic amino acids.[1.30] This evidence suggested that Aib was a very strong helix promoter.

It has been well documented that Aib and other residues disubstituted on the α-carbon, where the R groups are not extremely large, strongly promote helical structures.[1.31,1.32] The additional R group severely restricts the possible

conformations of the amino acid while in a peptide. The rotation around the nitrogen to the α-carbon (ϕ angle) and the α-carbon to the carbonyl (ψ angle) is restricted (Figure 1.9).[1.31-1.33] The calculations of allowable conformations of Aib in ϕ, ψ space determine that the allowed angles are restricted to those for the 3_{10}-helix (ϕ ≈ -60°/60°, ψ ≈ -30°/30° left-handed / right-handed helix) and the α-helix (ϕ ≈ -55°/55°, ψ ≈ -45°/45° left-handed / right-handed helix).[1.31-1.33]

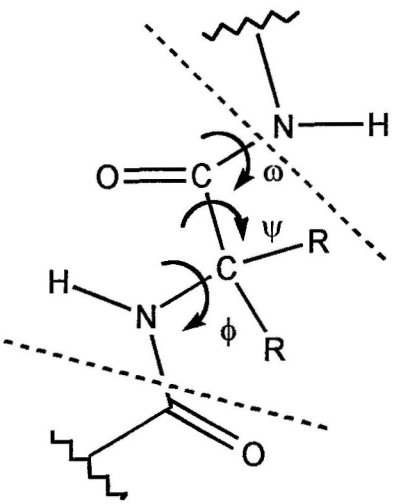

Figure 1.9. Torsional angles of the peptide backbone.

1.5.2 Other α,α-Disubstituted Amino Acids

Aib is the most common α,α-disubstituted amino acid (ααAA) studied, but many other ααAAs have been synthesized and their effects on peptide secondary structure examined.[1.32-1.41] A series of ααAAs have been developed which are

symmetric about the α-carbon and the α-carbon is not in a ring system (Figure 1.10).[1.32] Representative examples of amino acids in this family are: diethylglycine (Deg), di-*n*-propylglycine (Dp^{n}g), di-*n*-butylglycine (Db^{n}g), diphenylglycine (Dϕg), and dibenzylglycine (Db$_z$g). Unlike Aib, these amino acids promote the extended structure ($\phi \approx \psi \approx 180°$) and do not promote helicity.[1.32]

Deg	R= ethyl	Dϕg	R= phenyl
Dp^{n}g	R= *n*-propyl	Db$_z$g	R= benzyl
Db^{n}g	R= *n*-butyl		

Figure 1.10. Representative acyclic, symmetrical, non-polar ααAAs.

A variety of cyclic, aliphatic, ααAAs have been studied for their structure promoting ability (Figure 1.11).[1.32,1.34] 1-Aminocyclobutane carboxylic acid (Ac$_4$c), 1-aminocyclopentane carboxylic acid (Ac$_5$c), 1-aminocyclohexane carboxylic acid

(Ac_6c), and 1-aminocycloheptane carboxylic acid (Ac_7c) have been shown to promote the formation of 3_{10}- or α-helices.[1.32,1.34] 1-Aminocyclooctane carboxylic acid (Ac_8c) prefers to form a 3_{10}-helix/β-bend structure and 1-aminocyclopropane carboxylic acid (Ac_3c) forms a distorted 3_{10}-helix.[1.32] In general, cyclic, aliphatic ααAAs promote helical structures, whether 3_{10}- or α-helical.

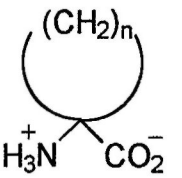

Ac_3c	n= 3	Ac_6c	n= 6
Ac_4c	n= 4	Ac_7c	n= 7
Ac_5c	n= 5	Ac_8c	n= 8

Figure 1.11. Representative cyclic, non-polar ααAAs.

Chiral ααAAs have also been prepared, and their structure promoting effects investigated. Chiral, cyclic ααAAs and methylated derivatives of proteinogenic amino acids represent the majority of chiral ααAAs prepared.[1.32,1.35-1.38] The cyclic

amino acids are thought to promote structures similar to those of their achiral counterparts. α-Methylphenylalanine (αMePhe), α-methylleucine (αMeLeu), α-methyltryptophan (αMeTrp), and α-methylvaline (αMeVal) have exhibited strong helix promoting tendencies in short peptides (Figure 1.12).[1.32,1.37] The ability of the methylated derivatives of proteinogenic amino acids to promote helical structures is notable, since all acyclic residues with both side chains larger than methyl promote an extended conformation. The above studies indicate that cyclic residues and acyclic residues, where at least one side chain is methyl, promote helical structures. In contrast, ααAAs with side chains consisting of acyclic functionalities larger than methyl are inclined to form extended structures.

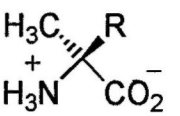

αMePhe	R= benzyl
αMeTrp	R= 3-methylindole
αMeLeu	R= isobutyl
αMeVal	R= isopropyl

Figure 1.12. Methylated derivatives of proteinogenic amino acids.

A variety of polar ααAAs bearing various functional groups (Figure 1.13) have been prepared for the investigation of amino acid binding to receptor complexes and for incorporation into biologically active peptides.[1.38-1.41] The polar ααAAs are generally thought to promote the same secondary structures as their parent non-polar compounds.

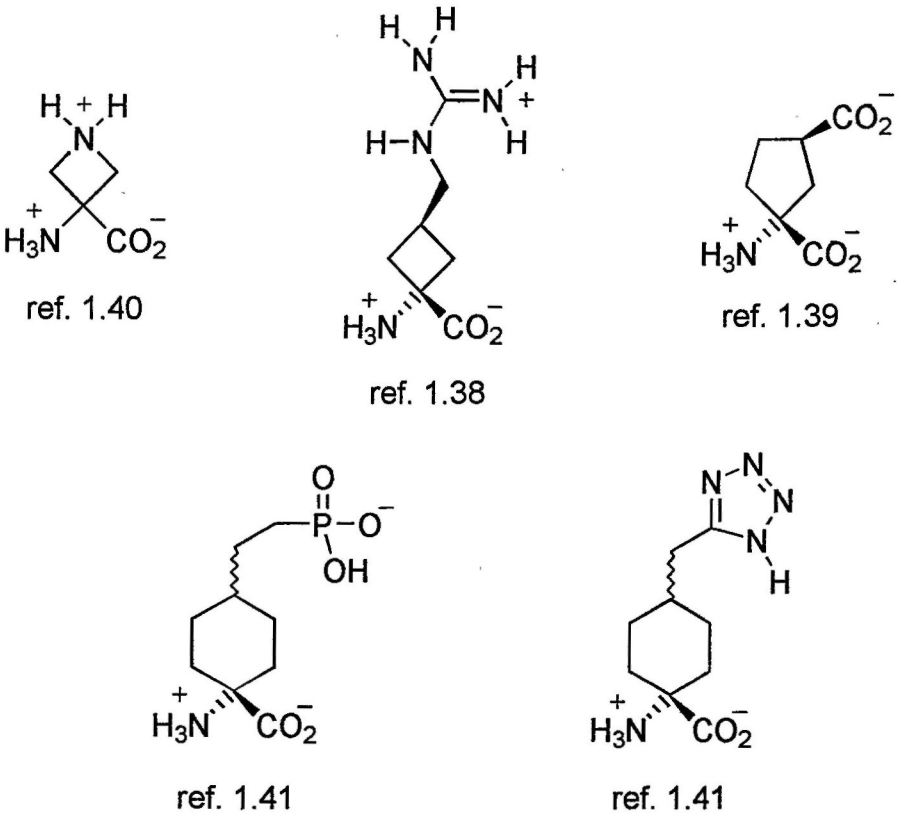

Figure 1.13. Representative polar ααAAs.

Most preparations of polar ααAAs report the synthesis of the unprotected amino acids, which limits their applicability in peptide synthesis.[1.39,1.40,1.41] Orthogonal protection of the side chain in respect to the α-amine is required for the incorporation of the amino acid into a peptide. Orthogonally protected, polar ααAAs suitable for incorporation are important tools in peptide design. They allow the synthesis of water soluble peptides containing high percentages of ααAAs and can be used to form the polar face in an amphipathic, highly helical peptide. Polar ααAAs thus provide a tool for the development of highly helical peptides as antimicrobial agents.

1.5.3 Incorporation of α,α-Disubstituted Amino Acids Into Peptides

The incorporation of one or multiple α,α-disubstituted amino acids into a peptide has proven to be an arduous procedure until recently.[1.33] The additional substituent on the α-carbon significantly increases steric bulk, rendering ααAAs couplings difficult.[1.42] Carbodiimides (Figure 1.14), which have traditionally been used in amino acid couplings, give unsatisfactory yields in ααAAs couplings.[1.43] Dicyclohexyl carbodiimide (DCC) and diisopropyl carbodiimide (DIC) are the most common carbodiimide based coupling reagents used in peptide assembly. Extended reaction times or the use of additives (i.e. 1-hydroxybenzotriazole (HOBt)) seldom improve the yields in the carbodiimide mediated ααAA couplings.[1.43] Also, first generation phosphonium and uronium salts (Figure 1.14) (i.e. (benzotriazolyloxy)-tris(dimethylamino)phophonium hexafluorophosphate (BOP) or *O*-benzotriazolyl-*N*,

N,N',N'-tetramethyluronium hexafluorophosphate (HBTU)) have yielded only mediocre results on ααAA couplings even with the addition of heat or lengthy reaction times.[1.42] First generation phosphonium and uronium salt based coupling reagents have HOBt (Figure 1.14) acting as the leaving group and subsequently forming the active ester.

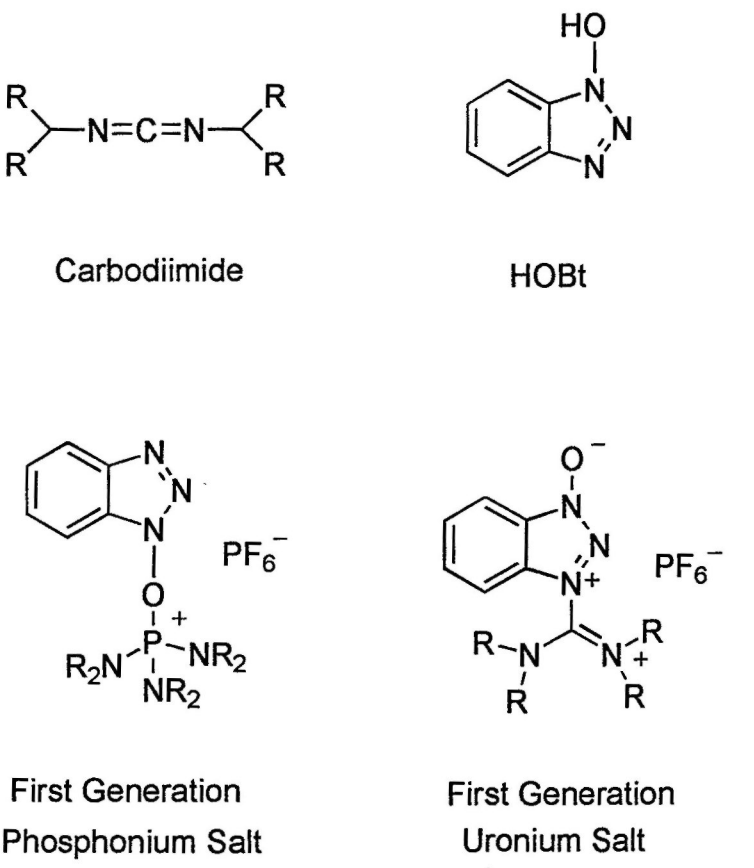

Figure 1.14. Traditional amino acid coupling reagents/additive.

Alternate methods have been utilized or developed in attempts to overcome the difficulties encountered with the above coupling reagents. Acid chlorides, oxazolones, *N*-carboxyanhyrides (NCAs), and 2-(dimethylamino)-3,3-dimethyl-azirine are some of the more common methods/reagents used (Figure 1.15).[1.42,1.44,1.45]

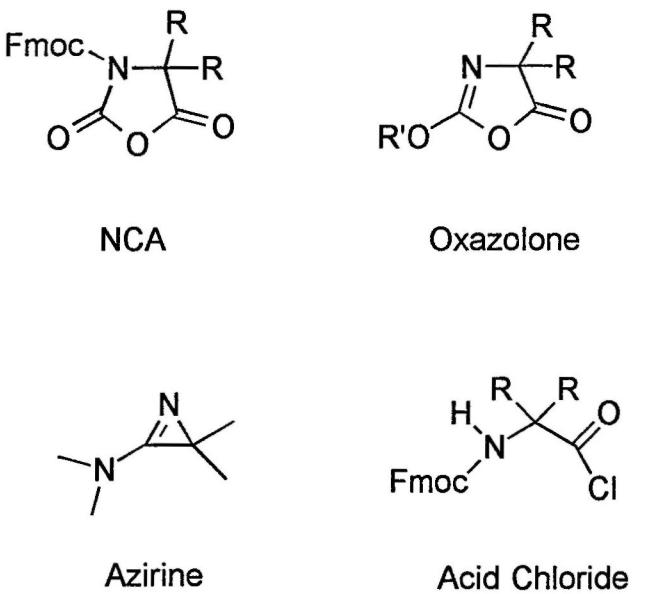

Figure 1.15. Alternate reagents for ααAA couplings.

Even though these methods have the capability of producing higher yields on ααAA couplings, specific drawbacks have limited their use. Acid chloride activation has been limited because of harsh conditions required for its formation and the acid chloride's susceptibility to oxazolone formation.[1.44] NCAs and oxazolones are seldom used because of a high degree of side product formation accompanying the couplings.[1.42,1.45] The post coupling hydrolysis required by the azirine method severely limits its applicability as a peptide synthesis reagent.[1.45] These alternate methods are not general or mild enough to allow repetitive, high yield couplings required by solid-phase peptide synthesis (SPPS).

New methods have been developed for the mild and efficient couplings of sterically hindered residues. Carpino's acid fluorides (Figure 1.16) give high yield couplings of ααAAs under mild conditions.[1.42,1.46,1.47] The acid fluoride method has proven to be equally effective in solution or on solid supports.[1.42,1.46,1.47] The original acid fluoride couplings used preformed acid fluorides which were reacted with the free amine of another amino acid in the presence of *N,N*-diisopropylethylamine (DIEA).[1.48,1.49] The acid fluoride is formed by treating an amino-protected amino acid with cyanuric fluoride and pyridine. Later, a method was developed for the *in situ* formation of the acid fluoride with tetramethylfluoroformamidinium hexafluorophosphate (TFFH) and subsequent coupling.[1.50] Even extremely hindered residue (i.e. *N*-methyl-Aib) couplings have

been shown to produce high yields with acid fluorides and a bis-trimethylsilylamide (BSA) activated nitrogen.[1.51]

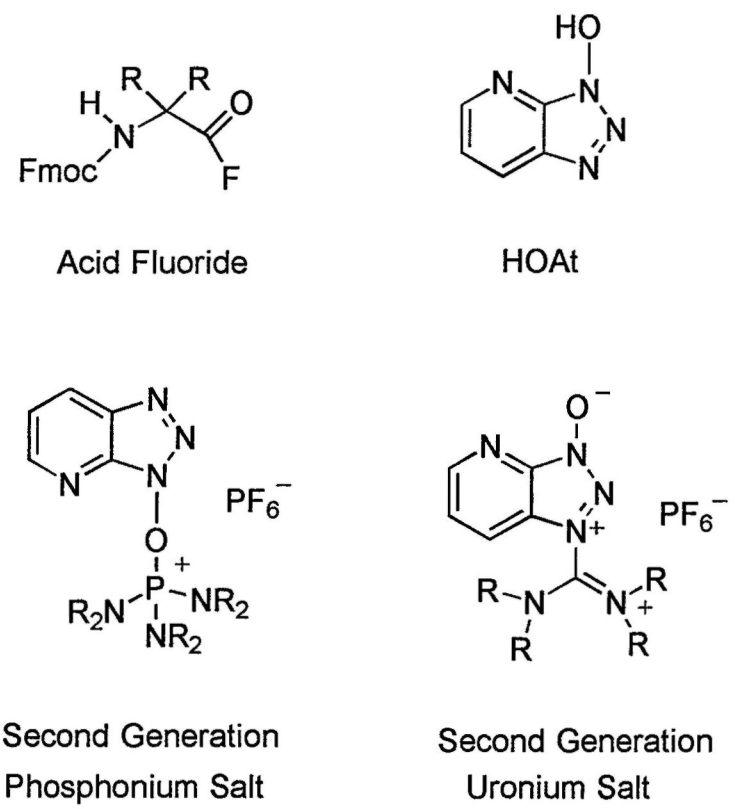

Figure 1.16. Current reagents used for ααAA couplings.

Second generation phosphonium and uronium salt coupling reagents (Figure 1.16) (i.e. 7-azabenzotriazole-1-yloxytris(pyrrolindino)phosphonium hexafluorophosphate (PyAOP) or *N*-[[(dimethylamino)-1*H*-1,2,3-triazolo[4,5-b]pyrindin-1-yl]methylene]-*N*-methylmethanaminium hexafluorophosphate *N*-oxide (HATU)) have also been examined in sterically hindered residue couplings.[1.52,1.53] The newer salts differ from the first generation salts only by the substitution of 1-hydroxy-7-azabenzotriazole (HOAt) (Figure 1.16) for HOBt. The second generation phosphonium and uronium salts have exhibited a high degree of efficiency in multiple ααAA couplings.[1.52,1.53]

1.6 Amino Acid Synthesis

A vast number of synthetic routes for the construction of amino acids and amino acid derivatives have been developed. Traditional α-amino acid syntheses produce racemic mixtures, but many of these methods may be modified to give enantioselective syntheses. Also, ααAAs have become popular in peptide design; consequently, many syntheses have been adapted to the formation of these non-proteinogenic amino acids.

The conversion of an α-halo carboxylic acid to an amino acid via a substitution reaction with ammonia or an ammonia equivalent (N_3 or potassium pthalimide) can be utilized as a route to amino acids (Figure 1.17). This procedure produces a racemic mixture of amino acids, unless a chiral α-haloacid is used as the

electrophile. The formation of an ααAA via amino introduction on an α-halo acid would be very sluggish due to steric constraints.

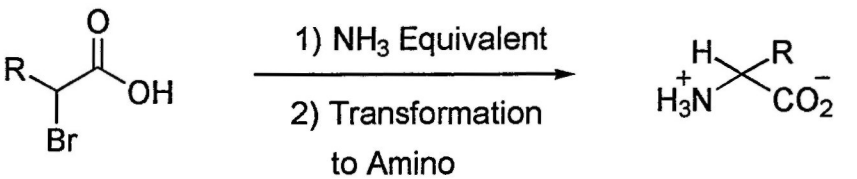

Figure 1.17. Amino acid synthesis via amino introduction on an α-halo carboxylic acid.

The well known Curtius, Hoffman, Schmidt, and other related rearrangements are viable pathways to amino acids (Figure 1.18).[1.54-1.56] The amino acid is produced following the hydrolysis of an isocyanate, which is formed as a result of the rearrangement of an *N*-bromo amide anion or an alkanoyl azide. The rearrangements may produce a specific enantiomer if a chiral R group is present because the configuration is maintained in the rearrangements.[1.57] ααAA may be synthesized via the Curtius, Hoffman, Schmidt, and other related rearrangements by using an appropriately substituted migrating carbon.

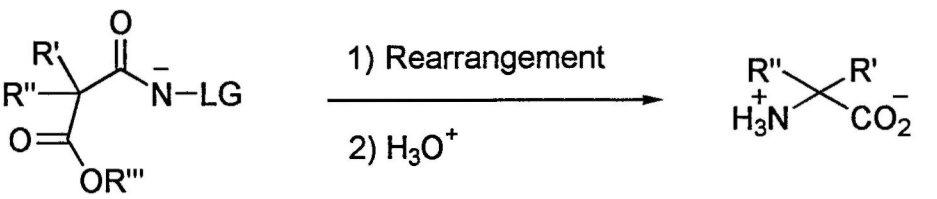

Figure 1.18. Amino acid synthesis via rearrangements.

α-Amino acids are readily generated by the reductive amination of α-keto acids (Figure 1.19). The reductive amination approach is not extensively utilized in chemical syntheses, but has found widespread application in enzymatic syntheses.[1.58] Amino acid formation via the reductive amination of an α-keto acid is a biosynthetic step. As a result, the enzymes are excellent catalysts for the transformation to L-amino acids.[1.58] The enzymatic reactions are highly enantiospecific, forming only one enantiomer in good yield. The reductive amination procedure can not be applied as a route to ααAAs because the α-carbon of the resulting amino acid is the carbonyl carbon in the stating material.

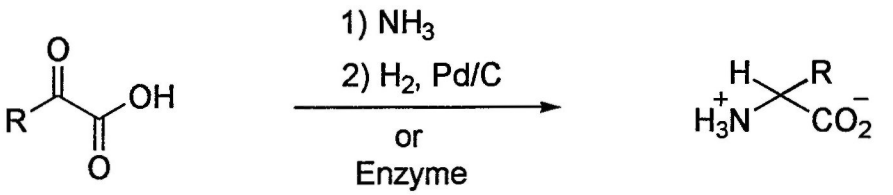

Figure 1.19. Amino acids synthesis via reductive amination.

The Strecker and Bucherer-Bergs are common methods of amino acid synthesis and are particularly prevalent in ααAA synthesis (Figure 1.20).[1.32-1.41,1.59,1.60] Both methods employ aldehydes and ketones as starting materials for α-amino acids and ααAAs, respectively. The Strecker synthesis reacts KCN and NH_4Cl with an aldehyde or ketone to form an amino nitrile, which is subsequently hydrolyzed to yield the amino acid. An aldehyde or ketone is treated with KCN and $NH_4(CO_3)_2$ to give the corresponding hydantoin in the Bucherer-Bergs synthesis. The hydantoin is cleaved with base to form the free amino acid.

Traditional Strecker and Bucherer-Bergs syntheses give a racemic mixture of the resulting amino acid, but this is often not a drawback in ααAA synthesis because many are symmetrical.[1.32] Asymmetric Strecker syntheses have been developed

using chiral amines for stereochemical control in the reaction.[1.58] The asymmetric methods produce acceptable enantiomeric excesses (ee), but other methods are more prevalent in asymmetric amino acid synthesis.

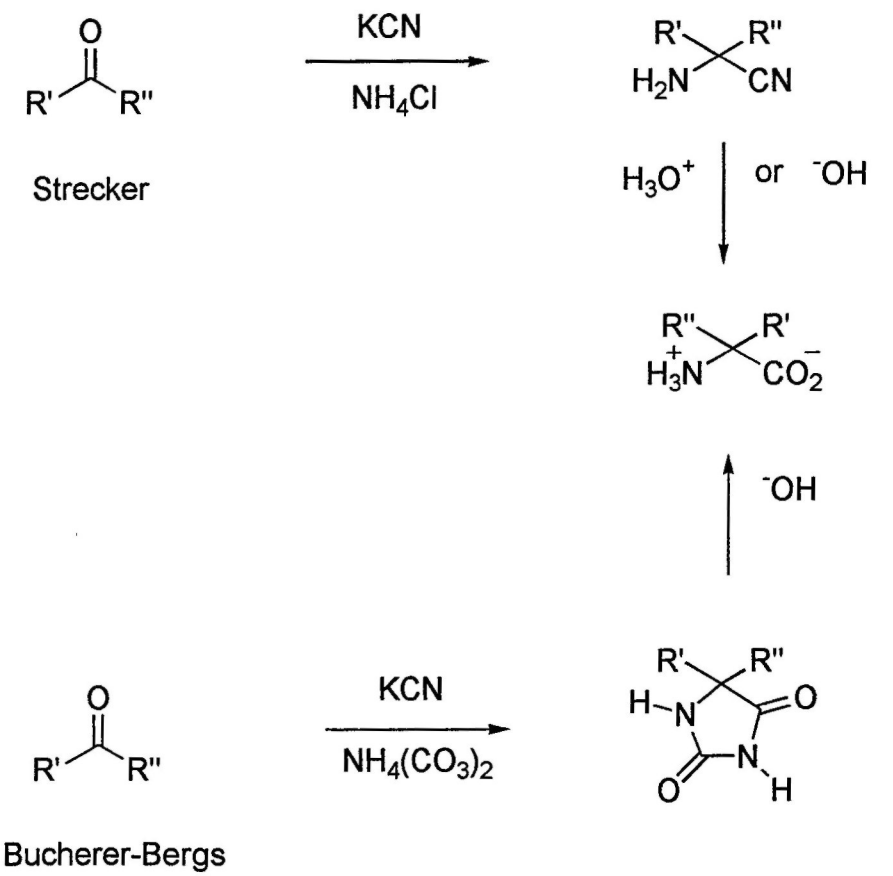

Figure 1.20. Strecker and Bucherer-Bergs Syntheses.

Asymmetric hydrogenation of α,β-dehydro-amino acids is an effective procedure for the introduction of chirality to an amino acid (Figure 1.21). A plethora of chiral, bis-phosphine ligands have been developed for asymmetric hydrogenations with rhodium, which generally produce ees of 90% or greater.[1.58] Wittig, Horner-Emmons, and condensation reactions are the most common synthetic routes to α,β-dehydro-amino acids.[1.58] The asymmetric hydrogenation is an effective method of enantioselective amino acid preparation, but it is limited by difficulty in α,β -dehydro-amino acid preparations and its inability to produce ααAAs.

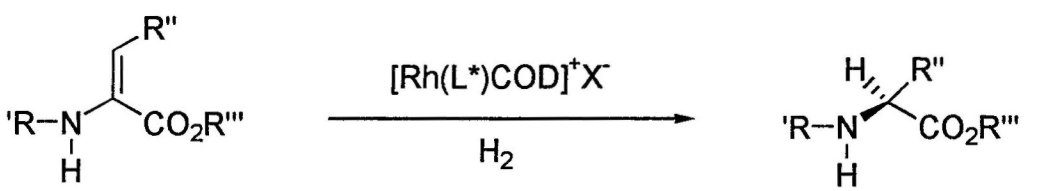

Figure 1.21. Amino acid synthesis via asymmetric hydrogenation.

The electrophilic or nucleophilic addition of a side chain or side chains to glycine synthons are effective and widely used methods of amino acid syntheses. The

benzophenone imine of glycine *t*-butyl ester is a common glycine anion equivalent used for the synthesis of α-amino acids, while a similar procedure may be employed for ααAA construction (Figure 1.22).[1.61] The reaction is generally done by deprotonation of the template, alkylation with R-X, and acidic hydrolysis to yield the amino acid. The above method has been recently extended to an enantioselective synthesis using chiral phase-transfer catalysis. The chiral phase-transfer catalysis method produces moderate yields of the desired amino acid enantiomer.[1.61]

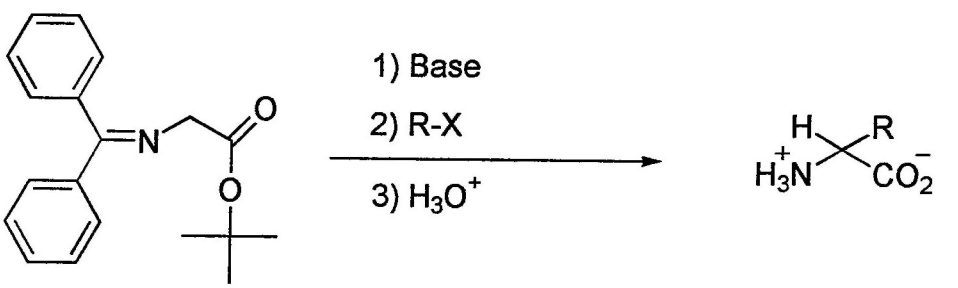

Figure 1.22. Amino acid synthesis with an achiral glycine template.

The development of chiral glycine synthons for the enantioselective synthesis of mono- and di-substituted amino acids has provided an excellent tool for the organic chemist. The chiral templates generally produce the amino acid in good yield with very high ee. Many of the chiral glycine equivalents have the ability to function either as an electrophile or a nucleophile. Numerous enantioselective templates have been developed, but four have proven to be very effective and versatile.[1.58]

One of the classic glycine templates is Schöllkopf's bis-lactim ether (Figure 1.23).[1.62] The bis-lactim ether is synthesized by forming the diketopiperazine of glycine and valine (D- or L-, depending upon which configuration of the amino acid is desired), followed by methylation of the oxygens. The amino acid synthesis begins with deprotonation of the lactim and alkylation, which adds on the opposite face of the template with respect to the isopropyl. The lactim may be deprotonated and alkylated again to form an ααAA precursor.[1.63] Following alkylation, the template is hydrolyzed to give the amino acid in the desired configuration.

Schöllkopf's template may also act as a chiral glycine cation equivalent. This is accomplished via chlorination of the lactim by treatment with base and hexachloroethane.[1.64] The chlorination results with the chloro and isopropyl groups in a cis arrangement. The chlorinated moiety is alkylated with olefins or arenes in the presence of a Lewis acid, which gives inversion of configuration of the chloronated carbon. The alkylated template is subsequently hydrolyzed as above to form the free amino acid.

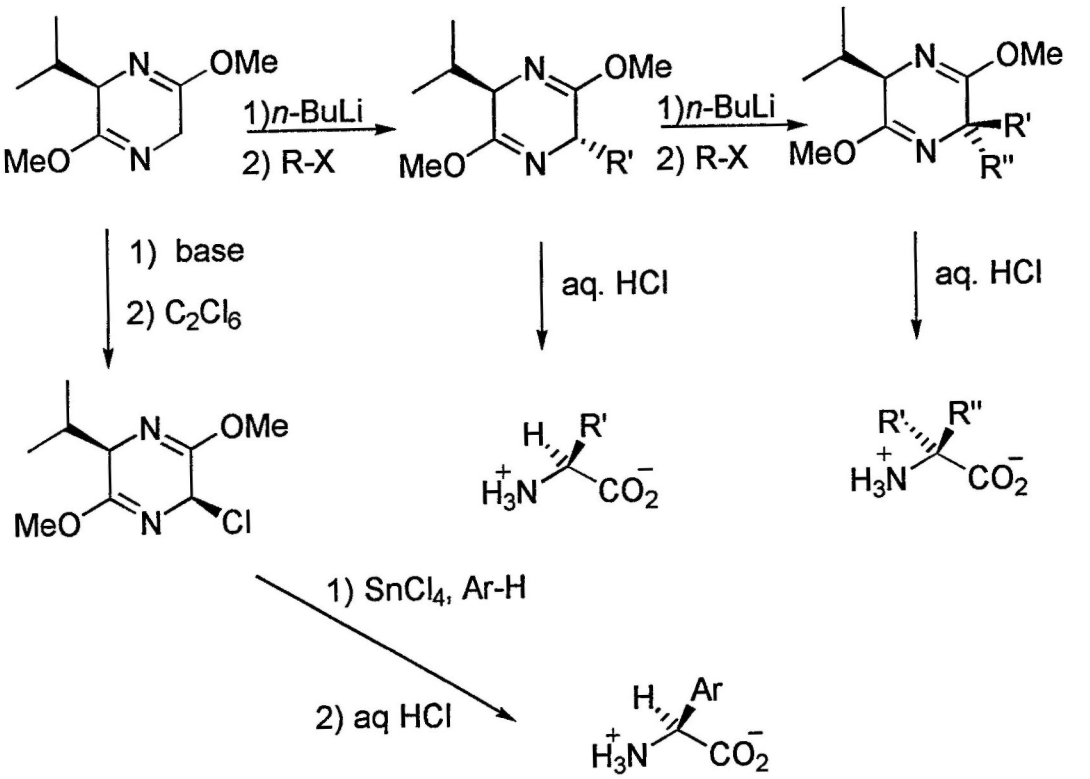

Figure 1.23. Amino acid synthesis using Schöllkopf's template.

Seebach's imidazolidinone chiral glycine template presents another efficient method for enantioselective amino acid synthesis (Figure 1.24).[1.65] The template is formed by the condensation of glycine-methyl amide and pivaldehyde,

t-butyloxycarbonyl (Boc) protection of the nitrogen, and separation of the isomers. The resulting template is deprotonated and alkylated for α-amino acid synthesis or deprotonated and alkylated again for ααAA synthesis.[1.63] The *t*-butyl group directs the alkylation to the opposite face of the template creating a new chiral center. Acidic hydrolysis of the alkylated template yields the desired amino acid in good yield and good ee.

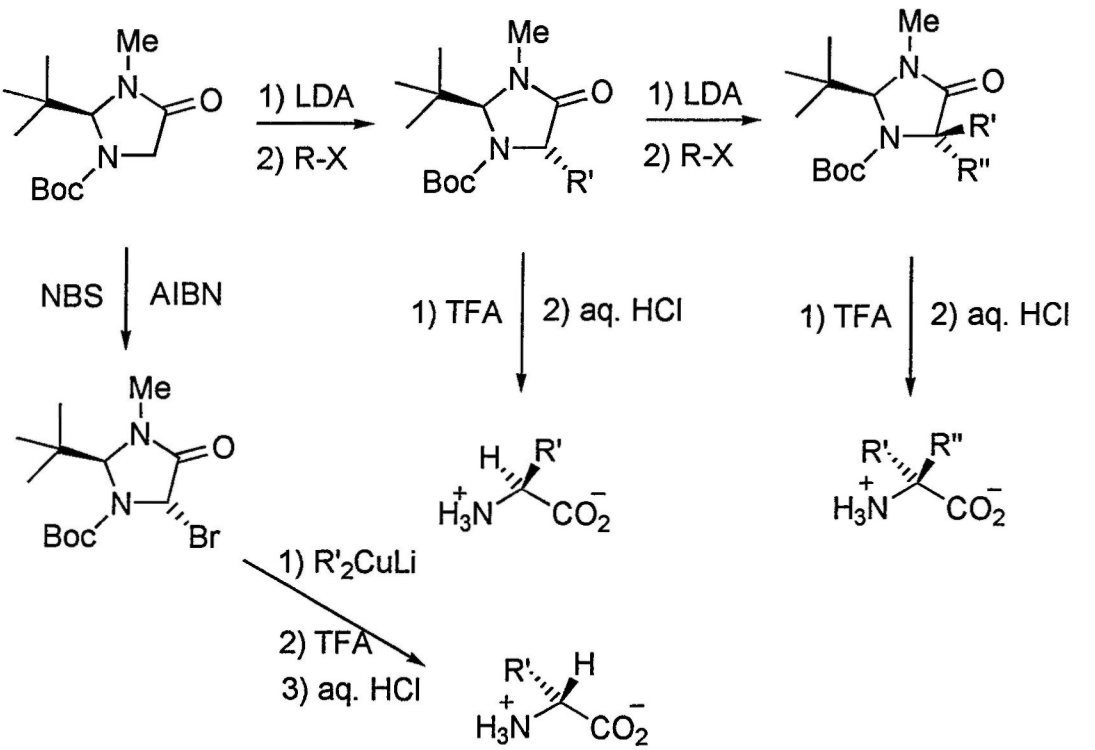

Figure 1.24. Amino acid synthesis using Seebach's template.

Bromination in the α-position of Seebach's template provides an enantioselective, cationic glycine equivalent.[1.66] The template is alkylated with an alkyl cuprate (R_2CuLi), or an arene in the presence of a Lewis acid, to give a monosubstituted amino acid following hydrolysis.

One of the most efficient and widely used chiral glycine equivalents was developed by Williams (Figure 1.25).[1.67] Protected diphenyloxazinones are employed as chiral electrophiles or nucleophiles in the Williams method. The diphenyloxazinones are synthesized by reacting erythro-α,β-diphenyl-β-hydroxyethylamine (either enantiomer, depending upon which configuration of the resulting amino acid is desired) with ethyl bromoacetate, Boc protection of the nitrogen, and acid catalyzed esterification. The amino acid synthesis proceeds by enolate formation with base, subsequent alkylation for α-amino acid formation or a second deprotonation-alkylation for the formation of ααAAs. The mono- or dialkylated template is treated with trifluoroacetic acid (TFA) and hydrogenated over palladium to form the free amino acid, or the template is cleaved with Li/NH_3 to give the Boc protected amino acid. In the case of aryl side chains, the above procedures are not used due to reduction of the side chains so, the template is cleaved by sequential treatment with Me_3SiI, aq. HCl, and $NaIO_4$ to yield the free amino acid.[1.68] William's template may also be brominated and alkylated in the presence of a Lewis acid to form the desired amino acid after template cleavage.[1.69]

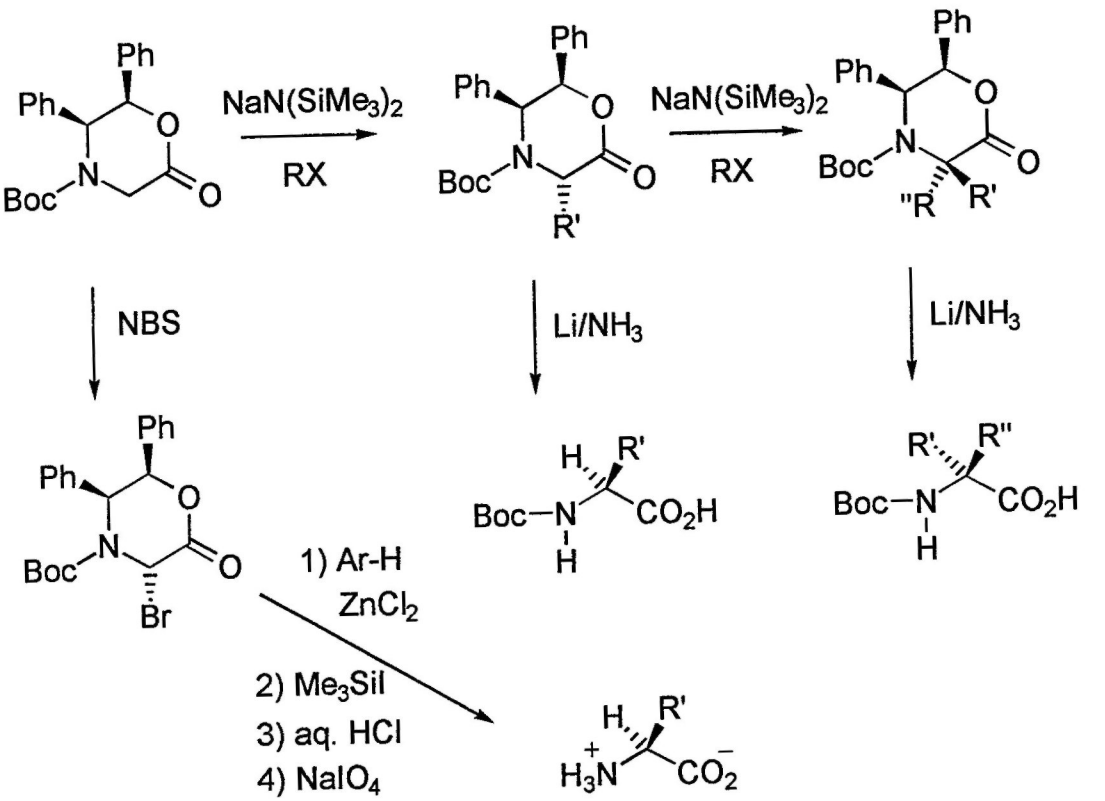

Figure 1.25. Amino acid synthesis using William's template.

Myers recently reported an enantioselective method for the synthesis of amino acids using inexpensive and easily obtained enantiomers of pseudoephedrine glycinimide (Figure 1.26).[1.70] The glycinimide is formed by treating psuedoephedrine

with *n*-butylLi followed by the addition of glycine methyl ester. The glycinimide moiety is treated with base and alkylated to yield the amino acid precursor. The protected amino acid is formed via basic hydrolysis and subsequent treatment with di-*tert*-butyl-dicarbonate or 9-fluorenylmethyl chloroformate.

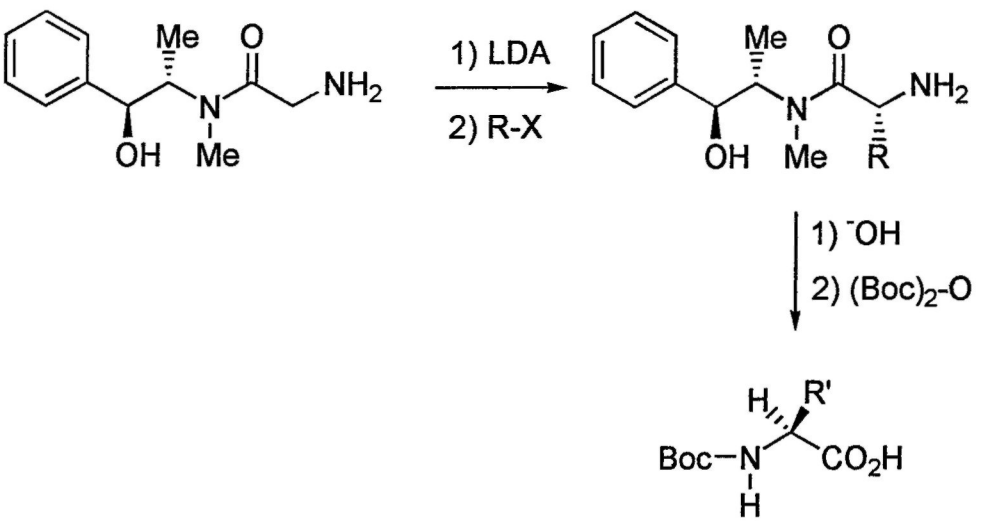

Figure 1.26. Amino acid synthesis using Myer's template.

The chiral glycine equivalents have made a significant contribution to the field of amino acid synthesis. Many of the templates used in syntheses are now commercially available which provides an easy route to enantiomerically pure amino acids. Even though the template methods are important, the significance of the other methods can not be ignored. Many amino acid syntheses concentrate on the assembly of elaborate side-chains where the amino acid functionalities may need to be introduced prior to completion of the side chain. Traditional methods also may be applied where the templates fail, or the template chemistries are not compatible with the side chains.

1.7 Secondary Structures Promoted by α,α-Disubstituted Amino Acids

The α-helix, 3_{10}-helix, and extended conformation are the predominant secondary structures promoted by ααAAs. The extended conformation is generally only promoted by acyclic ααAAs with sterically demanding α-substituents, but conclusive studies exploring the structural preferences of 9-membered ring or larger cyclic ααAAs have not yet been performed.[1.32] Cyclic ααAAs (8-membered or smaller) and ααAAs containing methyl as at least one side chain promote the formation of 3_{10}- and α-helices. The helix preference depends upon the design of the peptide, the environment, and the location and percentage of ααAAs.

The 3_{10}-/α-helix equilibrium is currently being investigated by many groups because the 3_{10}-helix is thought to be a protein folding intermediate and the 3_{10}-helix is postulated to play a role in receptor binding.[1.71-1.74] The 3_{10}-helix and the α-helix

have been well characterized in short peptides containing multiple ααAAs.[1.72,1.74] Aib has been almost exclusively used in the studies of helix preference in ααAAs rich peptides. Unfortunately, the use of the hydrophobic amino acid has precluded studies in aqueous media and required the experiments, either spectroscopic or crystallization, to be performed in organic solvents.

Researchers have suggested factors for the prediction of the type of helix formed in short ααAAs rich peptides (Table 1.1). The length of the peptide, percentage of ααAAs, location of monosubstituted amino acids, and the solvent effects are the primary factors thought to be involved in the 3_{10}-/α-helix equilibrium.[1.45,1.70-1.77] The peptide length is believed to be an important factor in the determination of the helix type preference. Karle reported that Aib rich peptides with five residues or less form 3_{10}-helices, and peptides with ten or more residues prefer an α-helix.[1.72] Aib rich peptides between five and ten residues in length have no definite helix preference and form either the 3_{10}-helix or the α-helix, although some believe there is a distinct length discrimination for the preferential formation of the 3_{10}-helix or the α-helix.[1.32,1.72] It was reported that peptides with seven residues or less will form a 3_{10}-helix, and peptides containing greater than eight residues will form an α-helix, unless the peptide contains an extremely high percentage of ααAAs.[1.32]

The percentage of ααAAs contained in a peptide is also capable of dictating the preference of helical formation. This factor plays the largest role in medium

length peptides (7-10 residues), which can form either the 3_{10}-helix or the α-helix. Seven residue or longer peptides with 50% or greater ααAAs are reported to form a 3_{10}-helix and those containing less than 50% ααAA content favor an α-helix.[1.72]

Table 1.1

Factors determining helix preference in Aib rich peptides.

α-Helix	3_{10}-Helix
-Longer peptides (~10 residues or longer)	-Shorter peptides (~5 residues or less)
-Less than 50% ααAA content	-Greater than 50% ααAA content
-Two monosubstituted amino acids next to each other	-No two monosubstituted amino acids next to each other
-Polar solvents, especially H_2O	-Non-polar solvents

The location of the monosubstituted amino acids in ααAA rich peptides has been suggested to be more influential on the 3_{10}-/α-helix equilibrium than the percentage of ααAAs. Peptides containing 75% Aib were examined for the effect of the location of monosubstituted residues on the helix preference.[1.45] The placement of two monosubstituted amino acids together in the peptide sequence caused α-helix

formation, while the separation of the monosubstituted residues by just one Aib or two Aibs forced the peptide into a 3_{10}-helical conformation.[1.45]

The 3_{10}-/α-helix equilibrium may be shifted to a particular helix type by the media. The polarity of organic solvents used in crystallization and NMR experiments has exhibited control in the 3_{10}-/α-helix equilibrium.[1.74-1.77] An Aib rich peptide has demonstrated formation of an α-helix in dimethyl sulfoxide (DMSO), but makes a clear transition to a 3_{10}-helix when the solvent is changed to chloroform.[1.75] Another experiment with Aib rich peptides revealed α-helix formation with water present in the solvent and 3_{10}-helix formation under anhydrous conditions.[1.76,1.77] Methanol and methanol/ethyl ether solvent systems were used in the crystallization of ααAA rich peptides which yielded an α-helix and 3_{10}-helix respectively.[1.74] The above experiments indicate that polar solvents promote the α-helix, while less polar solvents induce 3_{10}-helix formation.

Recent theoretical calculations have probed the effects of various polarity solvents on the 3_{10}-/α-helix equilibrium.[1.70,1.72] Thermodynamic data reveals that the α-helix is overall more energetically favorable while the 3_{10}-helix is entropically favored. The calculations have confirmed many of the experimental observations on the preference of the α-helix or the 3_{10}-helix. The 3_{10}-helix is calculated to be favored in shorter, Aib rich peptides, while the α-helix predominates in longer peptides. Also, the length where the two helical forms are isoenergetic is 7.5 residues, which falls within the range (~7-10 residues) which Karle and others

reported for equal preference for the α-helix or the 3_{10}-helix.[1.70,1.72] In this region, the solvent effects play a significant role in the 3_{10}-/α-helix equilibrium.

Four different mediums, vacuum, methylene chloride, acetonitrile, and water, were examined for their respective effects on the 3_{10}-/α-helix equilibrium of a poly-Aib 10-mer peptide. The 3_{10}-helix was found to have a slightly increased relative stability in lower polarity environments, but as the polarity of the media rises, the α-helix becomes increasing more stable. The trend of escalating stability of the α-helical conformation as solvent polarity is raised can be explained by peptide-solvent interactions.

The α-helix forms six intramolecular hydrogen bonds in a ten residue peptide leaving three N-terminal amide hydrogens and four C-terminal carbonyl oxygens without internal hydrogen bonding partners. Seven intramolecular hydrogen bonds are possible in a ten residue 3_{10}-helix. This hydrogen bonding pattern leaves only two N-terminal amide protons and three C-terminal carbonyls without internal hydrogen bonding partners (Figure 1.26). The additional exposed carbonyl and amide protons of the α-helix give rise to more favorable interactions with solvent, especially water, thereby increasing the stability of the α-helix.[1.70] The 3_{10}-helix gains stability in non-polar environments from the additional hydrogen bond present in the helix as compared to the α-helix.[1.70]

The conclusions drawn from theoretical calculations and experimental data agree on the solvent effects of the 3_{10}-/α-helix equilibrium. They conclude that

medium length (~7-10 residues) Aib rich peptides prefer to form a 3_{10}-helix in non-polar environments and favor an α-helix in polar media, especially water. This suggests that a 3_{10}-helix would be more likely to occur in the interior, hydrophobic region of a peptide, while the α-helix should be more prevalent in outer regions of a protein exposed to aqueous media.

1.8 Characterization of Peptides Rich in α,α-Disubstituted Amino Acids

The most definitive method of structural determination of peptides is X-ray diffraction analysis, but this method of structural analysis has its limitations.[1,2] Crystallization of peptides is a challenging task and obtaining peptide crystals of crystallographic quality is even more difficult. The actual structural analysis is time consuming and generally must be done by a protein crystallographer. X-ray analysis yields the most accurate and detailed analysis of peptide structure, but other, more accessible methods are commonly utilized.

The secondary structure of peptides can often be reliably elucidated by NMR spectroscopy. A variety of one and two dimensional NMR experiments (i.e. 1D proton, *J*-correlated spectroscopy (COSY), total correlation spectroscopy (TOCSY), and nuclear Overhauser effect spectroscopy (NOESY)) are used to determine the peptide structure.[1,2] The secondary structure is usually derived from strong, characteristic NOEs (Nuclear Overhauser Effect) in the spectrum. Helical forms of peptides, the 3_{10}-helix and the α-helix, exhibit strong, consecutive NOEs between

the amide hydrogen of the *i* residue and the amide hydrogen of the *i* + 1 residue, N,N(*i*, *i* + 1) and between the proton on the α-carbon of the *i* residue and the amide proton of the *i* + 3 residue, α,N(*i*, *i* + 3).[1.78] The 3_{10}-helix and the α-helix can be differentiated by the relative intensities of three intermediate range NOEs; α,N(*i*, *i* + 2) (strong in the 3_{10}-helix), α,N(*i*, *i* + 4) (strong in the α-helix), and α,β(*i*, *i* + 3) (strong in the α-helix).[1.78] These experiments may be used to determine the presence of a specific helix type of a peptide composed of proteinogenic amino acids, but they are not very applicable for Aib rich peptides. This arises from the lack of α-hydrogens, which are integral in the NMR experiments, in Aib and other ααAAs.

Kuki recently reported a method for the characterization of an Aib rich 3_{10}-helical peptide via NMR.[1.79] The experiment was done in DMSO, and each N,N (*i*, *i* +1) was assigned sequentially. After complete assignment of all of the amide crosspeaks, the intramolecular hydrogen bonds were counted to reveal the correct number for a 3_{10}-helix. Even though the hydrogen bond counting method was successful for the above system, it may not be applicable for all peptides and solvents. NMR spectroscopy has not found widespread applications for the characterization of Aib rich α- and 3_{10}-helices.

Circular dichroism (CD) offers a convenient and reliable method for the determination of peptide secondary structure. The major types of secondary structures exhibit distinct circular dichroism spectra making the structures easily

distinguishable.[1.1,1.2] The random coil shows a minimum near 195 nm and a maximum near 217 nm in the CD spectrum. The β-sheet spectrum is characterized by a negative band centered about 217 nm and a positive band around 195 nm. Helical peptides, the 3_{10}-helix and the α-helix, exhibit two minima near 208 nm and 222 nm and a positive band near 195 nm. The difference between the 3_{10}-helix spectrum and the α-helix spectrum is not as exaggerated, but they can be easily differentiated.[1.80] The ratio, R, of the intensity of the 222 nm band ($n \rightarrow \pi^*$) divided by the intensity of minima near 208 nm ($\pi \rightarrow \pi^*$) is used to differentiate between the 3_{10}-helix and the α-helix (Figure 1.27).

The ratio is approximately 1 for the α-helix, while the ratio is 0.4 or less for the 3_{10}-helix. Also, the positive band near 195 nm is much weaker for the 3_{10}-helix as compared to the α-helix. The overall spectrum of the 3_{10}-helix is also weaker than the α-helical spectrum. Few CD spectra of 3_{10}-helices have been reported, but the experimental spectra agree well with the theoretically calculated 3_{10}-helix CD spectrum.[1.80-1.82]

$$R = [\theta]_{n \rightarrow \pi^*} / [\theta]_{\pi \rightarrow \pi^*}$$

Figure 1.27. Equation for the determination of R values.

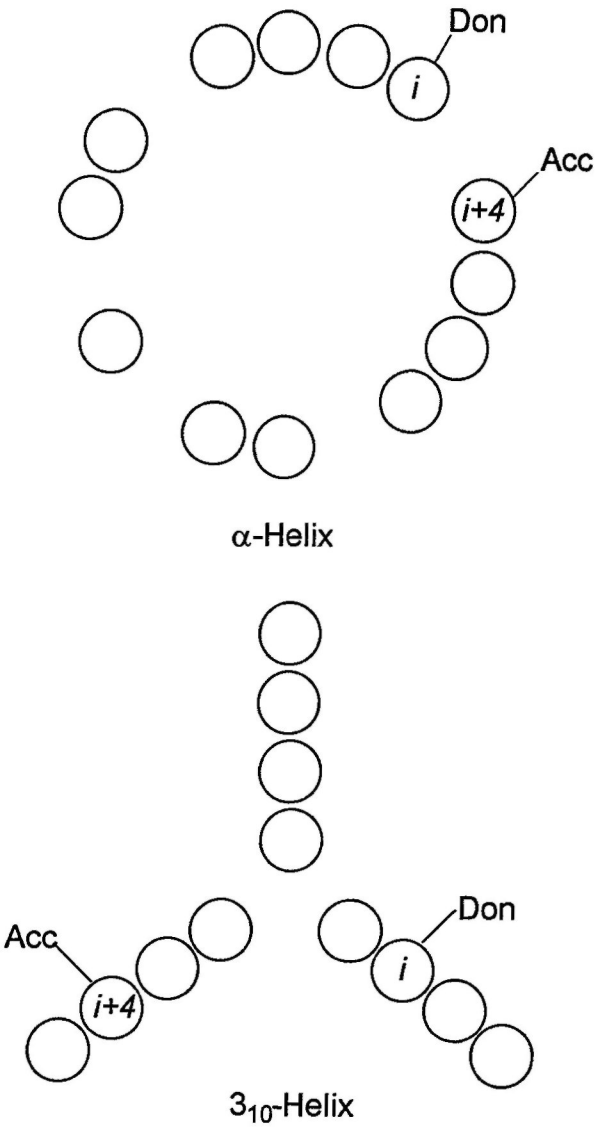

Figure 1.28. Donor/Acceptor system positioning in 3_{10}- and α-helices.

Fluorescence spectroscopy is capable of differentiating distances between defined sites on a peptide using a suitably chosen fluorescent donor/acceptor system.[1.83] The 3_{10}-/α-helix equilibrium may be probed with a fluorescence lifetime system by taking advantage of the unique distances and geometries of each type of helix. The distances between the donor and acceptor will differ depending upon the helical conformation assumed by the peptide, if the donor and acceptor system is appropriately placed (i and $i + 4$). The distance between the donor and acceptor will increase as the peptide changes from an α-helix to a 3_{10}-helix because the 3_{10}-helix is longer (1.94 Å/residue) than the α-helix (1.56 Å/residue).[1.4] The separation of the donor and acceptor will not only increase due to helix lengthening, but the donor and acceptor will move to opposite faces of the helix (Figure 1.28). With i to $i + 4$ positioning, the donor and acceptor will be "on top" of each other in the α-helix but exist on either side of the 3_{10}-helix. A recently reported system explored the 3_{10}-/α-helix equilibrium using this approach.[1.83] The study revealed distinct differences in fluorescent lifetimes while the peptide was in 3_{10}-helical and α-helical conformations. The secondary structures of the peptides were confirmed by circular dichroism.

1.9 References

1.1 Walton, A. G. *Polypeptides and Protein Structure*; Elsevier: New York, 1981.

1.2 Creighton, T. E. *Proteins: Structure and Molecular Properties*, 2nd ed.; W. H. Freeman and Co.: New York, 1993.

1.3 Moore, M. L. In *Synthetic Peptides: A User's Guide*; Grant, G. A., Ed.; W. H. Freeman and Co.: USA, 1992.

1.4 Toniolo, C.; Benedetti, E. *Trends Biochem. Sci.* **1991**, *16*, 350-353.

1.5 Smythe, M. L.; Huston, S. E.; Marshall, G. R. *J. Am. Chem. Soc.* **1995**, *117*, 5445-5452.

1.6 Pérez-Payá, E.; Houghten, R. A.; Blondelle, S. E. *J. Biol. Chem.* **1995**, *270*, 1048-1056.

1.7 Epand, R. M.; Shai, Y.; Segrest, J. P.; Anantharamaiah, G. M. *Biopolymers (Peptide Sci.)*, **1995**, *37*, 319-338.

1.8 Pathak, N.; Salas-Auvert, R.; Ruche, G.; Janna, M.; McCarthy, D.; Harrison, R. G. *Proteins: Structure, Function, and Genetics*, **1995**, *22*, 182-186.

1.9 Schiffer, M.; Edmunson, A. B. *Biophys. J.* **1967**, *7*, 121-135.

1.10 Zhong, L.; Putnam, R. J.; Johnson, W. C.; Rao, A. G. *Int. J. Pept. Protein Res.* **1995**, *45*, 337-347.

1.11 Saberwal, G.; Nagaraj, R. *Biochim. Biophys. Acta* **1994**, *1197*, 109-131.

1.12 Marion, D.; Zasloff, M.; Bax, A. *FEBS Lett.* **1988**, *227*, 21-26.

1.13 Mchaourab, H. S.; Hyde, J. S.; Feix, J. B. *Biochemistry* **1993**, *32*, 11895-11902.

1.14 Javadpour, M. M.; Juban, M. M.; Lo, W. J.; Bishop, S. M.; Alberty, J. B.; Cowell, S. M.; Becker, C. L.; McLaughlin, M. L. *J. Med. Chem.* **1996**, *39*, 3107-3113.

1.15 Dempsey, C. E. *Biochim. Biophys. Acta* **1990**, *1031*, 143-161.

1.16 Maloy, W. L.; Kari, U. P. *Biopolymers (Peptide Sci.)*, **1995**, *37*, 105-122.

1.17 Bevins, C. L.; Zasloff, M. *Ann. Rev. Biochem.* **1990**, *59*, 395-414.

1.18 Tytler, E. M.; Anantharamaiah, G. M.; Walker, D. E.; Mishra, V. K.; Palgunachari, M. N.; Segrest, J. P. *Biochemistry* **1995**, *34*, 4393-4401.

1.19 Bessalle, R.; Gorea, A.; Shalit, I.; Metzger, J. W.; Dass, C.; Desiderio, D. M.; Fridkin, M. *J. Med. Chem.* **1993**, *36*, 1203-1209.

1.20 Matsuzaki, K.; Harada, M.; Handa, T.; Munakoshi, S.; Fujii, N.; Yajima, H.; Miyajima,, K. *Biochim. Biophys. Acta* **1989**, *981*, 130-134.

1.21 Matsuzaki, K.; Sugishita, K.; Fujii, N.; Miyajima, K. *Biochemistry* **1995**, *34*, 3423-3429.

1.22 Blondelle, S. E.; Houghten, R. A. *Biochemistry* **1991**, *30*, 4671-4678.

1.23 Andreu, D.; Ubach, J.; Boman, A.; Wåhlin, B.; Wade, D.; Merrifield, R. B.; Boman, H. G. *FEBS Lett.* **1992**, *296*, 190-193.

1.24 Wade, D.; Boman, A.; Wåhlin, B.; Drain, C. M.; Andreu, D.; Boman, H. G.; Merrifield, R. B. *Proc. Natl. Acad. Sci. USA* **1990**, *87*, 4761-4765.

1.25 Bessalle, R.; Kapitkovsky, A.; Gorea, A.; Shalit, I.; Fridkin, M. *FEBS Lett.* **1990**, *274*, 151-155.

1.26 Blondelle, S. E.; Houghten, R. A. *Biochemistry* **1992**, *31*, 12688-12694.

1.27 Chou, P. Y.; Fasman, G. D. *Adv. Enzymol. Rel. Areas Mol. Biol.* **1978**, *47*, 45-148.

1.28 Scholtz, J. M.; Baldwin, R. L. *Annu. Rev. Biophys. Biomol. Struct.* **1992**, *21*, 95-118.

1.29 O'Neil, K. T.; DeGrado, W. F. *Science* **1990**, *250*, 646-651.

1.30 Nagaraj, R.; Balaram, P. *Acc. Chem. Res.* **1981**, *14*, 356-362.

1.31 Karle, I. L.; Balaram, P. *Biochemistry* **1990**, *29*, 6747-6756.

1.32 Benedetti, E. *Biopolymers (Peptide Sci.)*, **1996**, *40*, 3-44.

1.33 Balaram, P. *Curr. Opin. Struct. Biol.* **1992**, *2*, 845-851.

1.34 Toniolo, C.; Crimsa, M.; Formaggio, F.; Benedetti, E.; Santini, A.; Iacovino, R.; Diblasio, B; Pedone, C.; Kamphuis, J. *Biopolymers (Peptide Sci.)*, **1996**, *40*, 519-522.

1.35 Burgess, K.; Ho, K.; Pettitt, B. M. *J. Am. Chem. Soc.* **1995**, *117*, 54-65.

1.36 Burgess, K.; Ho, K.; Pal, B. *J. Am. Chem. Soc.* **1995**, *117*, 3808-3819.

1.37 Formaggio, F.; Toniolo, C.; Crisma, M.; Valle, G.; Kaptein, B.; Schoemaker, H. E.; Kamphuis, J.; DiBlasio, B.; Maglio, O.; Fattorusso, R.; Benedetti, E.; Santini, A. *Int. J. Pept. Protein Res.* **1995**, *45*, 70-77.

1.38 Gershonov, E.; Granoth, R.; Tzehoval, E.; Gaoni, Y.; Fridkin, M. *J. Med. Chem.* **1996**, *39*, 4833-4843.

1.39 Curry, K.; Peet, M. J.; Magnuson, D. S. K.; McLennan, H. *J. Med. Chem.* **1988**, *31*, 864-867.

1.40 Kozikowski, A. P.; Fauq, A. H. *Synlett* **1991**, 783-784.

1.41 Alonso, F.; Micó, I.; Nájera, C.; Sansano, J. M.; Yus, M. *Tetrahedron* **1995**, *51*, 10259-10280.

1.42 Wenschuh, H.; Beyermann, M.; Krause, E.; Brudel, M.; Winter, R.; Schümann, M.; Carpino, L. A.; Bienert, M. *J. Org. Chem.* **1994**, *59*, 3275-3280.

1.43 Frérot, E.; Coste, J.; Pantaloni, A.; Dufour, M.; Jouin, P. *Tetrahedron* **1991**, *47*, 259-270.

1.44 Carpino, L. A.; Chao, H. G.; Beyermann, M.; Bienert, M. *J. Org. Chem.* **1991**, *56*, 2635-2642.

1.45 Basu, G.; Bagchi, K.; Kuki, A. *Biopolymers* **1991**, *31*, 1763-1774.

1.46 Wenschuh, H.; Beyermann, M.; El-Faham, A.; Ghassemi, S.; Carpino, L. A.; Bienert, M. *J. Chem. Soc., Chem. Commun.* **1995**, 669-670.

1.47 Wenschuh, H.; Beyermann, M.; Haber, H.; Seydel, J. K.; Krause, E.; Bienert, M.; Carpino, L. A.; El-Faham, A.; Albericio, F. *J. Org. Chem.* **1995**, *60*, 405-410.

1.48 Carpino, L. A.; Sadat-Aalaee, D.; Chao, H. C.; DeSelms, R. H. *J. Am. Chem. Soc.* **1990**, *112*, 9651-9652.

1.49 Carpino, L. A.; Mansour, E. M. E.; Sadat-Aalaee, D. *J. Org. Chem.* **1991**, *56*, 2611-2614.

1.50 Carpino, L. A.; El-Faham, A. *J. Am. Chem. Soc.* **1995**, *117*, 5401-5402.

1.51 Wenschuh, H.; Beyermann, M.; Winter, R.; Bienert, M.; Ionescu, D.; Carpino, L. A. *Tetrahedron Lett.* **1996**, *37*, 5483-5486.

1.52 Carpino. L. A.; El-Faham, A.; Minor, C. A.; Albericio, F. *J. Chem. Soc., Chem. Commun.* **1994**, 201-203.

1.53 Albericio, F.; Cases, M.; Alsina, J.; Triolo, S. A.; Carpino, L. A.; Kates, S. A. *Tetrahedron Lett.* **1997**, *38*, 4853-4856.

1.54 Smith, P. A. In *Organic Reactions*, Vol. 3; Adams, R,; Bachmann, W. E.; Fieser, L. F.; Johnson, J. R.; Snyder, H. R., Eds.; John Wiley & Sons: New York, 1946; 337-448.

1.55 Wallis, E. S.; Lane, J. F. In *Organic Reactions*, Vol. 3; Adams, R,; Bachmann, W. E.; Fieser, L. F.; Johnson, J. R.; Snyder, H. R., Eds.; John Wiley & Sons: New York, 1946; 267-306.

1.56 Wolff, H. In *Organic Reactions*, Vol. 3; Adams, R,; Bachmann, W. E.; Fieser, L. F.; Johnson, J. R.; Snyder, H. R., Eds.; John Wiley & Sons: New York, 1946; 337-448.

1.57 March, J. *Advanced Organic Chemistry: Reactions, Mechanisms, and Structure*, 4th ed.; John Wiley & Sons: USA, 1992.

1.58 Duthaler, R. O. *Tetrahedron* **1994**, *50*, 1539-1650.

1.59 Bucherer, H. T.; Steiner, W. *J. Prakt. Chem.* **1934**, *140*,291-316.

1.60 Shafran, Y. M.; Bakulev, V. A.; Mokrushin, V. S. *Russ. Chem. Rev.* **1989**, *58*, 148-162.

1.61 O'Donnell, M. J.; Wu, S.; Huffman, J. C. *Tetrahedron* **1994**, *50*, 4507-4518.

1.62 Schöllkopf, U. *Pure & Appl. Chem.* **1983**, *55*, 1799-1806.

1.63 Wirth, T. *Agnew. Chem. Int. Ed. Engl.* **1997**, *36*, 225-227.

1.64 Schöllkopf, U.; Grüttner, S.; Anderskewitz, R.; Egert, E.; Dyrbush, M. *Agnew. Chem. Int. Ed. Engl.* **1987**, *26*, 683-684.

1.65 Fitzi, R.; Seebach, D. *Tetrahedron* **1988**, *44*, 5277-5292.

1.66 Schickli, C. P.; Seebach, D. *Liebigs Ann. Chem.* **1991**, 655-658.

1.67 Williams, R. M.; Im, M. *J. Am. Chem. Soc.* **1991**, *113*, 9276-9286.

1.68 Williams, R. M.; Hendrix, J. A. *J. Org. Chem.* **1990**, *55*, 3723-3728.

1.69 Williams, R. M.; Sinclair, P. J.; Zhai, D.; Chen, D. *J. Am. Chem. Soc.* **1988**, *110*, 1547-1557.

1.70 Myers, A. G.; Gleason, J. L.; Yoon, T.; Kung, D. W. *J. Am. Chem. Soc.* **1997**, *119*, 656-673.

1.71 Smythe, M. L.; Huston, S. E.; Marshall, G. R. *J. Am. Chem. Soc.* **1993**, *115*, 11594-11595.

1.72 Karle, I. L.; Flippen-Anderson, J. L.; Gurunath, R.; Balaram, P. *Protein Sci.* **1994**, *3*, 1547-1555.

1.73 Basu, G.; Kuki, A. *Biopolymers* **1992**, *32*, 61-71.

1.74 Otoda, K.; Kitagawa, Y.; Kimura, S.; Imanishi, Y. *Biopolymers* **1993**, *33*, 1337-1345.

1.75 Vijayakumar, E. K. S.; Balaram, P. *Biopolymers* **1983**, *22*, 2133-2140.

1.76 Karle, I. L.; Sukumar, M.; Balaram, P. *Proc. Natl. Acad. Sci. USA* **1986**, *83*, 9284-9288.

1.77 Karle, I. L.; Flippen-Anderson, J. L.; Sukumar, M.; Balaram, P. *Int. J. Pept. Protein Res.* **1988**, *31*, 567-576.

1.78 Millhauser, G. L.; Stenland, C. J.; Hanson, P.; Bolin, K. A.; van de Ven, F. J. M. *J. Mol. Biol.* **1997**, *267*, 963-974.

1.79 Basu, G.; Kuki, A. *Biopolymers* **1993**, *33*, 995-1000.

1.80 Toniolo, C.; Polese, A.; Formaggio, F.; Crimsa, M.; Kamphius, J. *J. Am. Chem. Soc.* **1996**, *118*, 2744-2745.

1.81 Manning, M. C.; Woody, R. W. *Biopolymers* **1991**, *31*, 569-586.

1.82 Iwata, T.; Lee, S.; Oishi, O.; Aoyagi, H.; Ohno, M.; Anzai, K.; Kirino, Y.; Sugihara, G. *J. Biol. Chem.* **1994**, *269*, 4928-4933.

1.83 Hungerford, G.; Martinez-Insua, M.; Birch, D. J. S.; Moore, B. D. *Angew. Chem. Int. Ed. Engl.* **1996**, *35*, 326-329.

Chapter 2

Antimicrobial α,α-Dialkylated Amino Acid Rich Peptides With *In-Vivo* Activity Against an Intracellular Pathogen*

2.1 Introduction

The efficacy of current antibiotics is declining at an alarming rate due to the proliferation of multi-drug resistant bacteria.[2.1-2.3] The lack of effectiveness of so many of the current antibiotics arises from most of them relying on the same mode of action. The approval of new antibiotics is slower than the rate of resistance proliferation, particularly the rate of development of new drugs with novel mechanisms of action. Antimicrobial peptides represent one example of the novel antimicrobial agents currently being developed to potentially address this need.[2.4] Basic amphipathic α-helical peptides often have broad spectrum *in vitro* antimicrobial activity at μM concentrations.[2.5] Although the details of the mechanism of action of antimicrobial peptides remains a matter of controversy, there is a consensus that these peptides selectively disrupt the cell membranes of susceptible cells.[2.6-2.8] The selectivity for disruption of bacterial over eucaryotic cells has been attributed to

*Reprinted in part with permission from *Journal of Medicinal Chemistry*, **1996**, *Volume 39*, pages 3603-3605; T. Scott Yokum, Philip H. Elzer, Mark L. McLaughlin, Antimicrobial α,α-Dialkylated Amino Acid Rich Peptides With *In-Vivo* Activity Against an Intracellular Pathogen.

exterior membrane charge differences, membrane potential differences, cholesterol content, and differences in the rate of membrane repair.[2.9-2.12] It has also become apparent that the distinction between an antimicrobial and a cytotoxic or lytic peptide depends on the eucaryotic cell line tested, for instance there are reports of antimicrobial/lytic peptides selectively destroying transformed instead of normal mammalian cells.[2.13,2.14] Herein, we report evidence that peptides in this class selectively destroy infected macrophages in hyperimmune BALB/C mice and release the intracellular pathogen, *Brucella abortus*, which is dispatched by the immune system. This *in vivo* activity may provide a unique approach to quicker, more efficient clearing of systemic intracellular pathogen infections which are particularly difficult to treat with normal antibiotics.[2.15]

Brucella are short, non-motile, non-sporulating, and non-encapsulated Gram-negative aerobic rods. Brucella are important veterinary pathogens and of the six known species four, namely *B. abortus*, *B. melitensis*, *B. suis*, and *B. canis* are pathogenic for man.[2.16,2.17] In animal infections, the organisms localize in the reproductive organs, mammary glands, supramammary lymph nodes, and other reticuloendothelial tissues and lead to abortion and infertility.[2.18] The zoonotic bacterial disease, brucellosis, has a significant impact on human health worldwide. The infection results in a chronic, debilitating disease known as undulant fever in humans.[2.19] Humans are exposed through direct contact with infected animals or infected animal products.[2.20] In the United States, human brucellosis is an

occupational hazard for veterinarians, abattoir workers, animal handlers, and laboratory workers. Due to the highly infectious nature of the brucella species via aerosolization, several members of the genus are candidates for biological weapons, placing military personnel at risk for infections.[2.21]

Human brucellosis is characterized by malaise, fever, anorexia, muscular weakness, arthritis, and dementia.[2.19] Cardiac and neurologic disorders may occur and, if untreated, may result in a mortality rate as high as 10%. Lengthy antibiotic therapy with one or multiple drugs for up to 30-45 days is required for the treatment of brucellosis, but relapses of infection often occur after treatment is discontinued. Unfortunately, antibiotic therapy does not relieve the symptoms of malaise, depression, and sometimes severe dementia associated with the disease. Currently, there are no vaccines available for humans, since the live vaccines used in the control of animal brucellosis, are virulent for man.

Brucella species survive and replicate in host macrophages.[2.22-2.24] Their ability to survive in a host's macrophages is thought to play a central role in enabling these organisms to produce disease.[2.25] Intracellular brucellae are sequestered from the innate and specific immune responses of the host and are not directly exposed to the complement cascade, neutrophils, or brucella specific antibodies.[2.26] There is clearly a need for the development of more effective treatments for human brucellosis. We present results that short, amphipathic, helical peptides may become the basis of an effective treatment for brucellosis. There are other diseases caused by intracellular

pathogens with an etiology similar to brucellosis, such as tuberculosis (Tb), which infects about a third of the world's population and kills more people than any other single infectious agent.[2.27]

2.2 Results

The antimicrobial peptides listed in Table 2.1 are *de novo* amphipathic peptides composed of 50-80% α,α-disubstituted amino acids (ααAAs) and a proteinogenic derivative (**2.1-2.12**). The design of these peptides is loosely based on the natural antimicrobial peptides, peptaibols.[2.28-2.30] Peptaibols have several α-aminoisobutyric acid (Aib) residues, are acetylated on the N-terminus, and have an amino alcohol at the C-terminus.[2.29] *De novo* peptides that include only a putative amphipathic helix have activity comparable to or greater than native antimicrobial peptides.[2.31,2.32] Amphipathic peptides with $\geq$ 18 residues can have very high cytotoxicity, but simply shortening the peptides to 14 residues reduces cytotoxicity and retains much of the antimicrobial activity.[2.33,2.34] Peptides **2.2-2.12** were synthesized to test the hypothesis that the Aib or Aib-like residues would stabilize helical conformations and retain biological activity as the peptides were further shortened.[2.35-2.37] Combinations of lysine with Aib or 1-amino-1-cyclohexanecarboxylic acid, Ch, and combinations of lysine with Aib and the novel amino acid, 4-aminopiperidine-4-carboxylic acid,[2.38] Api, were incorporated into peptides **2.2-2.12** (Figure 2.1). The protected form of Api, suitable for incorporation

via solid-phase peptide synthesis, was synthesized in five steps from commercially available 4-piperidinone monohydrate.

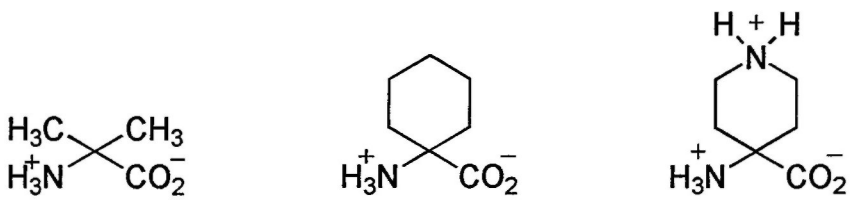

Figure 2.1. Structures of Aib, Ch, and Api amino acids.

The ααAA rich peptides **2.2-2.10** were synthesized using acid fluoride activation developed by Carpino and co-workers.[2.38-2.40] The peptides were assembled using a Milligen 9050 peptide synthesizer on a PAL-PEG-PS solid support. The couplings were done in *N,N*-dimethylformamide (DMF) using an 8-fold excess of preformed 9-fluorenymethyloxycarbonyl (Fmoc)-amino acid fluorides, 3 equivalents of diisopropylethylamine (DIEA), and a 1.5 hour recycling time. Fmoc removal was accomplished by treatment with a solution of 2% 1,8-diazobicyclo[4.5.0]undec-7-ene

(DBU), 20% piperidine in DMF. Side-chain deprotection and resin cleavage was done by treatment with trifluoroacetic acid (TFA) : triisopropylsilane : water : phenol (8.8:0.2:0.5:0.5) (reagent B) for 2 hours.[2.41] The peptides were purified by preparative reverse-phase HPLC on a C_4 column using a gradient of water and acetonitrile with 0.05% TFA in each. Molecular weight and amino acid composition were verified by MALDI mass spectrometry and amino acid analysis, respectively. Peptides **2.11** and **2.12** were prepared by manually coupling the first three residues on PAL-PEG-PS resin using eight equivalents of the amino acid fluoride and 2 equivalents of DIEA in refluxing methylene chloride.[2.38] The progress of the reaction was followed by periodic work-up of small aliquots of resin to determine the level of Fmoc release relative to the expected Fmoc release values.[2.42] After the first three steps were completed manually, the remainder of the peptides were machine synthesized in DMF, purified, and characterized as above for peptides **2.2-2.10**. The temperature increase not the solvent change is the significant factor, as the use of methylene chloride at room temperature failed to give acceptable yields.

Peptide **2.1** was synthesized via standard Fmoc solid phase synthesis conditions on a Milligen 9050 peptide synthesizer. Deprotection, purification, and characterization was done as above for peptides **2.2-2.12**.

The antimicrobial peptides in Table 2.2 are a collection of natural peptides (**2.13-2.15**), simplified analogs of natural peptides (**2.16-2.18**), *de novo* amphipathic peptides (**2.19-2.24**). Melittin was purchased as the naturally occurring C-terminus

carboxylate. Cecropin B, magainin 2, the simplified natural peptides analogs, and the *de novo* amphipathic peptides were prepared as previously reported as the C-terminus amides.[2.34]

Table 2.1

Sequences of peptides **2.1-2.12**.

Peptide	Sequence
2.1 Al-14	Lys-Ala-Ala-Lys-Lys-Ala-Ala-Lys-Ala-Ala-Lys-Lys-Ala-Ala-NH_2
2.2 Ai-14	Lys-Aib-Aib-Lys-Lys-Aib-Aib-Lys-Aib-Aib-Lys-Lys-Aib-Aib-NH_2
2.3 Ai-11	Lys-Lys-Aib-Aib-Lys-Aib-Aib-Lys-Lys-Aib-Aib-NH_2
2.4 Ai-11-ac	Ac-Lys-Lys-Aib-Aib-Lys-Aib-Aib-Lys-Lys-Aib-Aib-NH_2
2.5 Ch-14	Lys-Ch-Ch-Lys-Lys-Ch-Ch-Lys-Ch-Ch-Lys-Lys-Ch-Ch-NH_2
2.6 Ch-11	Lys-Lys-Ch-Ch-Lys-Ch-Ch-Lys-Lys-Ch-Ch-NH_2
2.7 Ch-13	Lys-Ch-Ch-Lys-Lys-Ch-Ch-Lys-Ch-Ch-Lys-Lys-Ch-----NH_2
2.8 Ch-10	Lys-Lys-Ch-Ch-Lys-Ch-Ch-Lys-Lys-Ch-----NH_2
2.9 Pi-10	Aib-Aib-Api-Lys-Aib-Aib-Api-Lys-Aib-Aib-NH_2
2.10 Pi-10-ac	Ac-Aib-Aib-Api-Lys-Aib-Aib-Api-Lys-Aib-Aib-NH_2
2.11 Ipi-10	Api-Aib-Aib-Lys-Aib-Aib-Lys-Aib-Aib-Api-NH_2
2.12 Ipi-10-ac	Ac-Api-Aib-Aib-Lys-Aib-Aib-Lys-Aib-Aib-Api-NH_2

Table 2.2

Sequences of peptides **2.13-2.24**.

Peptide	Sequence
2.13 Melittin	Gly-Ile-Gly-Ala-Val-Leu-Lys-Val-Leu-Thr-Thr-Gly-Leu-Pro-Ala-Leu-Ile-Ser-Trp-Ile-Lys-Arg-Lys-Arg-Gln-Gln-NH_2
2.14 Cecropin B amide	Lys-Trp-Lys-Val-Phe-Lys-Lys-Ile-Glu-Lys-Met-Gly-Arg-Asn-Ile-Arg-Asn-Gly-IleVal-Lys-Ala-Gly-Pro-Ala-Ile-Ala-Val-Leu-Gly-Glu-Ala-Lys-Ala-Leu-NH_2
2.15 Magainin 2 amide	Gly-Ile-Gly-Lys-Phe-Leu-His-Ser-Ala-Lys-Lys-Phe-Gly-Lys-Ala-Phe-Val-Gly-Glu-Ile-Met-Asn-Ser-NH_2
2.16 Melittin analog	Phe-Ala-Leu-Ala-Leu-Lys-Ala-Leu-Lys-Lys-Ala-Leu-Lys-Lys-Leu-Lys-Lys-Ala-Leu-Lys-Lys-Ala-Leu-NH_2
2.17 D-Melittin analog	D-(Phe-Ala-Leu-Ala-Leu-Lys-Ala-Leu-Lys-Lys-Ala-Leu-Lys-Lys-Leu-Lys-Lys-Ala-Leu-Lys-Lys-Ala-Leu)-NH_2
2.18 Cecropin analog	Arg-Trp-Arg-Leu-Phe-Arg-Arg-Ile-Asp-Arg-Val-Gly-Lys-Gln-Ile-Lys-Gln-Gly-Ile-Leu-Arg-Ala-Gly-Phe-Ala-Ile-Ala-Leu-Val-Gly-Asp-Ala-Arg-Ala-Val-NH_2
2.19 Kfa-21	$(Lys\text{-}Phe\text{-}Ala\text{-}Lys\text{-}Phe\text{-}Ala\text{-}Lys)_3\text{-}NH_2$
2.20 Kla-21	$(Lys\text{-}Leu\text{-}Ala\text{-}Lys\text{-}Leu\text{-}Ala\text{-}Lys)_3\text{-}NH_2$
2.21 Kkl-21	$(Lys\text{-}Leu\text{-}Ala\text{-}Lys\text{-}Lys\text{-}Leu\text{-}Ala)_3\text{-}NH_2$
2.22 Kal-21	$(Lys\text{-}Ala\text{-}Leu\text{-}Lys\text{-}Ala\text{-}Leu\text{-}Lys)_3\text{-}NH_2$
2.23 Klg-21	$(Lys\text{-}Leu\text{-}Gly\text{-}Lys\text{-}Lys\text{-}Leu\text{-}Gly)_3\text{-}NH_2$
2.24 Kaa-21	$(Lys\text{-}Ala\text{-}Ala\text{-}Lys\text{-}Lys\text{-}Ala\text{-}Ala)_3\text{-}NH_2$

Table 2.3

Peptide antibacterial activity and percent helicity.

Peptide	MIC (μM) vs. *E. coli*	MIC (μM) vs. *S. aureus*	% Helicity
2.1 Al-14	>178	>178	ND[a]
2.2 Ai-14	5.5	11	58[b]
2.3 Ai-11	55	>220	40[b]
2.4 Ai-11-ac	6.6	212	ND[c]
2.6 Ch-11	5.2	2.6	ND[c]
2.7 Ch-13	4.5	2.2	80[b]
2.8 Ch-10	5.7	2.8	46[b]
2.9 Pi-10	7.7	123	38[b]
2.10 Pi-10-ac	7.4	>230	45[b]
2.11 Ipi-10	3.8	>240	25[d]
2.12 Ipi-10-ac	7.4	>230	34[d]

[a] This peptide precipitates when the 25 mM SDS is added, precluding CD spectroscopic measurement.

[b] % α-helicity

[c] Insufficient quantities of these peptides were made for CD spectroscopic measurements.

[d] % 3_{10}-helicity

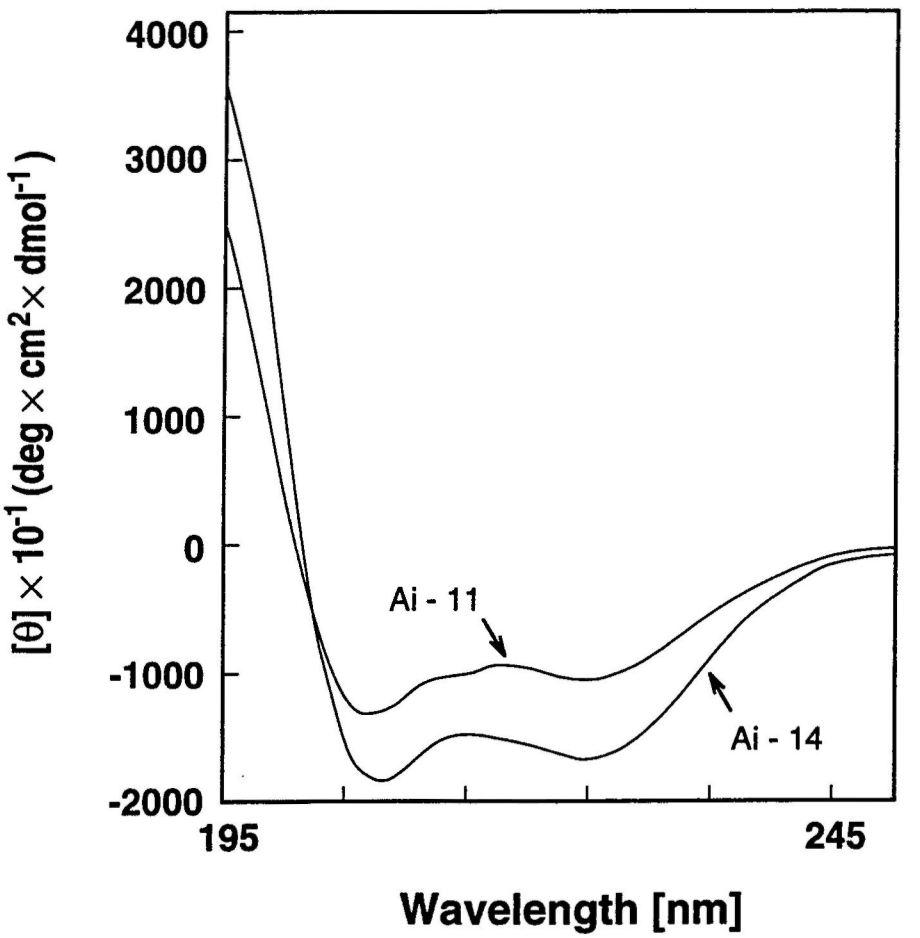

Figure 2.2. CD spectra of Ai-11 and Ai-14 in SDS.

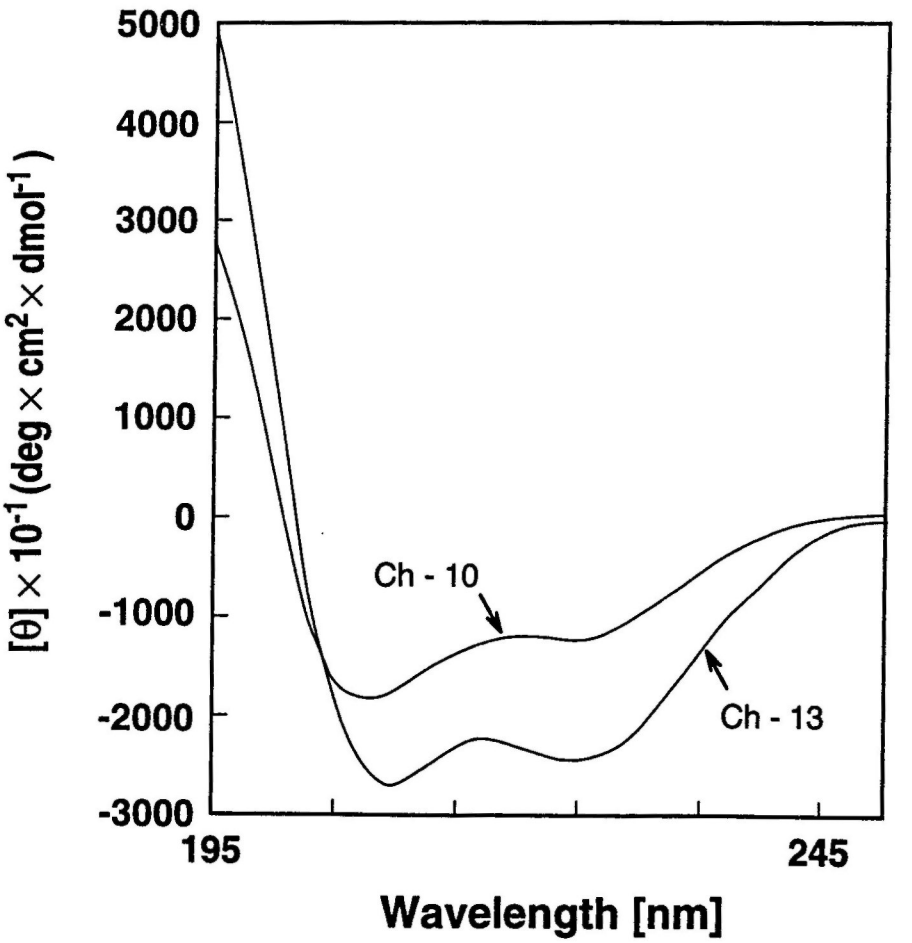

Figure 2.3. CD spectra of Ch-10 and Ch-13 in SDS.

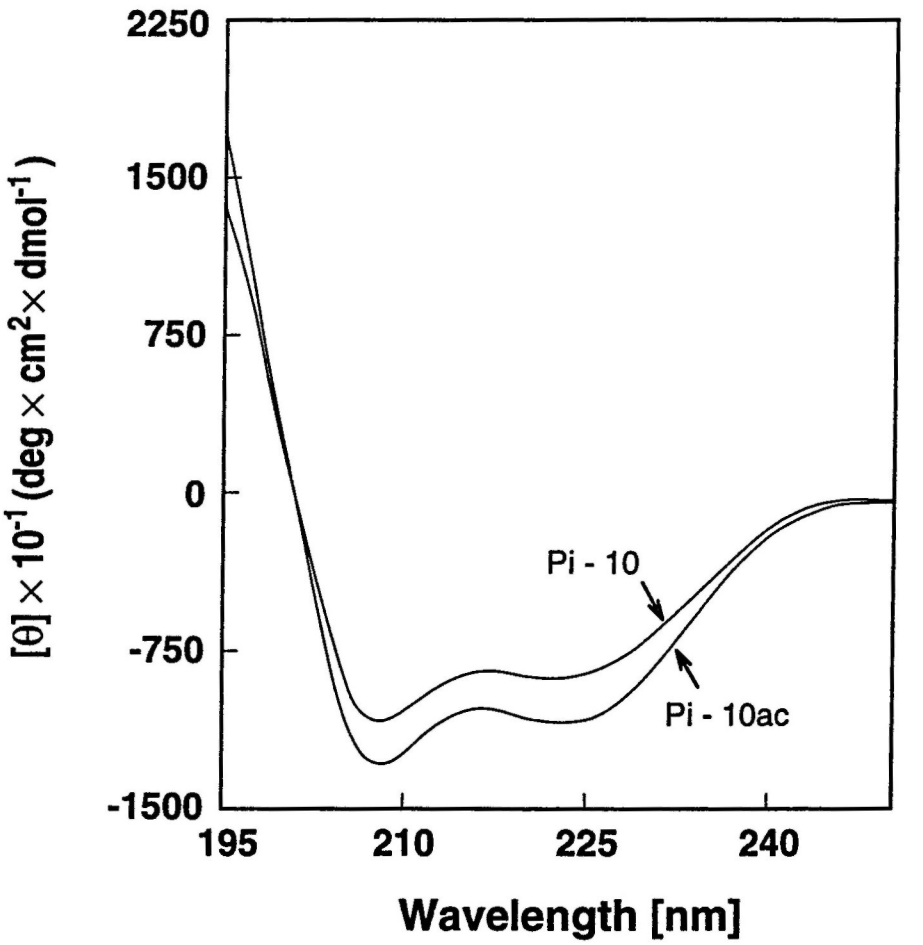

Figure 2.4. CD spectra of Pi-10 and Pi-10-ac in SDS.

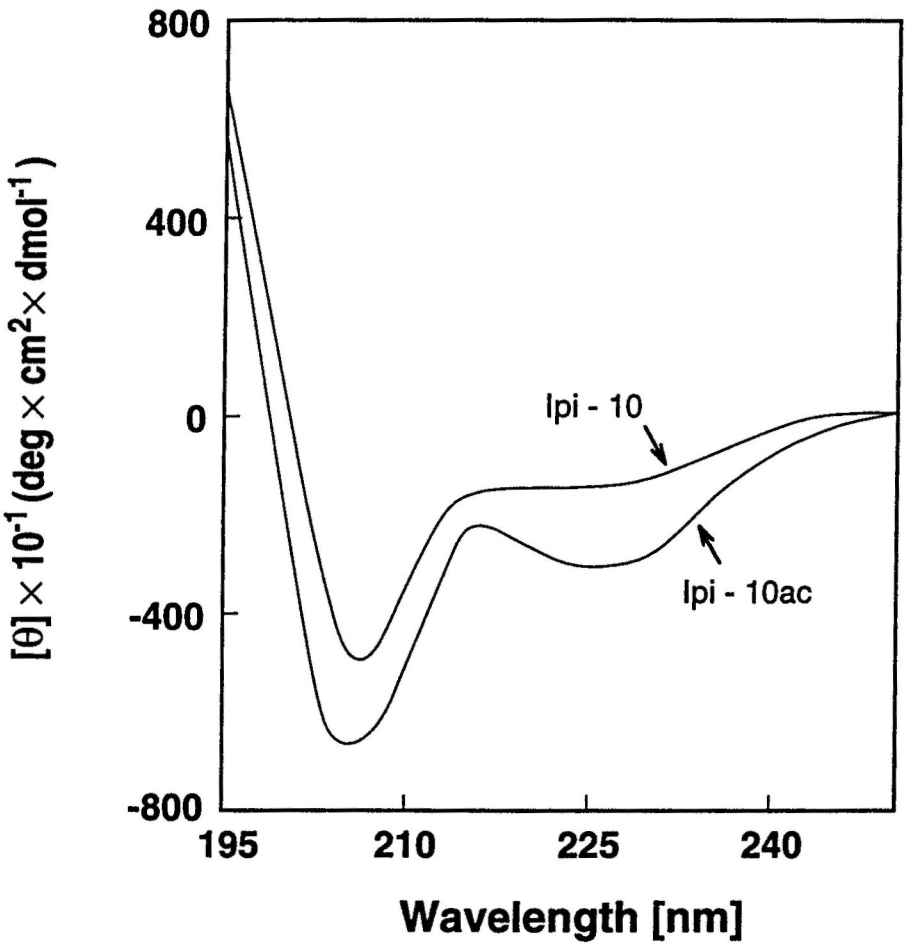

Figure 2.5. CD spectra of Ipi-10 and Ipi-10-ac in SDS.

The helicity of the ααAA rich peptides was determined via circular dichroism (CD) spectroscopy (Table 2.3 and Figures 2.2-2.5). The CD spectra were taken at 25° C in 25 mM sodium dodecyl sulfate (SDS) with peptide concentrations ranging from 100 μM to 200 μM. Peptides **2.2, 2.3, 2.7-2.10** displayed a significant degree of helicity (38-81%). The percent helicity was calculated using the formulas: % α-Helicity = $-100([\theta]_{222} + 3000)/33000$ and $[\theta]_{222} = [\theta]_{obs}(MRW/10lc)$ where MRW is the molecular weight of the peptide over the number of backbone amide bonds, l is the pathlength (cm), and c is the peptide concentration (mg/mL).[2.34] Peptides **2.11** and **2.12** displayed a CD spectra indicative of a 3_{10}-helical conformation (25% and 34% 3_{10}-helical, respectively). The percent helicity of the 3_{10}-helical peptides was estimated using the formula: % 3_{10}-helix = $(100)[[\theta]_{207} / -21{,}500]$.[2.43]

The direct antimicrobial activities of the peptide **2.1-2.12** were tested against representative Gram-positive (*S. aureus*) and Gram-negative (*E. coli*) bacteria (Table 2.3). The Aib containing peptides inhibit *E. coli* at significantly lower concentrations than *S. aureus* with ranges of 5.5 - 55 μM and 11 - >220 μM, respectively. The Ch containing peptides **2.7** and **2.8** inhibit *S. aureus* at lower concentrations than *E. coli* with ranges of 2.2 - 2.8 μM and 4.5 - 5.7 μM, respectively. The *in vitro* MIC activity of peptides **2.11** and **2.12** is 3.8 and 7.4 μM against *E. coli*. These peptides are inactive against *S. aureus*. The direct antimicrobial activity of peptides **2.13-2.24** against *E. coli* and *S. aureus* has been reported with MIC activity ranging from 1 - 19 μM.[2.34] However, none of the peptides have direct antimicrobial activity against

Brucella abortus at peptide concentrations as high as 100 μM.[2.44,2.45] In spite of the resistance of *Brucella abortus* to direct peptide killing *in vitro,* several of these peptides significantly reduce *Brucella abortus* levels in chronically infected mice compared to saline-treated infected mice (Tables 2.4 and 2.5).

The chronically infected mice were susceptible to peptide toxicity at much lower peptide doses than control animals. The highest non-lethal dose for infected mice was only 25 μg for melittin, whereas 500 μg doses were non-lethal for all of the Aib containing peptides and some of the peptides composed solely of proteinogenic amino acids. The toxicity observations were classified into three categories: none, stress, and toxic. None meant the peptide failed to show a difference relative to peptide-treated non-infected and saline-treated infected mice. Stress meant that the mice showed signs of distress; i.e. tremors, temporary paralysis, etc. Toxic meant that some of the mice in that treatment group died at the lowest dose that still reduced spleenic brucella levels. When the peptide dose was being titrated to the lowest effective dose, several of the infected mice died at peptide doses that were harmless to normal non infected mice. These mice died within 1-2 minutes of injection from massive internal bleeding. However, in many cases, the peptide dose could be titrated down to doses that showed significant reductions of spleen colonization and that had no obvious stress on the infected mice group.

Table 2.4

Indirect *in vivo* peptide activity against *Brucella abortus* in BALB/c mice of peptides **2.1-2.12**.

Peptide	Dose (μg)	% Brucella Reduction	Toxicity[b]	Stability[c]
2.1 Al-14	1000	0[a]	stress	ND
2.2 Ai-14	500	80	none	complete
2.3 Ai-11	500	63	none	complete
2.4 Ai-11-ac	500	30	none	complete
2.7 Ch-13	100	33[a]	none	complete
2.8 Ch-10	100	0[a]	toxic	complete
2.9 Pi-10	500	90	none	complete
2.10 Pi-10-ac	500	0[a]	toxic	ND
2.11 Ipi-10	500	55[a]	stress	ND
2.12 Ipi-10-ac	500	0[a]	stress	ND

[a] these are not significant, see the experimental section.

[b] classifications defined in the results section are based upon observations on the mice following peptide treatment.

[c] classifications defined in the results section.

Table 2.5

Indirect *in vivo* peptide activity against *Brucella abortus* in BALB/c mice of peptides **2.13-2.24**.

Peptide	Dose (μg)	% Brucella Reduction	Toxicity[b]	Stability[d]
2.13 Melittin	25	50	none	partial
2.14 Cecropin B amide	500	53[a]	none	none
2.15 Magainin 2 amide	500	54[a]	none	none
2.16 Melittin analog	500	90	toxic	none
2.17 D-Melittin analog	500	65	stress	partial
2.18 Cecropin analog	1000	44[a]	stress	none
2.19 Kfa-21	100	91	none[c]	none
2.20 Kla-21	100	51	none[c]	none
2.21 Kkl-21	100	0[a]	none[c]	none
2.22 Kal-21	100	63[a]	none[c]	ND
2.23 Klg-21	500	18[a]	stress	none
2.24 Kaa-21	1000	0[a]	stress	ND

[a] these are not significant, see the experimental section.

[b] classifications defined in the results section are based upon observations on the mice following peptide treatment.

[c] lethal at 500 μg.

[d] classifications defined in the results section.

The peptides containing high percentages of ααAAs are expected to be resistant to enzymatic hydrolysis, while the peptides containing all natural amino acids are expected to undergo rapid proteolysis *in vivo*. To gauge the relative lability, these peptides were treated *in vitro* with trypsin. All of the peptides contain lysine or arginine residues, so they can be expected to be susceptible to trypsin cleavage. The peptides were incubated with 100 μg/mL of trypsin for 20 minutes and assayed for remaining MIC activity against *E. coli* as previously reported.[2.46] Table 2.4 shows that all peptides containing 50-80% ααAAs were resistant to proteolysis and retained their original MIC activity. Only melittin retained any activity of the peptides composed of all natural amino acids, but surprisingly, the D-melittin analog retained only partial activity (Table 2.5).

Table 2.6 shows normal murine macrophage survival versus peptide concentration for the peptides from Tables 2.4 and 2.5 that show significant *in vivo* brucella reductions. Normal untreated murine macrophages have a survival rate of 90%, thus melittin and peptides **2.19** and **2.20** show very slight toxicity, which is not statistically significant at 0.1 μM. The melittin analogs show significant toxicity at 0.1 μM, the lowest peptide concentration tested. The Aib rich peptides showed no significant toxicity at 10 μM, but all showed significant toxicity at 50 μM. The highest dose that showed ≥70% macrophage survival was used as the starting dosage to determine if infected macrophages are selectively destroyed relative to non infected macrophages in Table 2.7.

Table 2.6

Normal macrophage survival versus peptide concentration.

Peptide	50 μM	10 μM	1 μM	0.1 μM
2.2 Ai-14	57	87	88	91
2.3 Ai-11	57	81	89	88
2.4 Ai-11-ac	59	86	82	92
2.9 Pi-10	68	90	89	95
2.13 Melittin	ND	<2	ND	85
2.16 Melittin analog	ND	38	ND	72
2.17 D-Melittin analog	ND	<2	ND	73
2.19 Kfa-21	ND	26	ND	87
2.20 Kla-21	ND	42	ND	90

Murine macrophages were incubated with *B. abortus* according to previously reported conditions shown to infect 40% of the macrophages.[2.23] The survival rate (90%) of this partially infected macrophage population was the same as the normal non infected macrophage survival rate over a 48 hour period. The peptides **2.16**, **2.17**, and **2.20** appear to be equally toxic toward normal and partially infected macrophages. Melittin and peptide **2.19** show slightly decreased survival among infected macrophages and the Aib containing peptides all show significantly lower

survival of the infected macrophages. Peptides **2.2** and **2.9** show an approximately 40% lower macrophage survival rate of the partially infected macrophage population. These values correlate with the maximum expected since about 40% of the macrophages are infected. Peptides **2.4** and **2.3** are killing less and more than the expected ideal value of 40%, respectively.

Table 2.7

In vitro peptide toxicity against normal and infected murine macrophages.

Peptide	Conc. (μM)	% Survival Normal Mϕ	% Survival Infected Mϕ	Significance[a]
2.2 Ai-14	10	87	54	S
2.3 Ai-11	10	81	38	S
2.4 Ai-11-ac	10	86	63	S
2.9 Pi-10	10	90	55	S
2.13 Melittin	0.1	85	78	S
2.16 Melittin analog	0.1	72	71	NS
2.17 D-Melittin analog	0.1	73	75	NS
2.19 Kfa-21	0.1	87	76	S
2.20 Kla-21	0.1	90	88	NS

[a] S, statistically significant; NS, not statistically significant

2.3 Discussion

It is well established that basic amphipathic α-helical peptides often have broad spectrum *in vitro* antimicrobial activity at μM concentrations and that more hydrophobic peptides in this class can have significant mammalian cell toxicity. Melittin is the best studied of this class of peptides which has an amphipathic domain with a relatively narrow polar face which presumably causes its high cytotoxicity.[2.5] *De novo* peptides containing only leucine and lysine residues in an approximate 2:1 ratio and having putative amphipathic α-helical sequences are the most cytotoxic peptides known in this class.[2.47] A definite length dependence on cytotoxicity was noted with these peptides showing that peptide shortening reduced cytotoxicity. We showed in a series of modestly hydrophobic *de novo* basic amphipathic peptides that cytotoxicity was nearly eliminated when peptides were shortened from 21 residues to 14 residues, whereas direct *in vitro* antimicrobial activity was mostly retained in 14-mers.[2.34] A subset of the 21-mers reported previously are shown as peptides **2.19-2.24** in Table 2.2. The helicity of these peptides in SDS micelles correlates with peptide cytotoxicity.[2.34]

The incorporation of ααAAs into short peptides can promote helicity, so peptides even shorter than 14-mers should retain activity if the peptides contained several ααAAs.[2.48-2.51] However, the incorporation of multiple ααAAs has proven to be difficult using traditional peptide coupling reagents.[2.51] The use of Aib and Aib-like residues has been limited in the past due to the difficulty of coupling or harsh

conditions used for their incorporation. Carpino's development of acid fluorides for amino acid couplings presented the first method for the mild and efficient solid-phase synthesis of Aib or Aib-like rich peptides.[2.38] *In situ* coupling reagents have since been developed for the incorporation of hindered residues, but in our hands, the acid fluoride couplings have proven to be the most effective.[2.51]

The only major synthetic difficulty encountered came in the coupling of the second residue in the Ch-11, Ch-14, and Ipi-10 peptides, which resulted in the deletion of the residue. The failure arises from the coupling of a cyclic ααAA in position 2 (in respect to the C-terminus) to an ααAA, cyclic or acyclic, in the first position (attached to the solid support). The deletion sequence is not encountered when coupling 2 acyclic ααAAs in position 1 and 2 or when coupling a cyclic ααAA and a proteinogenic amino acid in either position. The poor coupling yield of the second residue was overcome by refluxing the Fmoc-amino acid fluoride in methylene chloride with DIEA for 24 hours. The progress of the reaction was followed by quantitative Fmoc tests. The first 3 residues of Ipi-10 were coupled manually as above and the resin placed onto the instrument and the final 7 residues incorporated without difficulty. Ch-11 and Ch-14 were not resynthesized via the above method because the peptides obtained (Ch-10, Ch-13) from the residue deletion were amphipathic and showed good *in-vitro* antibacterial activity, but were lethal in *in-vivo* studies and it was postulated that the full length peptides would have been even more toxic.

To maximize the number of α,α-dialkylated amino acids and retain a high level of positive charge on the polar face of these peptides, the lysine-like α,α-dialkylated amino acid Api is introduced.[2.38] This residue with the γ-amine protected as the Boc-derivative allows the synthesis of an amphipathic peptide containing no natural amino acids. We have not yet attempted to synthesize a peptide devoid of natural amino acids because of the perceived problems in the synthesis and characterization. A peptide with only achiral α,α-dialkylated amino acids would show no CD spectra because there would be no preference for a left- or right-handed helix.

The peptides **2.2-2.12**, some as short as 10-mers, composed of 50-80% ααAAs show modest to substantial helicity in SDS micelles and good direct *in vitro* antimicrobial activity (Table 2.3). The replacement of Ala residues in peptide **2.1** with Aib residues in peptide **2.2** has a substantial effect on the biological activity. MIC assays were done with *E. coli* and *S. aureus*. Peptide **2.2** is at least 8-16 times more active than peptide **2.1**. Peptide **2.1** precipitates out of 25 mM SDS micelles so a comparison of secondary structure is precluded. Shortening peptide **2.2** to make peptide **2.3** showed diminished, but substantial activity against *E. coli*, and no activity against *S. aureus*. While Aib helps to promote helical conformations, it is not a very hydrophobic residue. The Ch residue was introduced to determine whether greater hydrophobic character would increase the activity of peptides with otherwise similar designs. Unfortunately, sufficient amounts of the analogous peptide sequence were not produced due to coupling problems with the second Ch residue from the

C-terminus. Peptide **2.7** had essentially the same activity as its closest Aib peptide counterpart, **2.2**, but peptide **2.8** with only 10 residues had increased activity over **2.7** and much higher activity than its closest Aib peptide counterpart, **2.3**. Peptide **2.9** with only 10 residues and only two natural amino acids also showed good antibacterial activity against *E. coli* and moderate activity against *S. aureus*.

The helicity of the Ai series of peptides was higher than what would be expected by peptides composed of solely proteinogenic amino acids, but were less helical than their Ch series counterparts. The increased helicity of the Ch containing peptides may be explained by the increased hydrophobic interactions of the Ch residues. Peptides **2.9** and **2.11** are sequence permutation isomers which are amphipathic as α-helical and 3_{10}-helical conformations, respectively.[2.43] While peptides **2.2-2.10** show CD spectra typical of α-helices, peptides **2.11** and **2.12** show CD spectra typical of 3_{10}-helices.[2.43] Iwata and co-workers designed putative 3_{10}-helical amphipathic peptides based on a repetitive triad sequence composed of all natural amino acids, i.e. H-(Leu-Arg-Leu)$_8$-OH.[2.52] These peptides showed a CD spectra expected for 3_{10}-helical peptides in model membrane media.[2.53] The peptides showed proton transfer activity across model membranes, but no antimicrobial activity.[2.52] So, we were pleasantly surprised by the excellent *in vitro* MIC activity that peptides **2.11** and **2.12** showed against *E. coli*. The most obvious structural differences causing Iwata's 3_{10}-helical peptides to be inactive and our 3_{10}-helical peptides to be active are peptide length and hydrophobicity. Iwata's peptides are

24-residues long and the hydrophobic face is composed of natural nonpolar residues which are much more hydrophobic than the Aib residues in peptide **2.11**. The excessive peptide length and high hydrophobicity of Iwata's peptides may stabilize biologically inactive peptide-membrane complexes.

We expected differences in the structure-activity relationships (SAR) for *in vivo* studies compared to previous *in vitro* antimicrobial and cytotoxicity measurements because peptide bioavailability and stability are potentially of paramount importance in determining *in vivo* bioactivity. Previous *in vitro* studies of melittin showed it to be one of the most cytotoxic natural peptides known and at 25 μg per mouse it is the most active peptide we found *in vivo*. The peptides are administered via injection into the lateral tail vein and circulation to the primary site of infection in the spleen is expected to be rapid. In spite of this, we initially thought that melittin would indiscriminately attack other cells in the blood before reaching the spleen, but none of the peptides, including melittin, showed any outward signs of toxicity in normal non-infected mice at concentrations 2-5 times higher than the dosages shown in Tables 2.4 and 2.5 for the infected mice. On the other hand, infected mice died within 1-2 minutes of injection at peptide dosages that were non lethal to normal non-infected mice. Necropsy of the peptide-overdosed, infected mice revealed massive internal bleeding with the lungs filled with blood. These observations are consistent with sepsis that could be brought on by the lysis of too many macrophages simultaneously releasing toxic concentrations of nitric oxide and

cytokines. In many cases, peptide concentration could be titrated down to dosages that showed no outward signs of peptide toxicity.

The rapid killing of infected mice at overdose peptide concentrations suggests the peptides attack target mammalian cells quickly. We believe the rapidity of this *in vivo* effect explains why peptides that should undergo very rapid nonspecific enzyme degradation show *in vivo* bioactivity. The peptides were treated *in vitro* with trypsin to estimate the relative degradation rates of these peptides *in vivo* and to determine if this factor of bioavailability correlated with bioactivity. The peptides composed of natural amino acids retained none of their original *in vitro E. coli* activity except melittin. We think melittin retained some of its original *in vitro* antimicrobial activity because it starts out so active. It is known that peptides in this class have the same bioactivity whether composed of all L- or all D-amino acids and the D-melittin analog, peptide **2.17**, has greater proteolytic stability than its L-isomer, peptide **2.16**.[2.46] In addition, all the peptides composed of 50-80% ααAAs were completely resistant to trypsin proteolysis.

The peptides showing significant brucellae reduction were tested *in vitro* against normal and infected murine macrophages. Macrophages were harvested from the spleens of normal mice and plated out in 96 well plates. Trypan blue exclusion was used as an indicator of macrophage viability. About 90% of the plated-out macrophages survived the stress of this manipulation, so only survival percentages <90% indicate peptide toxicity. These experiments were done to outline the peptide

concentrations to be used against the infected macrophages. The Aib containing peptides, **2.2**, **2.3**, **2.4**, and **2.9**, were tested at 0.1 - 50 μM and the maximum nontoxic to very slightly toxic dose was 10 μM. The longer and more hydrophobic peptides, **2.13**, **2.16**, **2.17**, **2.19**, and **2.20**, appear to be nontoxic or slightly toxic at 0.1 μM. The macrophages plated out as above were infected with *B. abortus* for 1 hr. The excess brucellae were washed away leaving behind intracellular brucellae. If each macrophage phagocytosizes just one brucellae, the brucellae counts indicate that 40% of the macrophages are infected. The nonviable macrophages cannot undergo phagocytosis and thus cannot contribute to any of intracellular brucellae counts. This percentage of experimental brucellae infection in murine macrophages is consist with literature values.[2.20] Trypan blue exclusion showed that this partially infected macrophage population had the same viability pre- and 1 to 48 hrs post-infection. Peptide effects on macrophage survival at the doses determined above were again assayed by trypan blue exclusion. Table 2.7 shows that melittin and peptide **2.19** have slightly greater infected macrophage killing. Peptides **2.16**, **2.17**, and **2.20** were nonselective at 0.1 μM peptide concentrations, showing no greater killing of infected macrophages over non-infected macrophages. Peptides **2.2**, **2.3**, **2.4**, and **2.9** kill infected macrophages significantly better than non-infected macrophages. The maximum percentage of macrophage killing for a peptide that selectively kills only infected macrophages should be about 55% survival. Peptides **2.2** and **2.9** correlate with this model perfectly. Peptide **2.4** may simply be less selective than peptides **2.2**

and **2.9** or the optimum peptide dosage may be slightly above or below 10 μM. The greater than 40% killing found for peptide **2.3** is not consistent with this simple model for selective killing of infected macrophages.

These peptides are unlikely to directly kill *B. abortus* at the concentrations ultimately obtained in the murine macrophages. *B. abortus* is relatively resistant to these antimicrobial peptides *in vitro*.[2.44,2.45] On average, these mice weigh 22 g, contain 3 mL of blood plasma, and 20 mL of total fluid. These peptides have molecular weights in 1-3.5 kD range, so the median peptide dose of 500 μg per mice for a 1 kD peptide gives an approximate peptide concentration range of ~ 160 μM in the plasma. This concentration is probably not relevant since the brucellae are sequestered within macrophages where the effective peptide concentration is likely to be lower. Even so, many of these peptides reduce spleenic brucella loads by about a factor of 10 in a single dose. When normal mice are experimentally infected with *B. abortus*, the macrophages phagocytosize the foreign cells killing some of the engulfed bacteria, but some of the brucellae avoid destruction and reproduce in the host macrophages producing a chronic infection. The intracellular brucella are insulated from the cellular and humoral immune response as well as the effect of added antibiotics because antibiotic concentrations within the macrophages probably never reach therapeutically effective concentrations.[2.54-2.56] After 4-6 weeks the mice become hyperimmune to the infection and a steady state count of brucellae are found in the spleens of these chronically infected mice. At this point, when infected

macrophages die and release brucellae, they are mostly dispatched by the primed immune system, but it can take a very long time for the intracellular pathogens to be cleared. We believe some of the peptides in Tables 2.1 and 2.2 selectively destroy the infected macrophages releasing the brucellae which are eliminated by the primed immune system.

Macrophages have among the most flexible of mammalian cell membranes and as such may be expected to be more highly susceptible to peptide cytotoxicity. The peptides that selectively lyse infected macrophages *in vitro* are apparently targeting some cell membrane variation between infected and normal non-infected macrophages. The *in vivo* reduction of brucellae was equally effective with peptides **2.16**, **2.17**, and **2.9**. Of these peptides, only **2.9** appears to preferentially lyse infected macrophages. We thought N-terminus acetylation would increase bioactivity since it is known that the acetylated peptides have greater helicity, but N-terminus acylation consistently reduced the *in vivo* antibrucellae activity. Peptide N-terminus acylation also reduces the overall charge of the peptides and increases the hydrophobicity of the peptide which may reduce the amount of peptide making it to the infected macrophages in the spleen.

2.4 Conclusions

Systemic intracellular pathogens are difficult to treat using standard antibiotic regimens and vaccines. Brucellosis treatment takes 1-1.5 months and Tb takes 6-9 months of antibiotic therapy.[2.54-2.58] A combination of optimized peptides or

peptide mimetics based on those reported herein along with standard antibiotics may lead to less time consuming treatments for diseases caused by intracellular pathogens.[2.59] Also peptides in this class have a modest direct antimycobacterial activity.[2.60]

The unexpected direct anti-*E. coli* activity of the amphipathic 3_{10}-helical peptides **2.11** and **2.12** is exciting as 3_{10}-helical peptides are about 20 % longer than α-helical peptides with the same number of residues. Shortened amphipathic 3_{10}-helical peptides may retain biological activity at shorter peptide lengths than analogous α-helical peptides of the same number of amino acid residues.

2.5 Experimental

2.5.1 Peptide Synthesis

Peptides **2.2-2.10** were synthesized via solid-phase peptide synthesis using a Milligen 9050 peptide synthesizer on a PAL-PEG-PS solid support. 8 equivalents of preformed Fmoc-acid fluorides, 3 equivalents of DIEA and a 1.5 h recycling time were used for the couplings. Residues were double coupled when they were a third in a series of α,α-disubstituted amino acids. A solution of 20% piperidine/2% 1,8-diazobicyclo[4.5.0]undec-7-ene (DBU) in DMF was used for Fmoc removal. Peptides **2.4, 2.10** and **2.12** were acetylated on the solid support by treatment with a 10% solution of acetic anhydride in methylene chloride and a catalytic amount of 4-dimethylaminopyridine for 20 minutes.

The peptides were simultaneously cleaved from the resin and side-chain deprotected using reagent B (8.8 : 0.2 : 0.5 : 0.5, trifluoroacetic acid (TFA) : triisopropylsilane : water : phenol).[2.41] The resulting acidic solution was diluted with 30% acetic acid, washed with ethyl ether (4 x 50 mL), and lyophilized. The crude peptides were purified by preparative reverse-phase HPLC on a Waters 15 μm Deltapak C_4 column using a water (0.05% TFA) and acetonitrile (0.05% TFA) gradient system. The gradient was run from 10% to 50% organic and the absorption monitored at 222 nm. Purities of the peptides were checked on a Vydac 5 μm C_{18} column using the same conditions. Matrix assisted laser desorption ionization (MALDI) mass spectrometry was used to verify peptide mass. Al-14, 1352 $(M + H)^+$; Ai-14, 1469.0 $(M + H)^+$; Ai-11, 1169.5 $(M + H)^+$; Ch-14, 1790.0 $(M + H)^+$; Ch-11, 1408.2 $(M + H)^+$; Ch-13 1662.4 $(M + H)^+$; Ch-10 1286.7 $(M + H)^+$; Pi-10, 1035.6 $(M + H)^+$; Pi-10-ac, 1078.0 $(M + H)^+$.

Peptides **2.11-2.12** were synthesized by manually coupling the first 3 residues onto a PAL-PEG-PS solid support. The couplings were done by refluxing 8 equivalents of the Fmoc-acid fluoride, 3 equivalents of DIEA, and the resin in methylene chloride. The couplings were allowed to reflux until an acceptable yield was determined by a quantitative Fmoc test.[2.42] After the first three residues were coupled to the resin, the remainder of the peptides were synthesized as above for peptides **2.2-2.10**.

Peptides **2.11-2.12** were purified as above for peptides **2.2-10** and their masses verified by matrix assisted laser desorption ionization mass spectrometry. Ipi-10, 1033.7 $(M + H)^+$; Ipi-10-ac, 1077.5 $(M + H)^+$.

Melittin was purchased from Sigma Chemical Co. and purified as above for peptides **2.2-2.12**.

2.5.2 Amino Acid Analysis

Amino acid analyses were performed according to ref 2.30. Briefly, the peptides were hydrolyzed in 6 N HCl and 0.01% phenol for 24 h at 110 °C. The samples were analyzed on a cation exchange column at 65° C and post-column ninhydrin derivitization at 130 °C. All amino acid analyses agreed with the expected values.

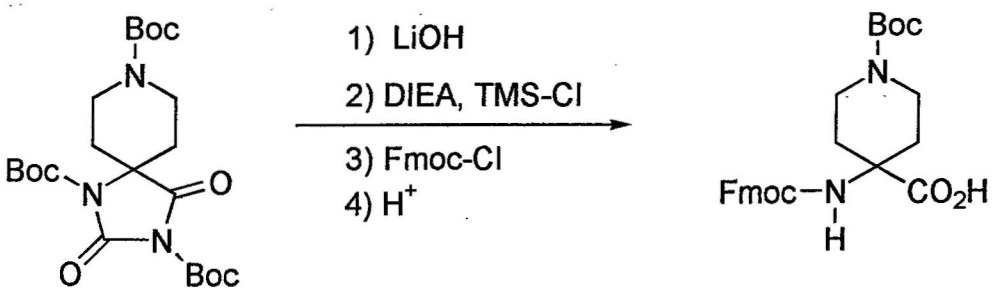

2.5.3 N^1-*tert*-butyloxycarbonyl-4-(amino-(9-fluorenylmethyloxycarbonyl))-piperidine-4-carboxylic acid

N^4, N^7, N^9-tris-*tert*-butyloxycarbonyl-8,10-dioxo-4,7,9-triaza-spiro[5,4] cyclodecane was prepared from *N*-*tert*-butyloxycarbonyl-4-piperidone according to

reference 2.38. In a 2L Erlenmeyer flask equipped with a stirring bar, N^4, N^7, N^9-tris-*tert*-butyloxycarbonyl-8,10-dioxo-4,7,9-triaza-spiro[5,4]cyclodecane (4.23 g, 9.0 mmol) was suspended in THF (800 mL). To this suspension 1N LiOH (72 mL, 72 mmol) was added with vigorous stirring. The resulting white suspension was stirred for 24 hrs. The final reaction mixture was concentrated with reduced pressure, extracted with diethyl ether (Et_2O) (2 x 125 mL), and the pH was adjusted to 7 with a solution of 20% citric acid. The resulting solid was filtered and dried *in vacuo* to yield 1-*tert*-butyloxycarbonyl-4-amino-piperidine-4-carboxylic acid ^1H NMR (200MHz, DMSO d_6) δ 3.60 (m, 4H), 1.88 (m, 4H), 1.39 (s, 9H) (1.54 g, 70%).

According to Bolin,[2.61] under inert atmosphere, 1-*tert*-butyloxycarbonyl-4-amino-piperidine-4-carboxylic acid (0.130 g, 0.532 mmol) was suspended in dry methylene chloride and DIEA (0.229 mL, 1.32 mmol) was added and allowed to stir at room temperature for five minutes. Trimethylsilyl chloride (0.116 g, 1.06 mmol) was added and the solution was heated to reflux for 3 h. The solution was placed in an ice bath and allowed to cool. Solid Fmoc-Cl (0.138 g, 5.32 mmol) was added and the solution was stirred for 4 h and allowed to warm to room temperature. The solvent was removed *in vacuo* and the solid was distributed between 50 mL of diethyl ether and 50 mL of 2.5% Na_2CO_3 solution. The aqueous layer was washed with Et_2O (50 mL) and acidified to pH 2 with 10% citric acid. The aqueous layer was washed with ethyl acetate (EtOAc) (3 x 50 mL). The EtOAc fractions were combined, dried ($MgSO_4$), and evaporated *in vacuo* to yield a yellow solid. The solid

was further purified by column chromatography over silica gel using 9:1 $CHCl_3$-CH_3OH. (0.211 g, 85%); ^1H NMR (200MHz, DMSO d_6) δ 1.39 (s, 9H), 1.65-1.89 (m, 2H), 1.91-2.15 (m, 2H), 2.90-3.09 (m, 2H), 3.55-3.76 (m, 2H), 4.19-4.32 (m, 3H), 7.22-7.54 (m, 5H), 7.70-7.80 (d, 2H), 7.85-7.96 (d, 2H), 8.30 (s, 1H); ^{13}C NMR (75 MHz, DMSO d_6) 28.01, 31.26, 46.72, 56.73, 65.26, 78.56, 79.11, 119.99, 125.21, 126.98, 127.54, 140.67, 143.76, 153.83, 155.26, 175.36 ppm; FAB MS (glycerol) 489 $(M + Na)^+$.

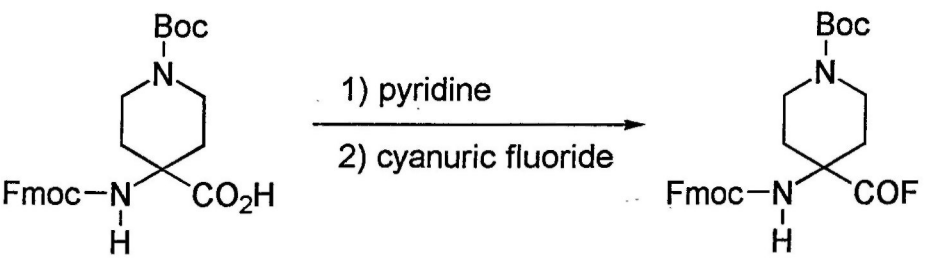

2.5.4 N^1-*tert*-butyloxycarbonyl-4-(amino-(9-fluorenylmethyloxycarbonyl))-piperidine-4-carboxylic acid fluoride

To a solution of N^1-*tert*-butyloxycarbonyl-4-(amino-(9-fluorenylmethyloxycarbonyl))-piperidine-4-carboxylic acid (3.0 g, 6.4 mmol) and pyridine (0.55 mL, 6.4 mmol) in dry methylene chloride (100 mL) cyanuric fluoride

(1.10 mL, 12.8 mmol) was added with cooling under argon. After 24 hrs, the solution was poured onto ice water (250 mL) and shaken. The entire solution was filtered and the organic layer was separated, dried ($MgSO_4$), and evaporated *in vacuo* to yield a tan solid (2.43 g, 81%); ^{1}H NMR (200MHz, DMSO d_6) δ 1.40 (s, 9H), 1.75-2.10 (m, 4H), 2.90-3.20 (m, 2H), 3.52-3.71 (m, 2H), 4.18-4.28 (t, 1H), 4.40-4.51 (d, 2H), 7.30-7.48 (m, 5H), 7.70-7.78 (d, 2H), 7.80-7.95(d, 2H), 8.30 (s, 1H).

2.5.5 General Acid Fluoride Synthesis

Under argon, the Fmoc-amino acid (1 equivalent) was dissolved in methylene chloride followed by the addition of pyridine (1.1 equivalents) and cyanuric fluoride (2 equivalents). The reaction was allowed to stir overnight for α,α-disubstituted amino acids or 4 h for proteinogenic amino acids. The reaction mixture was diluted with an additional 150 mL of methylene chloride, poured onto ice water, and filtered. The organic layer was washed with ice water (2x), dried over $MgSO_4$, and evaporated *in vacuo* to yield the acid fluoride as a white solid. The purity of the acid fluorides were checked by TLC and ^{1}H NMR in DMSO-d_6. For best results, the acid fluorides must be prepared fresh (within 24 h of use). After a prolonged period of time, the acid fluorides (especially Fmoc-Api(Boc)-F) degrade and become insoluble in the DMF/DIEA solution used for dissolution.

Fmoc-Ch-acid fluoride (90 % yield) ^{1}H NMR (250 MHz DMSO-d_6) δ 8.12 (s, 1H), 7.92 (d, 2H), 7.74 (d, 2H), 7.36 (m, 4H), 4.39 (d, 2H), 4.24 (t, 1H), 1.88 (m, 4H), 1.50 (m 4H), 1.24 (m, 2H), 0.86 (m, 2H).

Fmoc-Lys-(Boc)-acid fluoride (94 % yield) ^{1}H NMR (250 MHz DMSO-d_6) δ 8.12 (m, 1H), 8.08 (s 1H), 7.91 (d, 2H), 7.72 (d, 2H), 7.36 (m, 4H), 6.80 (m, 1H), 4.40 (t, 1H), 4.32 (m, 1H), 4.27 (d, 2H), 2.91 (m, 2H), 2.51 (m, 2H), 1.73 (m, 2H), 1.36 (s, 9H), 1.32 (m, 2H).

Fmoc-Aib-acid fluoride (89 % yield) ^{1}H NMR (250 MHz DMSO-d_6) δ 8.25 (s, 1H), 7.96 (d, 2H), 7.77 (d, 2H), 7.44 (m, 4H), 4.46 (d, 2H), 4.28 (t, 1H), 1.49 (s, 6H).

2.5.6 Circular Dichroism

Circular dichroism measurements were taken on a (+)-camphor sulfonic acid calibrated Aviv 60DS spectropolarimeter at 25 °C. The measurements were recorded over 250-195 nm using a 0.1 cm pathlength quartz cell, 1.2 nm bandwidth, 10 nm/min scan speed, and a 5 second time constant. Background spectra were acquired prior to each sample spectra and the two subtracted. Three repetitive scans were recorded and averaged to improve resolution. Peptide concentrations of 0.1 mM or 0.2 mM were used for the experiments. The reported mean residue elipticity, [θ] (deg cm^2 dmol^{-1}) is derived from the observed elipticity, $[\theta]_{obs}$ (millidegrees), using the formula $[\theta] = [\theta]_{obs}$ (MRW/10lc). MRW is the mean residue molecular weight of the peptide (molecular weight of the peptide divided by the number of peptide bonds), l is the pathlength (cm), and c is the peptide concentration (mg/mL).

2.5.7 MIC Assays

E. coli American type culture collection (ATCC) 25922 and *S. aureus* ATCC 25922 were used as representative Gram-positive and Gram-negative bacteria in the MIC assays. The bacterial cultures were grown in nutrient broth to midlog phase and standardized using a McFarland standard before dilution. A 512 μg/mL peptide stock solution was prepared and 1:2 serial dilutions were prepared and added to the culture media to give final peptide concentrations of 256-2 μg/mL.

50 μL of cells (5×10^4) and 50 μL of the desired peptide solution were added to a sterile well and the MIC determined by the lowest concentration that inhibited cell growth. The inhibition of cell growth was indicated by the absence of turbidity after four hours. The MIC values are reported as the median value for at least three experiments.

2.5.8 Enzymatic Stability Assays

The assays were performed according to reference 2.46. Peptide stock solutions from above were incubated with an equal volume of a 100 μg/mL solution of trypsin (Type II-S from Porcine pancrease (Sigma Chemical Co.)) for 20 minutes at 36° C. The peptide stock solutions were serially diluted and assayed against *E. coli* as above for remaining MIC activity. The stabilites were classified in three categories: none, partial, and complete. None meant that after incubation with the trypsin, the peptide showed no MIC activity (< 256 μg/mL). Partial meant that the peptide exhibited an MIC at a higher value than untreated, but lower than 256 μg/mL.

Complete meant that the enzyme had no effect on the peptide's MIC activity. The classifications were determined from the minimum of three experiments.

2.5.9 *In vivo B. abortus* Studies

Stock cultures of virulent *B. abortus* strain 2308 was passaged in BALB/c mice and isolated in pure culture from spleens. Stock cultures were prepared from 48 h growth on Schaedler blood agar plates and stored at -80 °C. For infections, the contents were freshly thawed, pooled and diluted in sterile PBS to a concentration of $5x10^5$ colony forming units (cfu) per mL. Exact numbers were established by subsequent viable counts. Stock cultures for macrophage assays were derived from the stocks above from a single solid passage.

Mice. Female BALB/c mice were purchased at 9 weeks of age from the Department of Laboratory Animal Medicine at the LSU School of Veterinary Medicine breeding colony. The animals were held for 1 week prior to use.

Titration of sublethal doses of peptides. Peptides were dissolved in PBS at an initial concentration of 1000 μg per 100 μL. Mice infected with *B. abortus* for 4-6 weeks were injected iv with 100 μL of peptide solution and any adverse reactions were noted (death, tremors, respiratory difficulty, or paralysis). If adverse reactions are evident the peptide was diluted 1:2 or 1:5 to titrate the highest non toxic dose. Non-infected mice treated as above were observed for 3 d.

Challenge infection of mice with B. abortus and peptide treatment. Mice were infected via the lateral tail vein with approximately $5x10^4$ cfu of *B. abortus* in 100 μL

of PBS. Approximately 4-6 weeks post infection, the mice were injected iv with a sublethal dose of peptide and a control group was injected with diluent. After 24 hrs, the peptide treatment group mice were sacrificed by CO_2 asphyxiation and their spleens and livers asceptically removed. The tissues were homogenized in 10 mL of PBS, serially diluted, and plated in triplicate. Colonies were counted after 3 days of incubation at 37 °C under a atmosphere of 10% CO_2. Bacterial loads in the peptide treated animals were compared to the diluent controls.

2.5.10 Macrophage assays

Preparation of cells. Modifications of the procedures described previously were used to harvest and infect murine resident peritoneal macrophages with strain 2308.[2.20,2.21] Briefly, following euthanasia, cells were harvested by lavage from the peritoneal cavity of ten-week old BALB/c mice using 8 mL of DMEM (Dulbecco's Modified Eagle Medium) + 5 % fetal calf serum (FCS) and 5 U/mL sodium heparin (Sigma). The cells were cultured in 96 well plates at a concentration of $1.5x10^5$ per well in 200 µL of DMEM + 5% FCS at 37° C in 5% CO_2. Cell cultures were enriched for macrophages by washing away non-adherent cells after overnight incubation with phosphate buffered saline (PBS) + 0.5% FCS and 200 µL of fresh media was added to the cultures.

Determination of non-cytotoxic concentration of peptides. Normal macrophage cultures were treated with 0 to 200 µM of the test peptide. The peptides were incubated with the cells for 1 hour at 37° C in 5% CO_2. The cells were washed

3 times with PBS + 5% FCS to remove any residual peptide. Peptide treated cells were stained with 0.04% trypan blue in DMEM + 5% FCS. 100-200 cells per well were counted using an inverted microscope and the number of stained cells were recorded. Five wells were examined per peptide concentration. Percent survival was calculated by subtracting the number of blue (dead) cells from the total cells and normalized.

Infection of cells with Brucella. *B. abortus* opsonized with a sub-agglutinating dilution (1:2000) of hyperimmune BALB/c mouse sera in DMEM + 5% FCS was added to the macrophages at a ratio of approximately 100 bacteria per macrophage. Phagocytosis proceeded for 2 h at 37° C, extracellular organisms were removed by washing 3 times with phosphate buffered saline (PBS) + 0.5% FCS and fresh DMEM. No FCS was added to the wells.

In vitro peptide treatment. Using non-cytotoxic concentrations as described above, peptides were added to infected and non-infected cell cultures for 1 hour at 37° C, 5% CO_2. The cells were washed 3 times with PBS + 5% FCS to remove any residual peptide. Percent viability was determined as described above.

2.5.11 Direct Bacterial Effects of Peptides on *B. abortus*

To determine the direct bactericidal effects of the various peptides on the viability of *B. abortus*, $1x10^7$ cfu of strain 2308 in PBS was incubated at 37° C with 10-100 μM of each peptide. At 0, 5, and 10 minutes an aliquot of the peptide

bacterial mixture was diluted and plated in triplicate and viable counts of bacteria determined. The control group contained no peptide.

2.5.12 Statistics

A mean value for each spleen count was obtained by averaging the triplicate values following log10 conversion. Data was expressed as log difference or percent bacterial reduction compared to the appropriate controls. Statistical comparisons between experimental groups was performed using the two-tailed Student's t test; p values less than 0.05 were considered significant.[2.62]

2.5.13 Biological Containment and Animal Use

All procedures involving live Brucella were performed in a Biological Level 3 (BL-3) containment facility at the LSU-SVM following Centers for Disease Control/National Institutes of Health guidelines.[2.63] In conducting research using animals, the investigators adhered to the "Guide for the Care and Use of Laboratory Animals," prepared by the Committee on Care and Use of Laboratory Animals of the Institute of Laboratory Animal Resources, National Research Council.[2.64]

2.6 References

2.1 Travis, J. *Science*, **1994**, *264*, 360-362.

2.2 Davies, J. *Science*, **1994**, *264*, 375-382.

2.3 Gabay, J. E. *Science*, **1994**, *264*, 373-374.

2.4 Maloy, W. L.; Kari, U. P. *Biopolymers (Peptide Science)* **1995**, *37*, 105-122.

2.5 Saberwal, G.; Nagaraj, R. *Biochim. Biophys. Acta* **1994**, *1197*, 109-131.

2.6 Kaiser, E. T.; Kezdy, F. J. *Ann. Rev. Biophys. Chem.* **1987**, *16*, 561-81.

2.7 Epand, R.; Shai, Y.; Segrest, J. P.; Anantharamaiah, G. M *Biopolymers (Peptide Science)* **1995**, *37*, 319-338.

2.8 He, K.; Ludtke, S. J. ; Worcester, L.; Huang, H. W. *Biochemistry* **1995**, *34*, 16764-16769.

2.9 Matsuzaki, K.; Harada, M.; Handa, T.; Munakoshi, S.; Fujii, N.; Yajima, H.; Miyajima, K. *Biochim. Biophys. Acta* **1989**, *981*, 130-134.

2.10 Matsuzaki, K.; Sugishita, K. Fujii, N.; Miyajima, K. *Biochem*istry **1995**, *34*, 3423-3429.

2.11 Tytler, E. M.; Anantharamaiah, G. M.; Walker, D. E.; Mishra V. K., Palgunachari; M. N.; Segrest, J. P. *Biochemistry* **1995**, *34*, 4393-4401.

2.12 Jaynes, J. M. Lytic Peptides Portend an Innovative Age in the Management and Treatment of Human Disease. *Drug & News Perspectives* **1990**, *3*, 69-78.

2.13 Jaynes, J. M.; Julian, G. R.; Jeffers, G. W.; White, K. L.; Enright, F. M. *Peptide Res.* **1989**, *2*, 157-160.

2.14 Cruciani, R. A.; Barker, J. L.; Zasloff, M.; Chen, H.-C.; Colamonici, O. *Proc. Natl. Acad. Sci., USA* **1991**, *88*, 3792-3796.

2.15 Moulder, J. W. *Microbiol. Rev.* **1985**, *49*, 298-337.

2.16 Timoney, J. F.; Gillespie, J. H.; Scott, F. W; Barlough, J. E. *The Genus Brucella. Hagan's and Brunner's Microbiology and Infectious Diseases of Domestic Animals,* 8th Ed. Cornell Univ. Press, Comstock Publishing Assoc., Ithaca, New York, 1988.

2.17 Burrows, W. Brucella. In *Textbook of Microbiology.* 19th Ed., W. B. Saunders Co., Philadelphia, Pennsylvania, 1968.

2.18 Nicoletti, P. *Adv. Vet. Sci. Compar. Med.* **1980**, *24*, 70-98.

2.19 Young, E. J. Clinical Manifestations of Human Brucellosis. *Brucellosis: clinical and laboratory aspects.* E.J. Young and M.J. Corbel (ed.) CRC Press, Boca Raton, FL. 1989, 97-126.

2.20 Nicoletti, P.In *Brucellosis: clinical and laboratory aspects.* Young, E.J., Corbel, M.J. Eds. CRC Press, Boca Raton, FL. 1989, 41-67.

2.21 Huxsoll, D. L., Patrick, W. C., III; Parrott, C. D. *J. Am. Vet. Med. Assoc.* **1987**, *190*, 714-722.

2.22 Detilleux, P. G.; Deyoe, B. L.; Cheville, N. F. *In Vitro. Infect. Immun.* **1990**, *58*, 2320-2328.

2.23 Jiang, X.; Baldwin, C. L. *Infect. Immun.* **1993**, *61*, 124-134.

2.24 Jones, S. M.; Winter, A. J. *Infect. Immun.* **1992**, *60*, 3011-3014.

2.25 Enright, F. M.; Araya, L. N.; Elzer, P. H.; Rowe, G. E.; Winter, A. J. *Vet. Immunol. Immunopathol.* **1990**, *26*, 171-182.

2.26 Corbeil, L. B.; Blau, K.; Inzana, T. J.; Neilsen, K. H.; Jacobson, R. H.; Corbeil, R. R. *Infect. Immun.* **1988**, *56*, 3251-3261.

2.27 Bloom, B.R. *Tuberculosis: Pathogenesis, Protection and Control.* ASM Press, Washington, DC 1994.

2.28 Benedetti, E.; Bavoso, A.; Di Blasio, B.; Pavone, V.; Pedone, C.; Toniolo, C.; Bonora, G. M.. *Proc. Natl. Acad. Sci. U.S.A.* **1982**, *79*, 7951-7954.

2.29 Nagaraj, R.; Balaram, P. *Acc. Chem. Res.* **1981**, *14*, 356-362.

2.30 Sansom, M. S. P. *Prog. Biophys. Mol. Biol.* **1991**, *55*, 139-236.

2.31 Lee, S.; Mihara, H.; Aoyagi, H.; Kato, T.; Izumuja, N.; Yamasaki, N. *Biochim. Biophys. Acta* **1986**, *862*, 211-219.

2.32 Blondelle, S. E.; Houghten, R.A. *Biochemistry* **1992**, *31*, 12688-12694.

2.33 Cornut, I.; Buttner, K.; Dasseux, J.-L.; Dufourcq, J. *FEBS Lett.* **1994**, *349*, 29-33.

2.34 Javadpour, M. M.; Juban, M. M.; Lo, W.-C. J.; Bishop, S. M.; Alberty, J. B.; Cowell, S. M.; Becker, C. L.; McLaughlin, M. L. *J. Med. Chem.* **1996**, *39*, 3107-3113.

2.35 Degrado, W. F.; Raleigh, D. P.; Handel, T. *Curr. Opin. Struct. Biol.* **1991**, *1*, 984-993.

2.36 Karle, I. L.; Balaram, P. *Biochemistry*, **1990**, *29*, 6747-6756.

2.37 Balaram, P. *Curr. Opin. Struct. Biol.* **1992**, *2*, 845-851.

2.38 Wysong, C. L.; Yokum, T. S.; Morales, G. A.; Gundry, R. L.; McLaughlin, M. L.; Hammer, R. P. *J. Org. Chem.*, **1996**, *61*, 7650-7651.

2.39 Wenschuh, H.; Beyermann, M., Krause, E.; Brudel, M.; Winter, R.; Schumann, M.; Carpino, L.; Bienert, M. *J. Org. Chem.* **1994**, *59*, 3275-3280.

2.40 Wenschuh, H.; Beyermann, M., Haber, H.; Seydel, J. K.; Krause, E.; Bienert, M.; Carpino, L.; El-Faham, A.; Albericio, F. *J. Org. Chem.* **1995**, *60*, 405-410.

2.41 Van Abel, R. J.; Tang, Y.; Rao, V. S. V.; Dobbs, C. H.; Tran, D.; Barany, G.; Selsted, M. E. *Int. J. Pept. Protein Res.* **1995**, *45*, 401-409.

2.42 Fields, G. B.; Tian, Z.; Barany, G.. In *Synthetic Peptides: A User's Guide*; Grant, G. A., Ed.; W. H. Freeman and Co.: USA, 1992.

2.43 Yokum, T.S.; Gauthier, T. J.; Hammer, R. P.; McLaughlin, M. L. *J. Am. Chem. Soc.* **1997**, *119*, 1167-1168.

2.44 Martinez de Tejada, G. T.; Pizarro-Cerda, J.; Moreno, E.; Moriyon, I. *Infect Immun.* **1995**, *63*, 3054-3061.

2.45 Halling, S. M. *Veterinary Microbiology*. **1996**, *51*, 187-192.

2.46 Wade, D., Boman, A., Wåhlin, B., Drain, C. M., Andreu, D., Boman, H. G., Merrifield, R. B. *Proc. Natl. Acad. Sic. U.S.A.* **1990**, *87*, 4761-4765.

2.47 Cornut, I.; Buttner, K.; Dasseux, J.-L.; Dufourcq, J. *FEBS Lett.* **1994**, *349*, 29-33.

2.48 Prasad, B. V. V.; Balaram, P. *CRC Crit. Rev. Biochem.* **1984**, *16*, 307-348.

2.49 Marshall, G. R.; Hodgkin, E. E.; Langs, D. A. Smith, G. D., Zabrocki, J.; Leplawy, M. T. *Proc. Natl. Acad. Sci. U.S.A.* **1990**, *87*, 487-491.

2.50 Augspurger, J. D.; Bindra, V. A.; Scheraga, H. A.; Kuki, A. *Biochemistry* **1995**, *34*, 2566-2576.

2.51 Wysong, C. L.; Yokum, T. S.; McLaughlin, M. L.; Hammer, R. P. *CHEMTECH* **1997**, *27*, 26-33.

2.52 Iwata, T.; Lee, S.; Oishi, O.; Aoyagi, H.; Ohno, M.; Anzai, K.; Kirino, Y.; Sugihara, G. *J. Biol. Chem.* **1994**, *269*, 4928-4933.

2.53 Toniolo, C.; Polese, A.; Formaggio, F.; Crisma, M.; Kamphuis, J. *J. Am. Chem. Soc.* **1996**, *118*, 2744-2745.

2.54 Holmes, B.; Quie, P.G.; Windhorst, D.B.; Pollarad, B.; Good, R.A. *Nature* **1966**, *210*, 1131-1132.

2.55 Kaufman, S.H.E. *Rev. Infect. Dis.* **1987**, *9*, S650-S659.

2.56 Vildé, J.L.; Dournon, E.; Rajagopalan, P. *Antimicrobial Agents and Chemotherapy.* **1986**, *30*, 743-748.

2.57 Hand, W.L.; King-Thompson, N.L. *Antimicrobial Agents and Chemotherapy* **1986**, *29*, 135-140.

2.58 Bloom, B.R., ed. *Tuberculosis: Pathogenesis, Protection, and Control.* ASM Press, Washington, DC 1994.

2.59 Spatola, A. In *Chemistry and Biochemistry of Amino Acids, Peptides, and Proteins*, Vol. VII, Weinstein, B., Ed., Dekker, New York, NY. 1983; pp. 267-357.

2.60 Miyakawa, Y.; Ratnakar, P.; Rao, A. G.; Costello, M. L.; Mathieu-Costello, O.; Lehrer, R. I.; Catanzaro, A. *Infec. Immun.* **1996**, *64*, 926-932.

2.61 Bolin, D. R.; Sytwu, I.-I.; Humiec, F.; Meienhofer, J. *Int. J. Peptide Protein Res.* **1989**, 353-359

2.62 Snedecor, G.W., & W.G. Cochran. *Statistical methods.* Iowa State University Press, Ames, IA 1985.

2.63 United States Department of Health and Human Services. *Biosafety in microbiological and biomedical laboratories.* H.H.S. Publication No. (CDC) 93-8395. Washington, DC: U.S. Government Printing Office, 1993.

2.64 United States Department of Health and Human Services. *Guide for the care and use of laboratory animals.* H.H.S. Publication No. (NIH) 86-23. Washington, DC U.S. Government Printing Office, 1985.

Chapter 3

Synthesis of a Series of Polar, Orthogonally Protected, α,α-Disubstituted Amino Acids*

3.1 Introduction

α,α-Disubstituted amino acids (ααAAs), **3.1** (where R, R' ≠ H), are widely used in peptide design because of their structure promoting abilities (Figure 3.1).[3.1-3.4] α-Aminoisobutyric acid (Aib) and Aib-like residues (where R, R' are not extremely bulky) promote helicity in peptides to a much greater extent than the proteinogenic, monosubstituted residues.[3.1-3.4] Their helix promoting ability arises from the restriction of allowed ϕ, ψ angles to those favoring helical structures.[3.1-3.4] Aib and Aib-like residues have been incorporated into peptides to promote the formation of 3_{10}- helices and α-helices.[3.1-3.5] The preferential formation of a 3_{10}-helix or an α-helix depends upon the design of the peptide, percentage of ααAAs, and location of the ααAAs.[3.5-3.9] The vast majority of peptides synthesized for the

*Reprinted in part from *Tetrahedron Letters, Volume 38*, T. Scott Yokum, Matthew G. Bursavich, Sarina A. Piha-Paul, David A. Hall, Mark L. McLaughlin, Synthesis of a Series of Polar, Orthogonally Protected, α,α-Disubstituted Amino Acids, Copyright 1997, pages 4013-4016, with kind permission from Elsevier Science Ltd. The Boulevard, Langford Lane, Kidlington, OX5 1GB, UK.

studies of the factors governing the formation of the 3_{10}-helix or the α-helix are hydrophobic peptides rich in non-polar ααAAs.[3.1-3.9] The extensive use of hydrophobic peptides in the study of the 3_{10}-/α-helix equilibrium has precluded experiments in aqueous solutions and limited them to organic media.[3.1-3.6]

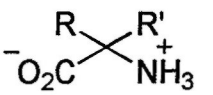

3.1

Figure 3.1. General structure of α,α-disubstituted amino acids.

Polar ααAAs have the ability to solubilize ααAA rich peptides in aqueous solution and permit studies in this medium while allowing the peptides to retain a high percentage of ααAAs. Very few examples of polar ααAAs suitable for incorporation into peptides have been reported in the literature.[3.10-3.12] Polar ααAAs are important design tools for the synthesis of short, highly helical, water soluble peptides containing high percentages of ααAAs. These peptides are integral to the study of

the $3_{10}/\alpha$-helix equilibrium, the investigation of the stability of the 3_{10}-helix in aqueous media, and in the design of short antimicrobial peptides.[3.5,3.13] Herein, we report the synthesis of a series of polar ααAAs suitably protected for incorporation into peptides via solid-phase peptide synthesis.

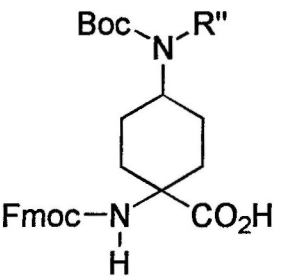

3.2

Figure 3.2. General structure of the target amino acids.

3.2 Results and Discussion

The general structure of the amino acids is shown above, **3.2** (Figure 3.2). The amino acids are constructed from a 6-membered ring backbone due to the high helix promoting effects previously exhibited by cyclic ααAAs in short

peptides.[3.5,3.13] The polar functionality is introduced onto the cyclic backbone via reductive amination. The reductive amination procedure provides flexibility for the incorporation of a wide variety of R" groups, such as hydrophobic chains, additional polar groups, or fluorescent probes. The side chain nitrogen, introduced by the reductive amination, will be protonated under physiological conditions and under conditions normally used for aqueous spectroscopic characterization.

The synthesis was designed using high yielding transformations so only small amounts of impurities would be present. This allows the crude product to be carried on to the next step without isolation of the intermediates. As a result, no compounds were purified until the target molecule. Analytical methods were used only to confirm the presence of the crude product (i.e. diagnostic peaks in the NMR, parent ion in GC/MS, etc.) except in the final product.

The synthesis begins with a reductive amination on the commercially available 1,4-cyclohexanedione monoethylene ketal, **3.3**, with the desired amine (1.1 equivalents), acetic acid (1.0 equivalent), and sodium triacetoxyborohydride (1.6 equivalents) in 1,2-dichloroethane (DCE) to give **3.4** (Figure 3.3).[3.14] Sodium cyanoborohydride was also used as the reducing agent, but gave unsatisfactory yields as compared to the acetoxy compound. The ketone functionality is unmasked by treating **3.4** with a 20% trifluoroacetic acid/water solution and heating to reflux in tetrahydrofuran (THF) for 24 hours to yield ketone **3.5** (Figure 3.3).

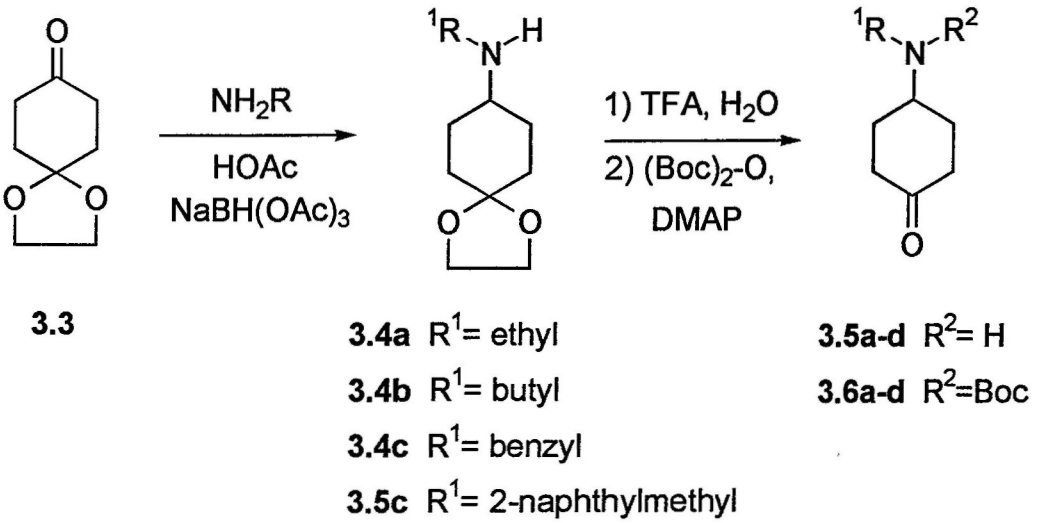

Figure 3.3. Synthesis of ketones **3.6 a-d**.

To obtain an amino acid suitable for 9-fluorenylmethyloxycarbonyl (Fmoc) solid-phase peptide synthesis (SPPS), the side chain must be orthogonally protected with respect to the α-nitrogen. An orthogonal protection scheme is a protection scheme where the different protecting groups employed are removed by alternate cleavage mechanisms (i.e. Fmoc (piperidine in DMF), *t*-butyloxycarbonyl (Boc) (trifluoroacetic acid (TFA)), allyloxycarbonyl (Pd^0)).[3.15] Traditional Fmoc SPPS uses Fmoc as the temporary (α) protection, TFA labile permanent (side-chain) protection and TFA labile linkage to the solid support. Thus, the nitrogen on ketone

3.5 is protected with Boc using triethylamine (Et_3N) (1.50 equivalents), $(Boc)_2$-O (1.20 equivalents) and a catalytic amount of 4-dimethylaminopyridine (DMAP) in THF to give **3.6** (Figure 3.3).

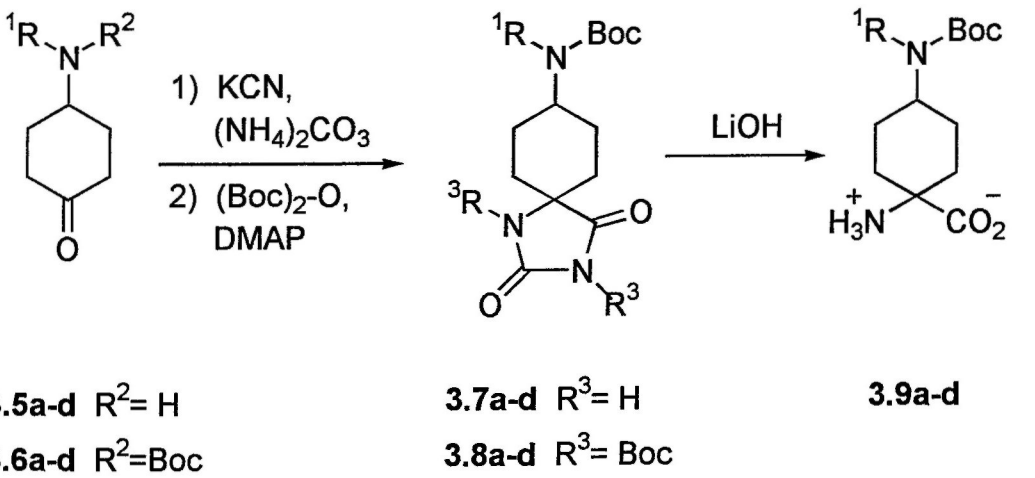

Figure 3.4. Synthesis of amino acids **3.9 a-d**.

Ketone **3.6** is then converted to hydantoin **3.7** using a Bucherer-Bergs procedure (Figure 3.4).[3.10,3.16-3.18] The Bucherer-Bergs procedure is known to give the α-product where α- and δ-nitrogens are expected to have the cis stereochemistry.[3.18] The hydantoin could be conventionally hydrolyzed using harsh

conditions (i.e. barium hydroxide in a Parr™ Bomb) which could effect the Boc protecting group. Both the α- and side chain nitrogens would be left unprotected if the side chain Boc was removed during conventional hydrolysis. Selective protection of the nitrogens is not a trivial task, but would be required for the synthesis of an amino acid suitable for incorporation using standard solid-phase peptide synthesis. We use a mild hydrolysis method developed by Rebek to avoid the potential complications with removal of the side-chain Boc.[3.10,3.19] This method activates the hydantoin nitrogens by reaction with $(Boc)_2$-O (2 equivalents per hydantoin nitrogen) and DMAP (0.1 equivalent) to give **3.8** (Figure 3.4).[3.9,3.17] The selective hydrolysis is accomplished with 1N lithium hydroxide (8 equivalents) and THF as a co-solvent at room temperature to give amino acid **3.9** (Figure 3.5).

The α-nitrogen is protected with Fmoc using trimethylsilyl chloride (TMS-Cl) (2.5 equivalents), diisopropylethylamine (DIEA) (3.0 equivalents), and Fmoc-Cl (1.1 equivalents) in methylene chloride (Figure 3.5). Protecting the α-nitrogen of a very hydrophobic amino acid of this type is difficult using traditional methods with aqueous/organic mixtures because of the extreme non-polar nature of the protected side chain. We use a method developed by Bolin and co-workers which solubilizes the amino acid by neutralizing the free amino function with DIEA and forming the silyl ester with TMS-Cl in neat organic media.[3.20] The neutral, organic soluble amino acid is now reacted with Fmoc-Cl to yield the fully protected amino acid.[3.20] The

crude product obtained from the Fmoc reaction is purified via silica gel column chromatography eluting with chloroform/methanol mixtures to give pure **3.10**.

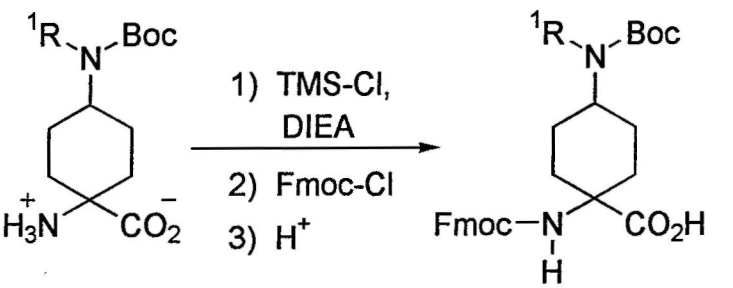

3.9a-d **3.10a-d**

Figure 3.5. Synthesis of protected amino acids **3.10 a-d**.

3.3 Conclusions

The method provides a general route to polar ααAAs with R groups of varying hydrophobicity. This method could also be easily adapted to the synthesis of fluorescent or other tagged ααAAs. We plan to study the effects of the hydrophobic chains on antimicrobial activity and helicity.

3.4 Experimental

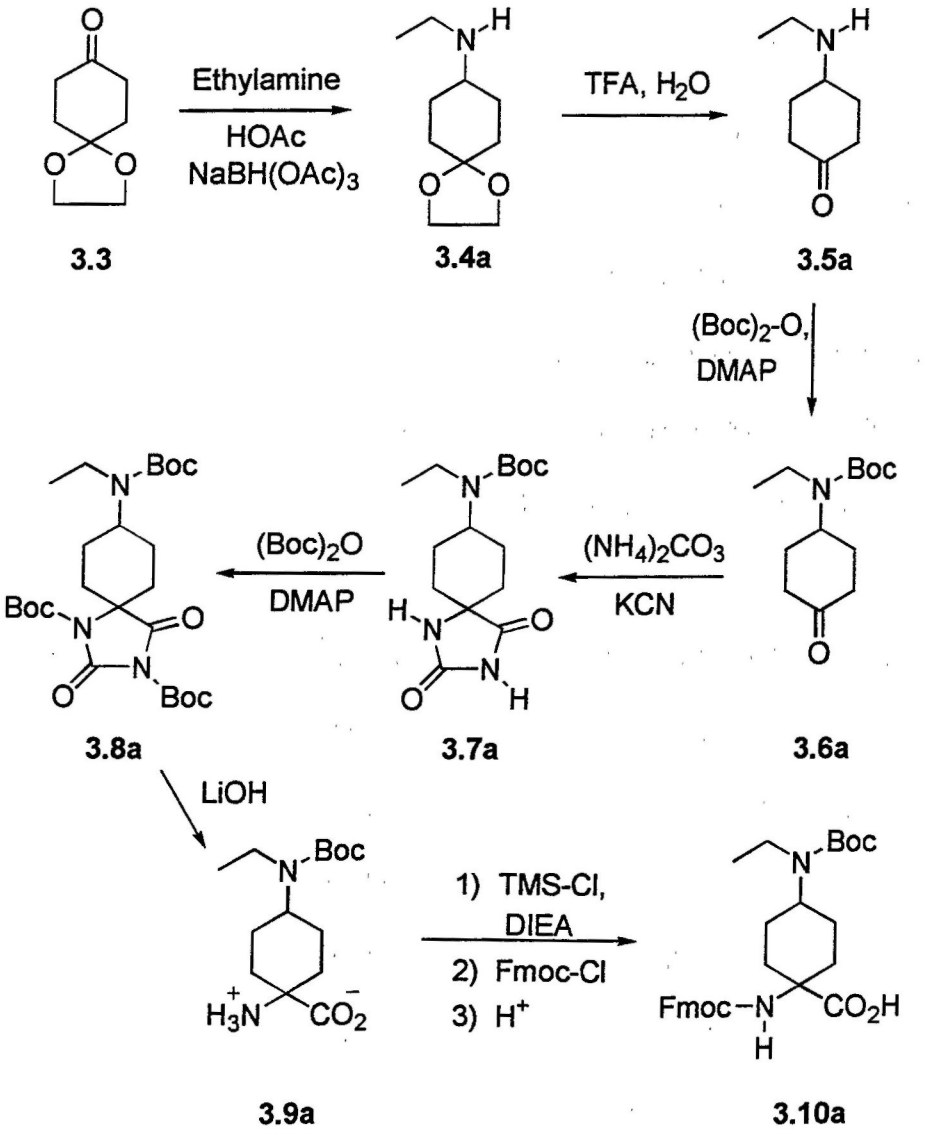

3.3 **3.4a** **3.5a**

3.8a **3.7a** **3.6a**

3.9a **3.10a**

3.4.1 N^4-*tert*-butyloxycarbonyl-N^4-ethyl-N^1-(9-fluorenylmethyloxycarbonyl)-1,4-bis-aminocyclohexane-1-carboxylic acid (3.10a)

N-ethyl-4-amino-7,10-dioxa-spiro[5,4]cyclodecane (**3.4a**). An Ar-purged flask was charged with 4-oxo-7,10-dioxa-spiro[5,4]cyclodecane (**3.3**) (5.00 g, 32.0

mmol) and 150 mL of DCE. Acetic acid (1.83 mL, 32.0 mmol) and (2.30 mL, 35.2 mmol) ethylamine were added sequentially to this solution. After stirring for 30 minutes, $NaBH(OAc)_3$ (10.86 g, 51.3 mmol) was added to the flask. The reaction mixture was monitored by GC-MS analysis. Once all starting material had been consumed (18 h), the reaction mixture was concentrated under reduced pressure and taken up in 200 mL of methylene chloride. The organic solution was washed with 10 % Na_2CO_3 (3 x 100 mL), dried over $MgSO_4$ and concentrated under reduced pressure. The resulting solid (5.15 g) was carried on to the next step without further purification. GC/MS m/z 185 $(M)^+$.

N-ethyl-4-aminocyclohexanone (**3.5a**). A solution of *N*-ethyl-4-amino-7,10-dioxa-spiro[5,4]cyclodecane (**3.4a**) (5.04 g, 27.2 mmol) in 55 mL of THF was treated with 20 mL of 20 % TFA/ H_2O solution and refluxed at 80° C until GC-MS showed that all starting material had been consumed. The solvents were removed under reduced pressure and the resulting oil taken up in 100 mL of methylene chloride. The organic solution was washed with 10% Na_2CO_3 (3 x 100 mL), dried ($MgSO_4$), and concentrated under reduced pressure. The resulting oil (3.10 g) was carried on to the next step without further purification. GC/MS m/z 141 $(M)^+$.

N-tert-butyloxycarbonyl-N-ethyl-4-aminocyclohexanone (**3.6a**). In a flask equipped with a mercury bubbler, *N*-ethyl-4-aminocyclohexanone (**3.5a**) (3.10 g, 22.0 mmol) was dissolved in 100 mL of methylene chloride and treated with Et_3N (4.58 mL, 32.90 mmol). After 5 minutes of stirring, $(Boc)_2$-O (5.75 g, 26.34 mmol) and

DMAP (0.27 g, 2.19 mmol) were added. The resulting mixture was stirred vigorously for 24 h and the organic solution was diluted with an additional 100 mL of methylene chloride. This solution was washed with 1 N HCl (2 x 70 mL), 10 % Na_2CO_3 (1 x 50 mL), brine (1 x 50 mL), and dried over $MgSO_4$. The solvent was removed under reduced pressure and the resulting oil (4.68 g) was used without further purification. ^1H NMR (200 MHz, $CDCl_3$) δ 1.38 (large singlet, indicating Boc).

N^4-*tert*-butyloxycarbonyl-N^4-ethyl-4-amino-7,9-diaza-8,10-dioxo-spiro[5,4] cyclodecane (**3.7a**). A solution of *N*-*tert*-butyloxycarbonyl-*N*-ethyl-4-aminocyclohexanone (**3.6a**) (4.73 g, 19.58 mmol) in 25 mL of methanol was treated with a solution of $(NH_4)_2CO_3$ (5.06 g, 52.69 mmol) and KCN (3.43 g, 52.69 mmol) in 25 mL of H_2O. The mixture was refluxed at 65° C for 48 h. The solution was removed from heat and the methanol removed under reduced pressure. Vacuum filtration of the resulting suspension gave a brown solid. The solid was dissolved in the minimum amount of methylene chloride and precipitated by the addition of hexanes. A white solid (3.52 g) was collected by vacuum filtration and carried on to the next step without further purification. ^{13}C NMR (75 MHz, $CDCl_3$) δ 178.78, 157.00, 154.38 (indicating 3 carbonyls present).

N^4-*tert*-butyloxycarbonyl-N^4-ethyl-4-amino-7,9-diaza-7,9-bis-*tert*-butyloxy-carbonyl-8,10-dioxo-spiro[5,4]cyclodecane (**3.8a**). In a 500 mL flask equipped with a mercury bubbler, N^4-*tert*-N^4-ethyl-butyloxycarbonyl-4-amino-7,9-diaza-8,

10-dioxo-spiro[5,4] cyclodecane (**3.7a**) (1.49 g, 4.79 mmol) was suspended in 100 mL of THF and treated with $(Boc)_2$-O (4.18 g, 19.14 mmol) and DMAP (0.58 g, 0.48 mmol). The mixture was stirred vigorously for 48 h at room temperature. The solvents were removed under reduced pressure and the resulting residue was taken up in 150 mL of methylene chloride, washed with 10 % citric acid solution (2 x 100 mL), 10 % Na_2CO_3 (3 x 100 mL), and dried over $MgSO_4$. The solvent was removed under reduced pressure to yield a solid (2.42 g) which was used without further purification. ^{1}H NMR (200 MHz, $CDCl_3$) δ 1.49, 1.39, 1.37 (3 large singlets, indicating 3 Bocs) ^{13}C NMR (50 MHz, $CDCl_3$) δ 170.94, 154.82, 149.18, 147.14, 144.93 (indicating 5 carbonyls present).

N^4-*tert*-butyloxycarbonyl-N^4-ethyl-1,4-bis-aminocyclohexane-1-carboxylic acid (**3.9a**). In a 500 mL flask, N^4-*tert*-butyloxycarbonyl-N^4-ethyl-4-amino-7,9-diaza-7,9-bis-*tert*-butyloxycarbonyl-8,10-dioxo-spiro[5,4]cyclodecane (**3.8a**) (1.50 g, 2.93 mmol) was suspended in 260 mL of THF and treated with 24 mL of 1 N LiOH. The mixture was stirred vigorously overnight at room temperature. The resulting suspension was diluted with an additional 100 mL of 1 N LiOH and the THF removed under reduced pressure. The remaining aqueous solution was washed with diethyl ether (3 x 100 mL) and the pH of the aqueous layer adjusted from 11 to 7 with 10 % citric acid solution. The aqueous layer was concentrated under reduced pressure, cooled, and filtration on Buchner funnel resulted in a white solid (0.82 g) which was

used without further purification. ^{1}H NMR (200 MHz, DMSO d_6) δ 1.39 (large singlet, indicating only 1 Boc).

N^4-*tert*-butyloxycarbonyl-N^4-ethyl-N^1-(9-fluorenylmethyloxycarbonyl)-1,4-bis-aminocyclohexane-1-carboxylic acid (**3.10a**). To an Ar-flushed three-neck flask containing N^4-*tert*-butyloxycarbonyl-N^4-ethyl-1,4-bis-aminocyclohexane-1-carboxylic acid (**3.9a**) (0.82 g, 2.81 mmol), 100 mL of methylene chloride and DIEA (1.47 mL, 8.43 mmol) were added. Following 5 minutes of stirring, TMS-Cl (0.89 mL, 7.03 mmol) was added via syringe. The solution was heated to reflux for 3 hours followed by cooling in an ice bath. To this cooled solution, Fmoc-Cl (0.80 g, 3.09 mmol) was added and stirred for 4 hr. The resulting solution was washed with 1 N HCl (2 x 50 mL), dried over $MgSO_4$ and the solvent removed under reduced pressure to yield a yellow solid. Purification of the crude mixture by column chromatography (92:8 chloroform:methanol) resulted in a white solid, N^4-*tert*-butyloxycarbonyl-N^4-ethyl-N^1-(9-fluorenylmethyloxycarbonyl)-1,4-bis-aminocyclohexane-1-carboxylic acid (**3.10a**). (0.26 g in an overall yield of 15.1%). ^{1}H NMR (250 MHz, DMSO d_6) δ 7.94 (d, 2H), 7.79 (d, 2H), 7.62 (s, 1H), 7.45 (t, 2H), 7.38 (t, 2H), 4.32 (m, 3H), 3.82 (bm, 1H), 3.16 (bm, 2H), 2.25 (bm, 2H), 1.74 (bm, 4H), 1.50 (bm, 2H), 1.46 (s, 9H), 1.12 (t, 3H). ^{13}C NMR (100 MHz, DMSO d_6) δ 175.88, 155.24, 154.24, 143.82, 140.73, 127.65, 127.00, 125.33, 120.01, 78.26, 65.20, 57.28, 54.20, 46.75, 43.80, 31.02, 28.15, 25.05, 16.02. FAB-MS (glycerol) m/z 509.3 $(M+H)^+$.

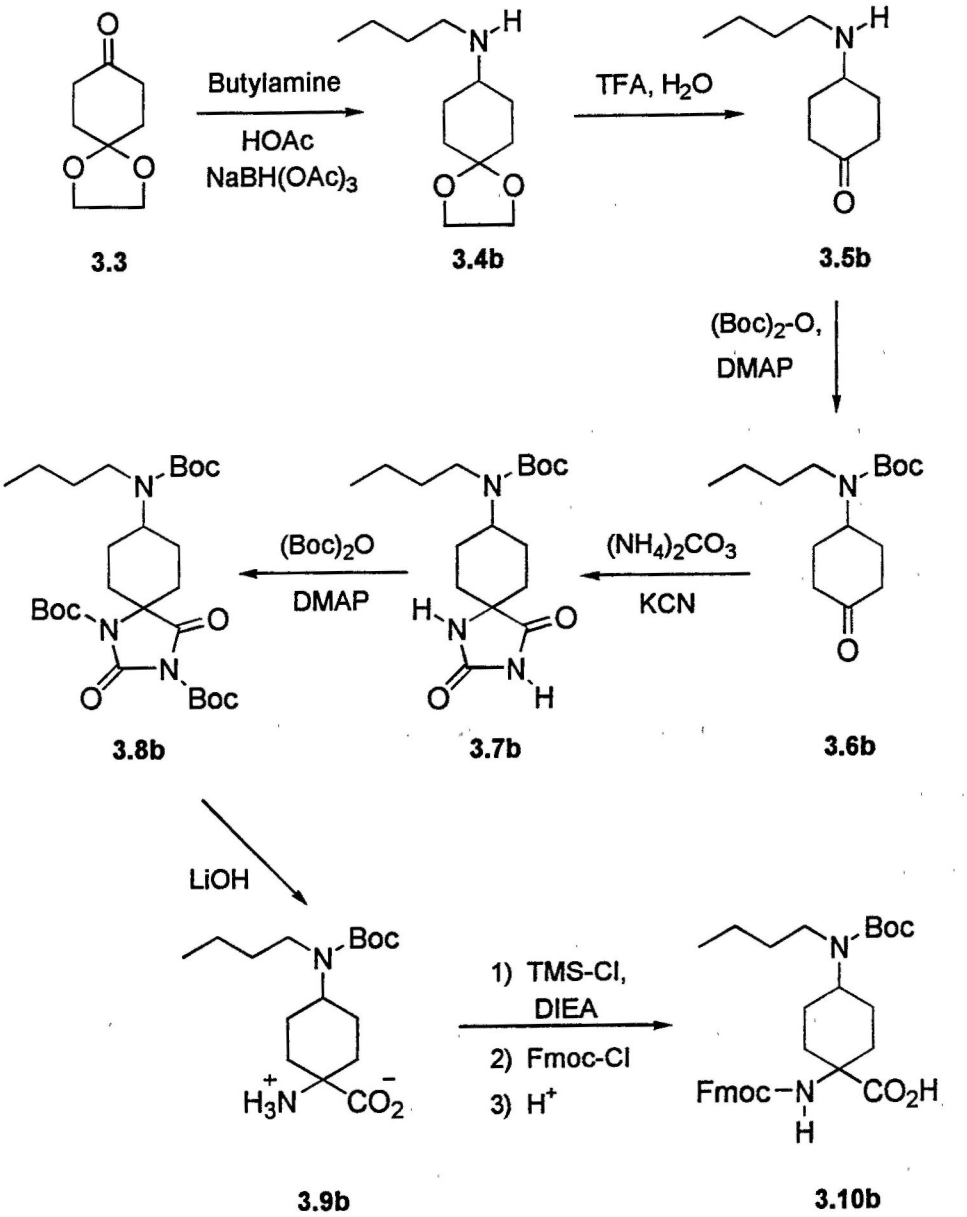

3.4.2 N^4-butyl-N^4-*tert*-butyloxycarbonyl-N^1-(9-fluorenylmethyloxycarbonyl)-1,4-bis-aminocyclohexane-1-carboxylic acid (3.10b)

N-butyl-4-amino-7,10-dioxa-spiro[5,4]cyclodecane (**3.4b**). An Ar-purged flask was charged with 4-oxo-7,10-dioxa-spiro[5,4]cyclodecane (**3.3**) (5.00 g, 32.0

mmol) and 150 mL of DCE. Acetic acid (1.83 mL, 32.0 mmol) and (3.48 mL, 35.2 mmol) butylamine were added sequentially to this solution. After stirring for 30 minutes, $NaBH(OAc)_3$ (10.86 g, 51.3 mmol) was added to the flask. The reaction mixture was monitored by GC-MS analysis. Once all starting material had been consumed (18 h), the reaction mixture was concentrated under reduced pressure and taken up in 200 mL of methylene chloride. The organic solution was washed with 10 % Na_2CO_3 (3 x 100 mL), dried over $MgSO_4$ and concentrated under reduced pressure. The resulting solid (6.76 g) was carried on to the next step without further purification. GC/MS m/z 213 $(M)^+$.

N-butyl-4-aminocyclohexanone (**3.5b**). A solution of *N*-butyl-4-amino-7,10-dioxa-spiro[5,4]cyclodecane (**3.4b**) (6.70 g, 31.4 mmol) in 55 mL of THF was treated with 19 mL of 20 % TFA/ H_2O solution and refluxed at 80° C until GC-MS showed that all starting material had been consumed. The solvents were removed under reduced pressure and the resulting oil taken up in 100 mL of methylene chloride. The organic solution was washed with 10% Na_2CO_3 (3 x 100 mL), dried ($MgSO_4$), and concentrated under reduced pressure. The resulting oil (5.31 g) was carried on to the next step without further purification. GC/MS m/z 169 $(M)^+$.

N-butyl-*N*-*tert*-butyloxycarbonyl-4-aminocyclohexanone (**3.6b**). In a flask equipped with a mercury bubbler, *N*-butyl-4-aminocyclohexanone (**3.5b**) (5.31 g, 31.4 mmol) was dissolved in 100 mL of methylene chloride and treated with Et_3N (4.15 mL, 29.75 mmol). After 5 minutes of stirring, $(Boc)_2$-O (7.79 g, 35.71 mmol) and

DMAP (0.36 g, 2.98 mmol) were added. The resulting mixture was stirred vigorously for 24 h and the organic solution was diluted with an additional 100 mL of methylene chloride. This solution was washed with 1 N HCl (2 x 70 mL), 10 % Na_2CO_3 (1 x 50 mL), brine (1 x 50 mL), and dried over $MgSO_4$. The solvent was removed under reduced pressure and the resulting oil (7.75 g) was used without further purification. ^1H NMR (200 MHz, $CDCl_3$) δ 1.38 (large singlet, indicating Boc).

N^4-butyl-N^4-*tert*-butyloxycarbonyl-4-amino-7,9-diaza-8,10-dioxo-spiro[5,4] cyclodecane (**3.7b**). A solution of *N*-butyl-*N*-*tert*-butyloxycarbonyl-4-aminocyclohexanone (**3.6b**) (7.64 g, 28.3 mmol) in 25 mL of methanol was treated with a solution of $(NH_4)_2CO_3$ (6.75 g, 70.2 mmol) and KCN (4.57 g, 70.2 mmol) in 25 mL of H_2O. The mixture was refluxed at 65° C for 48 h. The solution was removed from heat and the methanol removed under reduced pressure. Vacuum filtration of the resulting suspension gave a brown solid. The solid was dissolved in the minimum amount of methylene chloride and precipitated by the addition of hexanes. A white solid (6.53 g) was collected by vacuum filtration and carried on to the next step without further purification. ^{13}C NMR (50 MHz, $CDCl_3$) δ 178.28, 156.45, 154.41 (indicating 3 carbonyls present).

N^4-butyl-N^4-*tert*-butyloxycarbonyl-4-amino-7,9-diaza-7,9-bis-*tert*-butyloxycarbonyl-8,10-dioxo-spiro[5,4]cyclodecane (**3.8b**). In a 500 mL flask equipped with a mercury bubbler, N^4-butyl-N^4-*tert*-butyloxycarbonyl-4-amino-7,

9-diaza-8,10-dioxo-spiro[5,4] cyclodecane (**3.7b**) (2.06 g, 6.07 mmol) was suspended in 100 mL of THF and treated with $(Boc)_2$-O (5.33 g, 24.42 mmol) and DMAP (0. 75 g, 0. 61 mmol). The mixture was stirred vigorously for 48 h at room temperature. The solvents were removed under reduced pressure and the resulting residue was taken up in 150 mL of methylene chloride, washed with 10 % citric acid solution (2 x 100 mL), 10 % Na_2CO_3 (3 x 100 mL), and dried over $MgSO_4$. The solvent was removed under reduced pressure to yield a solid (4.55 g) which was used without further purification. ^{1}H NMR (200 MHz, $CDCl_3$) δ 1.47, 1.57, 1.58 (3 large singlets, indicating 3 Bocs) ^{13}C NMR (50 MHz, $CDCl_3$) δ 170.98, 154.88, 149.14, 147.08, 144.95 (indicating 5 carbonyls present).

N^4-butyl-N^4-*tert*-butyloxycarbonyl-1,4-bis-aminocyclohexane-1-carboxylic acid (**3.9b**). In a 500 mL flask, N^4-butyl-N^4-*tert*-butyloxycarbonyl-4-amino-7,9-diaza-7,9-bis-*tert*-butyloxycarbonyl-8,10-dioxo-spiro[5,4]cyclodecane (**3.8b**) (1.00 g, 1.85 mmol) was suspended in 165 mL of THF and treated with 15 mL of 1 N LiOH. The mixture was stirred vigorously overnight at room temperature. The resulting suspension was diluted with an additional 50 mL of 1 N LiOH and the THF removed under reduced pressure. The remaining aqueous solution was washed with diethyl ether (3 x 50 mL) and the pH of the aqueous layer adjusted from 11 to 7 with 10 % citric acid solution. The aqueous layer was concentrated under reduced pressure, cooled, and filtration on Buchner funnel resulted in a white solid (0.30 g) which was used without further purification. ^{1}H NMR (200 MHz, DMSO d_6) δ 1.39 (large

singlet, indicating only 1 Boc), ^{13}C NMR (50 MHz, DMSO d_6) δ 172.08, 154.40 (indicating only 2 carbonyls present).

N^4-butyl-N^4-*tert*-butyloxycarbonyl-N^1-(9-fluorenylmethyloxycarbonyl)-1,4-bis-aminocyclohexane-1-carboxylic acid (**3.10b**). To an Ar-flushed three-neck flask containing N^4-butyl-N^4-*tert*-butyloxycarbonyl-1,4-bis-aminocyclohexane-1-carboxylic acid (**3.9b**) (0.28 g, 0.88 mmol), 100 mL of methylene chloride and DIEA (0.46 mL, 2.64 mmol) were added. Following 5 minutes of stirring, TMS-Cl (0.28 mL, 2.20 mmol) was added via syringe. The solution was heated to reflux for 3 hours followed by cooling in an ice bath. To this cooled solution, Fmoc-Cl (0.25 g, 0.97 mmol) was added and stirred for 4 hr. The resulting solution was washed with 1 N HCl (2 x 50 mL), dried over $MgSO_4$ and the solvent removed under reduced pressure to yield a yellow solid. Purification of the crude mixture by column chromatography (9:1 chloroform:methanol) resulted in a white solid, N^4-butyl-N^4-*tert*-butyloxycarbonyl-N^1-(9-fluorenylmethyloxycarbonyl)-1,4-bis-aminocyclohexane-1-carboxylic acid (**3.10b**). (0.26 g in an overall yield of 28.4%). ^1H NMR (300 MHz, DMSO d_6) δ 7.88 (d, 2H), 7.73 (d, 2H), 7.56 (s, 1H),7.42 (t, 2H), 7.31 (t, 2H), 4.26 (m, 3H), 3.70 (bm, 1H), 3.02 (bm, 2H), 2.16 (bm, 2H), 1.69 (bm, 4H), 1.42 (bm, 4H), 1.40 (s, 9H), 1.24 (m, 2H), 0.89 (t, 3H). ^{13}C NMR (50MHz, $CDCl_3$) δ 178.54, 155.68, 155.38, 143.73, 141.28, 127.64, 127.01, 124.96, 119.89, 79.47, 66.63, 58.16, 54.00, 47.19, 43.56, 32.76, 31.64, 28.47, 25.21, 20.25, 13.88. FAB-MS (glycerol) m/z 537.5 $(M+H)^+$.

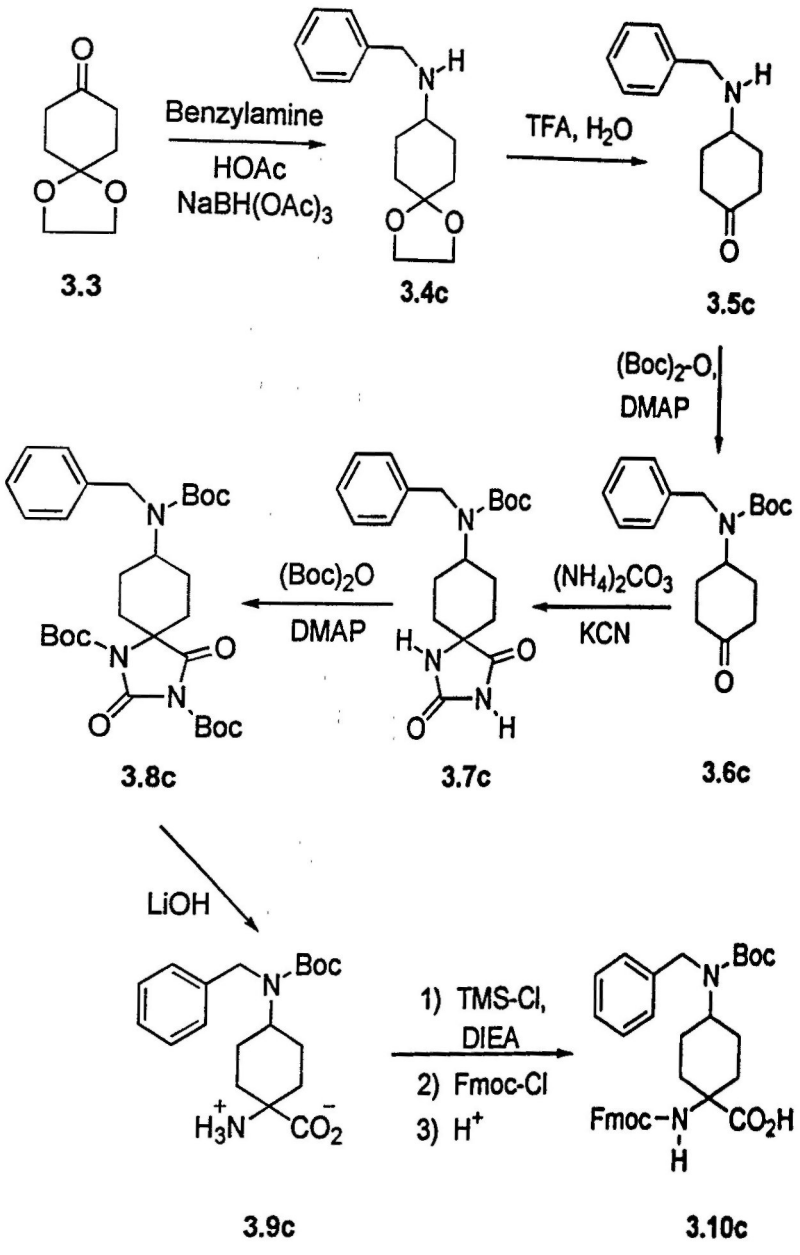

3.4.3 N^4-benzyl-N^4-*tert*-butyloxycarbonyl-N^1-(9-fluorenylmethyloxycarbonyl)-1,4-bis-aminocyclohexane-1-carboxylic acid (3.10c)

N-benzyl-4-amino-7,10-dioxa-spiro[5,4]cyclodecane (3.4c). An Ar-purged flask was charged with 4-oxo-7,10-dioxa-spiro[5,4]cyclodecane (3.3) (10.00 g, 64.0

mmol) and 200 mL of DCE. Acetic acid (3.67 mL, 64.0 mmol) and (7.69 mL, 70.4 mmol) butylamine were added sequentially to this solution. After stirring for 30 minutes, $NaBH(OAc)_3$ (21.71 g, 102.5 mmol) was added to the flask. The reaction mixture was monitored by GC-MS analysis. Once all starting material had been consumed (18 h), the reaction mixture was concentrated under reduced pressure and taken up in 200 mL of methylene chloride. The organic solution was washed with 10 % Na_2CO_3 (3 x 100 mL), dried over $MgSO_4$ and concentrated under reduced pressure. The resulting solid (15.84 g) was carried on to the next step without further purification. GC/MS m/z 247 $(M)^+$.

N-benzyl-4-aminocyclohexanone (**3.5c**). A solution of *N*-benzyl-4-amino-7,10-dioxa-spiro[5,4]cyclodecane (**3.4c**) (15.84 g, 64.0 mmol) in 55 mL of THF was treated with 19 mL of 20 % TFA/ H_2O solution and refluxed at 80° C until GC-MS showed that all starting material had been consumed. The solvents were removed under reduced pressure and the resulting oil taken up in 200 mL of methylene chloride. The organic solution was washed with 10% Na_2CO_3 (3 x 100 mL), dried ($MgSO_4$), and concentrated under reduced pressure. The resulting oil (13.00 g) was carried on to the next step without further purification. GC/MS m/z 203 $(M)^+$.

N-benzyl-*N*-*tert*-butyloxycarbonyl-4-aminocyclohexanone (**3.6c**) In a flask equipped with a mercury bubbler, *N*-benzyl-4-aminocyclohexanone (**3.5c**) (13.0 g, 64.0 mmol) was dissolved in 200 mL of methylene chloride and treated with Et_3N (9.59 mL, 68.87 mmol). After 5 minutes of stirring, $(Boc)_2$-O (22.55 g, 103.33

mmol) and DMAP (0.84 g, 6.98 mmol) were added. The resulting mixture was stirred vigorously for 24 h and the organic solution was diluted with an additional 100 mL of methylene chloride. This solution was washed with 1 N HCl (2 x 120 mL), 10 % Na_2CO_3 (1 x 100 mL), brine (1 x 100 mL), and dried over $MgSO_4$. The solvent was removed under reduced pressure and the resulting oil (19.42 g) was used without further purification. ^1H NMR (200 MHz, $CDCl_3$) δ 1.39 (large singlet, indicating Boc).

N^4-benzyl-N^4-*tert*-butyloxycarbonyl-4-amino-7,9-diaza-8,10-dioxo-spiro[5,4] cyclodecane (**3.7c**). A solution of *N*-benzyl-*N*-*tert*-butyloxycarbonyl-4-aminocyclohexanone (**3.6c**) (8.51 g, 28.0 mmol) in 25 mL of methanol was treated with a solution of $(NH_4)_2CO_3$ (8.09 g, 70.2 mmol) and KCN (5.48 g, 84.2 mmol) in 25 mL of H_2O. The mixture was refluxed at 65° C for 48 h. The solution was removed from heat and the methanol removed under reduced pressure. Vacuum filtration of the resulting suspension gave a brown solid. The solid was dissolved in the minimum amount of methylene chloride and precipitated by the addition of hexanes. A white solid (7.49 g) was collected by vacuum filtration and carried on to the next step without further purification. ^{13}C NMR (50 MHz, $CDCl_3$) δ 178.13, 156.23, 155.50 (indicating 3 carbonyls present).

N^4-benzyl-N^4-*tert*-butyloxycarbonyl-4-amino-7,9-diaza-7,9-bis-*tert*-butyloxy-carbonyl-8,10-dioxo-spiro[5,4]cyclodecane (**3.8c**). In a 500 mL flask equipped with a mercury bubbler, N^4-benzyl-N^4-*tert*-butyloxycarbonyl-4-amino-7,9-diaza-8,

10-dioxo-spiro[5,4] cyclodecane (**3.7c**) (3.00 g, 8.05 mmol) was suspended in 200 mL of THF and treated with $(Boc)_2$-O (7.03 g, 32.20 mmol) and DMAP (0.97 g, 0.80 mmol). The mixture was stirred vigorously for 48 h at room temperature. The solvents were removed under reduced pressure and the resulting residue was taken up in 200 mL of methylene chloride, washed with 10 % citric acid solution (2 x 100 mL), 10 % Na_2CO_3 (3 x 100 mL), and dried over $MgSO_4$. The solvent was removed under reduced pressure to yield a solid (3.27 g) which was used without further purification. ^{1}H NMR (200 MHz, $CDCl_3$) δ 1.49, 1.48, 1.36 (3 large singlets, indicating 3 Bocs).

N^4-benzyl-N^4-*tert*-butyloxycarbonyl-1,4-bis-aminocyclohexane-1-carboxylic acid (**3.9c**). In a 500 mL flask, N^4-benzyl-N^4-*tert*-butyloxycarbonyl-4-amino-7,9-diaza-7,9-bis-*tert*-butyloxycarbonyl-8,10-dioxo-spiro[5,4]cyclodecane (**3.8c**) (3.26 g, 5.68 mmol) was suspended in 150 mL of THF and treated with 49 mL of 1 N LiOH. The mixture was stirred vigorously overnight at room temperature. The resulting suspension was diluted with an additional 50 mL of 1 N LiOH and the THF removed under reduced pressure. The remaining aqueous solution was washed with diethyl ether (3 x 50 mL) and the pH of the aqueous layer adjusted from 11 to 7 with 10 % citric acid solution. The aqueous layer was concentrated under reduced pressure, cooled, and filtration on Buchner funnel resulted in a white solid (1.83 g) which was used without further purification. ^{1}H NMR (200 MHz, DMSO d_6) δ 1.43 (large singlet, indicating only 1 Boc).

N^4-benzyl-N^4-*tert*-butyloxycarbonyl-N^1-(9-fluorenylmethyloxycarbonyl)-1,4-bis-aminocyclohexane-1-carboxylic acid (**3.10c**). To an Ar-flushed three-neck flask containing N^4-benzyl-N^4-*tert*-butyloxycarbonyl-1,4-bis-aminocyclohexane-1-carboxylic acid (**3.9c**) (1.83 g, 5.25 mmol), 100 mL of methylene chloride and DIEA (2.47 mL, 15.75 mmol) were added. Following 5 minutes of stirring, TMS-Cl (1.66 mL, 13.12 mmol) was added via syringe. The solution was heated to reflux for 3 hours followed by cooling in an ice bath. To this cooled solution, Fmoc-Cl (1.49 g, 5.78 mmol) was added and stirred for 4 hr. The resulting solution was washed with 1 N HCl (2 x 50 mL), dried over $MgSO_4$, and the solvent removed under reduced pressure to yield a yellow solid. Purification of the crude mixture by column chromatography (95:5 chloroform:methanol) resulted in a white solid, N^4-benzyl-N^4-*tert*-butyloxycarbonyl-N^1-(9-fluorenylmethyloxycarbonyl)-1,4-bis-aminocyclohexane-1-carboxylic acid (**3.10c**). (0.87 g in an overall yield of 13.7%). ^{1}H NMR (250 MHz, $CDCl_3$) δ 7.73 (d, 2H), 7.57 (d, 2H), 7.36 (t, 2H), 7.29 (m, 7H), 4.89 (s, 1H) 4.41 (d, 2H), 4.33 (s, 2H), 4.16 (t, 1H), 4.00 (bm, 1H), 2.11 (bm, 2H), 1.79 (bm, 2H), 1.54 (bm, 4H), 1.40 (s, 9H). ^{13}C NMR (100 MHz, DMSO d_6) δ 175.87, 155.40, 155.25, 143.81, 140.72, 140.02, 128.15, 127.63, 127.02, 126.70, 126.49, 125.35, 120.08, 79.19, 65.21, 57.25, 54.16, 46.76, 46.10, 31.02, 28.01, 25.07. FAB-MS (glycerol) m/z 571.2 $(M+H)^+$.

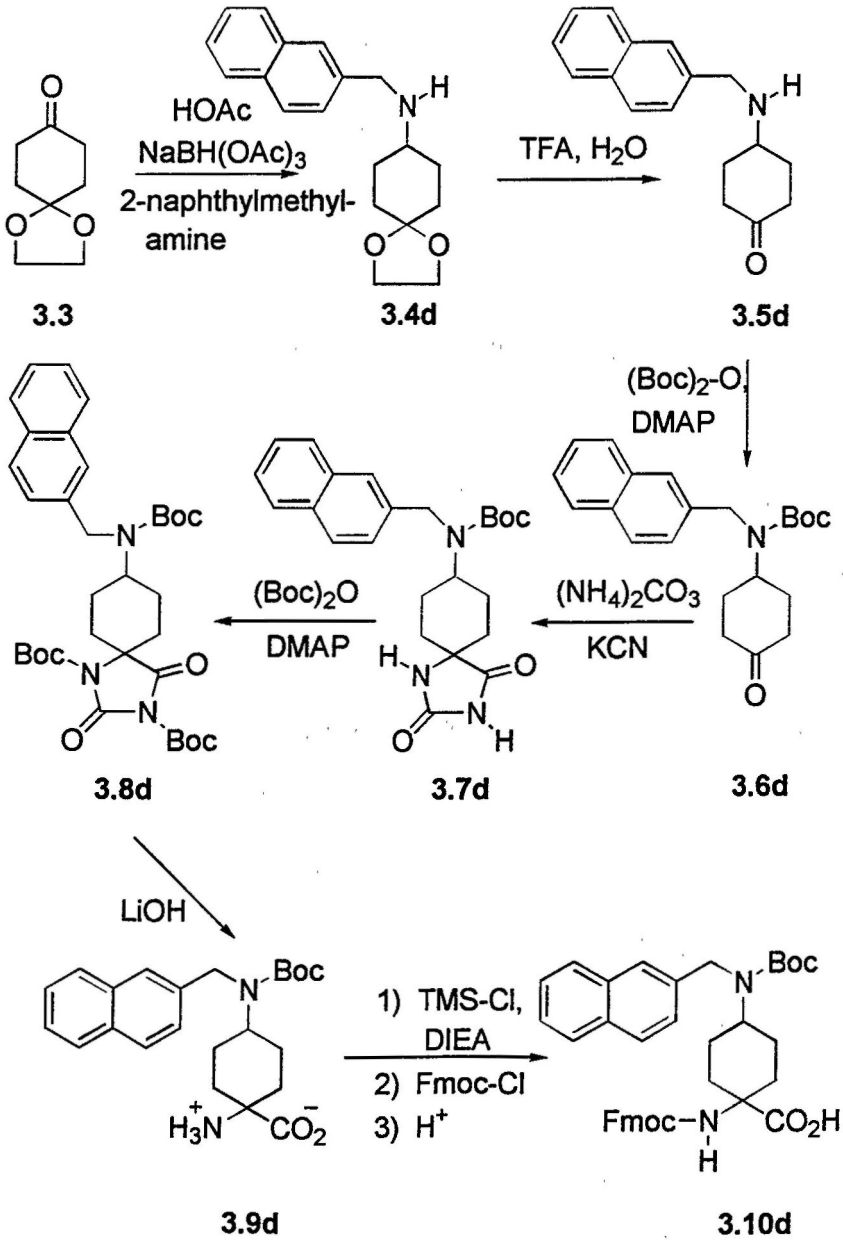

3.4.4 N^4-*tert*-butyloxycarbonyl-N^1-(9-fluorenylmethyloxycarbonyl)-N^4-(2-naphthylmethyl)-1,4-bis-aminocyclohexane-1-carboxylic acid (3.10d)

N-(2-naphthylmethyl)-4-amino-7,10-dioxa-spiro[5,4]cyclodecane (**3.4d**). An Ar-purged flask was charged with 4-oxo-7,10-dioxa-spiro[5,4]cyclodecane (**3.3**)

(5.00 g, 32.0 mmol) and 150 mL of DCE. Acetic acid (1.83 mL, 32.0 mmol) and (5.11 g, 35.2 mmol) 2-naphthylmethylamine were added sequentially to this solution. After stirring for 30 minutes, $NaBH(OAc)_3$ (21.71 g, 102.5 mmol) was added to the flask. The reaction mixture was monitored by GC-MS analysis. Once all starting material had been consumed (18 h), the reaction mixture was concentrated under reduced pressure and taken up in 200 mL of methylene chloride. The organic solution was washed with 10 % Na_2CO_3 (3 x 100 mL), dried over $MgSO_4$, and concentrated under reduced pressure. The resulting solid (7.94 g) was carried on to the next step without further purification. GC/MS m/z 296 $(M)^+$.

N-(2-naphthylmethyl)-4-aminocyclohexanone (**3.5d**). A solution of *N*-(2-naphthylmethyl)-4-amino-7,10-dioxa-spiro[5,4]cyclodecane (**3.4d**) (7.94 g, 26.8 mmol) in 60 mL of THF was treated with 20 mL of 20 % TFA/ H_2O solution and refluxed at 80° C until GC-MS showed that all starting material had been consumed. The solvents were removed under reduced pressure and the resulting oil taken up in 200 mL of methylene chloride. The organic solution was washed with 10% Na_2CO_3 (3 x 100 mL), dried ($MgSO_4$), and concentrated under reduced pressure. The resulting oil (6.78 g) was carried on to the next step without further purification. GC/MS m/z 253 $(M)^+$.

N-tert-butyloxycarbonyl-N-(2-naphthylmethyl)-4-aminocyclohexanone (**3.6d**). In a flask equipped with a mercury bubbler, *N*-(2-naphthylmethyl)-4-aminocyclohexanone (**3.5d**) (6.78 g, 26.8 mmol) was dissolved in 200 mL of

methylene chloride and treated with Et_3N (3.73 mL, 26.80 mmol). After 5 minutes of stirring, $(Boc)_2$-O (18.92 g, 86.70 mmol) and DMAP (0.35 g, 2.89 mmol) were added. The resulting mixture was stirred vigorously for 24 h and the organic solution was diluted with an additional 100 mL of methylene chloride. This solution was washed with 1 N HCl (2 x 120 mL), 10 % Na_2CO_3 (1 x 100 mL), brine (1 x 100 mL), and dried over $MgSO_4$. The solvent was removed under reduced pressure and the resulting oil (9.46 g) was used without further purification. ^{1}H NMR (200 MHz, DMSO d_6) δ 1.40 (large singlet, indicating Boc).

N^4-*tert*-butyloxycarbonyl-*N*^{4}-(2-naphthylmethyl)-4-amino-7,9-diaza-8,10-dioxo-spiro[5,4] cyclodecane (**3.7d**). A solution of *N-tert*-butyloxycarbonyl-*N*-(2-naphthylmethyl)-4-aminocyclohexanone (**3.6d**) (9.46 g, 26.80 mmol) in 25 mL of methanol was treated with a solution of $(NH_4)_2CO_3$ (8.27 g, 86.1 mmol) and KCN (5.61 g, 86.1 mmol) in 25 mL of H_2O. The mixture was refluxed at 65° C for 48 h. The solution was removed from heat and the methanol removed under reduced pressure. Vacuum filtration of the resulting suspension gave a brown solid. The solid was dissolved in the minimum amount of methylene chloride and precipitated by the addition of hexanes. A white solid (7.66 g) was collected by vacuum filtration and carried on to the next step without further purification. ^{13}C NMR (50 MHz, DMSO d_6) δ 178.99, 157.29, 154.83 (indicating 3 carbonyls present).

N^4-*tert*-butyloxycarbonyl-N^4-(2-naphthylmethyl)-4-amino-7,9-diaza-7,9-bis-tert-butyloxycarbonyl-8,10-dioxo-spiro[5,4]cyclodecane (**3.8d**). In a 500 mL flask

equipped with a mercury bubbler, N^4-*tert*-butyloxycarbonyl-N^4-(2-naphthylmethyl)-4-amino-7,9-diaza-8,10-dioxo-spiro[5,4] cyclodecane (**3.7d**) (1.03 g, 2.43 mmol) was suspended in 200 mL of THF and treated with $(Boc)_2$-O (1.59 g, 7.29 mmol) and DMAP (0.03 g, 0.24 mmol). The mixture was stirred vigorously for 48 h at room temperature. The solvent was removed under reduced pressure and the resulting residue was taken up in 200 mL of methylene chloride, washed with 10 % citric acid solution (2 x 100 mL), 10 % Na_2CO_3 (3 x 100 mL), and dried over $MgSO_4$. The solvents were removed under reduced pressure to yield a solid (1.31 g) which was used without further purification. ^{1}H NMR (200 MHz, $CDCl_3$) δ 1.58, 1.47, 1.44 (3 large singlets, indicating 3 Bocs).

N^4-*tert*-butyloxycarbonyl-N^4-(2-naphthylmethyl)-1,4-bis-aminocyclohexane-1-carboxylic acid (**3.9d**). In a 500 mL flask, N^4-*tert*-butyloxycarbonyl-N^4-(2-naphthylmethyl)-4-amino-7,9-diaza-7,9-bis-*tert*-butyloxycarbonyl-8,10-dioxo-spiro [5,4]cyclodecane (**3.8d**) (1.31 g, 2.11 mmol) was suspended in 200 mL of THF and treated with 50 mL of 1 N LiOH. The mixture was stirred vigorously overnight at room temperature. The resulting suspension was diluted with an additional 50 mL of 1 N LiOH and the THF removed under reduced pressure. The remaining aqueous solution was washed with diethyl ether (3 x 50 mL) and the pH of the aqueous layer adjusted from 11 to 7 with 10 % citric acid solution. The aqueous layer was concentrated under reduced pressure, cooled, and filtration on Buchner funnel

resulted in a white solid (0.84 g) which was used without further purification. ^{13}C NMR (50 MHz, DMSO d_6) δ 181.36, 154.82 (indicating only 2 carbonyls present).

N^4-*tert*-butyloxycarbonyl-N^1-(9-fluorenylmethyloxycarbonyl)-N^4-(2-naphthylmethyl)-1,4-bis-aminocyclohexane-1-carboxylic acid (**3.10d**). To an Ar-flushed three-neck flask containing N^4-*tert*-butyloxycarbonyl-N^4-(2-naphthylmethyl)-1,4-bis-aminocyclohexane-1-carboxylic acid (**3.9d**) (0.84 g, 2.11 mmol), 100 mL of methylene chloride and DIEA (1.18 mL, 6.78 mmol) were added. Following 5 minutes of stirring, TMS-Cl (0.69 mL, 5.42 mmol) was added via syringe. The solution was heated to reflux for 3 hours followed by cooling in an ice bath. To this cooled solution, Fmoc-Cl (0.70 g, 2.71 mmol) was added and stirred for 4 hr. The resulting solution was washed with 1 N HCl (2 x 75 mL), dried over $MgSO_4$, and the solvent removed under reduced pressure to yield a yellow solid. Purification of the crude mixture by column chromatography (95:5 chloroform:methanol) resulted in a white solid, N^4-*tert*-butyloxycarbonyl-N^1-(9-fluorenylmethyloxycarbonyl)-N^4-(2-naphthylmethyl)-1,4-bis-aminocyclohexane-1-carboxylic acid (**3.10d**). (0.70 g in an overall yield of 18.7%). ^1H NMR (300 MHz, DMSO d_6) δ 8.48 (s, 1H), 7.96 (m, 2H), 7.80 (m, 2H), 7.69 (m, 3H), 7.30 (bm, 8H), 4.92 (s, 2H), 4.85 (d, 1H), 4.75 (m, 2H), 3.60 (bm, 1H), 2.13 (bm, 2H), 1.74 (bm, 4H), 1.51 (bm, 2H)1.46 (s, 9H). ^{13}C NMR (100 MHz, $CDCl_3$) δ 183.93, 155.99, 155.85, 143.86, 141.41, 134.68, 133.79, 130.92, 129.01, 127.75, 127.14, 126.20, 125.99, 125.78, 125.65, 125.40, 125.10,

123.44, 119.99, 80.29, 66.61, 58.20, 54.50, 47.40, 45.00, 32.72, 28.52, 25.55. FAB-MS (glycerol) m/z 621.0 $(M+H)^+$.

3.5 References

3.1 Prasad, B. V. V.; Balaram, P. *CRC Crit. Rev. Biochem.* **1984**, *16*, 307-348.

3.2 Balaram, P. *Curr. Opin. Struct. Biol.* **1992**, *2*, 845-851.

3.3 Toniolo, C.; Benedetti, E. *Trends Biochem. Sci.* **1991**, *16*, 350-353.

3.4 Benedetti, E. *Biopolymers (Peptide Sci.)*, **1996**, *40*, 3-44.

3.5 Yokum, T. S.; Gauthier, T. J.; Hammer, R. P.; Mclaughlin, M. L. *J. Am. Chem. Soc.*, **1997**, *119*, 1167-1168.

3.6 Toniolo, C.; Polese, A.; Formaggio, F.; Crisma, M.; Kamphuis, J. *J. Am. Chem. Soc.* **1996**, *118*, 2744-2745.

3.7 Karle, I. L.; Flippen-Anderson, J. L.; Gurunath, R.; Balaram, P. *Protein Science* **1994**, *3*, 1547-1555.

3.8 Basu, G.; Bagchi, K.; Kuki, A. *Biopolymers* **1991**, *31*, 1763-1774.

3.9 Basu, G.; Kuki, A. *Biopolymers* **1993**, *33*, 995-1000.

3.10 4-Aminopiperidine-4-carboxylic acid is the only polar α,α-AA known to promote helical structures; Wysong, C. L.; Yokum, T. S.; Morales, G. A.; Gundry, R. L.; McLaughlin, M. L.; Hammer, R. P. *J. Org. Chem.* **1996**, *61*, 7650-7651.

3.11 Gershonov, E.; Granoth, R.; Tzehoval, E.; Gaoni, Y.; Fridkin, M. *J. Med. Chem.* **1996**, *39*, 4833-4843.

3.12 Burgess, K.; Lim, D.; Ho, K.; Ke, C. *J. Org. Chem.* **1994**, *59*, 2179-2185.

3.13 Yokum, T. S.; Elzer, P. H.; McLaughlin, M. L. *J. Med. Chem.* **1996**, *39*, 3603-3605.

3.14 Abdel-Magid, A. F.; Maryanoff, C. A.; Carson, K. G.; *Tetrahedron Lett.* **1990**, *31*, 5595-5598.

3.15 Kates, S.A.; Solé, N.A.; Johnson, C.R., Hudson, D.; Barany, G.; Albericio, F. *Tetrahedron Lett.* **1993**, *34*, 1549-1552.

3.16 Bergs, H. German Patent 566,094 (May 26, 1929); Chem. Abst. **1933**, *27*, 1001.

3.17 Bucherer, H. T.; Steiner, W. *J. Prakt. Chem.* **1934**, *140*, 291-316.

3.18 Edward, J. T.; Jitrangsri, C. *Can. J. Chem.* **1975**, *53*, 3339-3350.

3.19 Kubik, S.; Meissner, R. S.; Rebek, J. *Tetrahedron Lett.* **1994**, *35*, 6635-6638.

3.20 Bolin, D. R.; Sytwu, I.-I.; Humiec, F.; Meienhofer, J. *Int. J. Pept. Protein Res.* **1989**, 353-359.

Chapter 4

Solvent Effects on the 3_{10}- /α-Helix Equilibrium in Short Amphipathic Peptides Rich in α,α-Disubstituted Amino Acids*

4.1 Introduction

Prediction of peptide secondary structure (α-helix, β-sheet, 3_{10}-helix, etc.) *a priori* from amino acid sequence is a primary goal of *de novo* protein design and protein folding studies.[4.1-4.3] Relative to the α-helix and β-sheet, the factors favoring formation of the 3_{10}-helix (*i, i + 3* hydrogen bonding; constituting ~10% of protein structure) are only beginning to be understood.[4.4-4.8] The 3_{10}/α-helix equilibrium is being intensely studied because the 3_{10}-helix is a likely protein folding intermediate to the α-helix conformation.[4.9-4.14] Also, short stretches of 3_{10}-helix occur frequently in globular proteins and protein recognition steps may involve facile transitions between the α-helix and 3_{10}-helix.[4.14-4.16] Experiments probing the 3_{10}/α-helix equilibrium have almost exclusively focused on short hydrophobic peptides composed

*Reprinted in part with permission from *Journal of the American Chemical Society*, **1997**, *Volume 119*, pages 1176-1186; T. Scott Yokum, Ted J. Gauthier, Robert P. Hammer, Mark L. McLaughlin, Solvent Effects on the 3_{10}- /α-Helix Equilibrium in Short Amphipathic Peptides Rich in α,α-Disubstituted Amino Acids.

of several α,α-disubstituted amino acids (ααAAs), such as oligomers of α-aminoisobutyric acid (Aib, α-methylalanine) (Figure 4.1).[4.17-4.20] Studies of these peptides have been limited to spectroscopic measurements in organic solvents (e.g., dimethylsulfoxide, methanol, trifluoroethanol (TFE), acetonitrile (CH_3CN), etc.) or X-ray structure determinations of peptides crystallized from organic solvents.[4.21-4.24] In contrast, α-helix stability has been studied in aqueous and aqueous/organic milieu with short well-defined peptides.[4.25-4.27] Herein, we report the synthesis of three short, amphipathic, water-soluble peptides containing 80% ααAAs and the effects of aqueous/organic solvent composition on the 3_{10}/α-helix equilibrium by circular dichrosim (CD) spectroscopy.

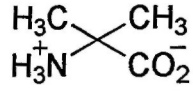

Figure 4.1. Structure of Aib.

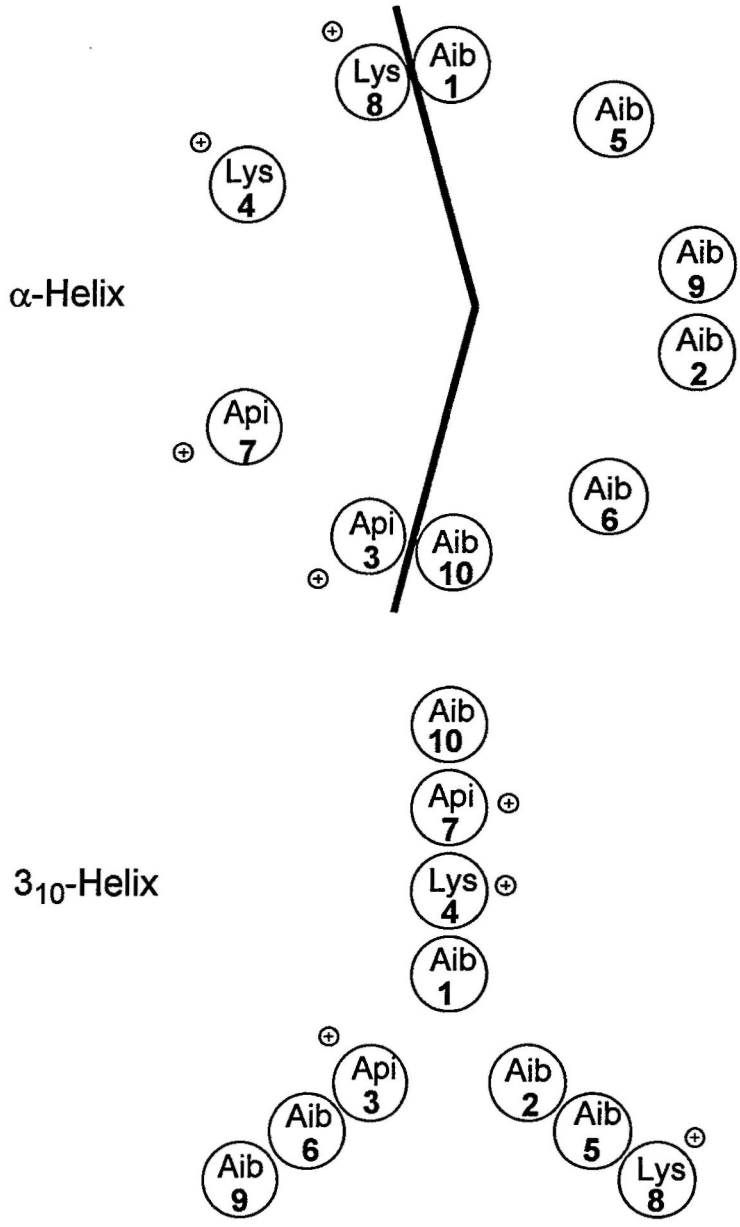

Pi-10 H-Aib-Aib-Api-Lys-Aib-Aib-Api-Lys-Aib-Aib-NH_2

Figure 4.2. The α- and 3_{10}-helical wheel diagrams and sequence of Pi-10.

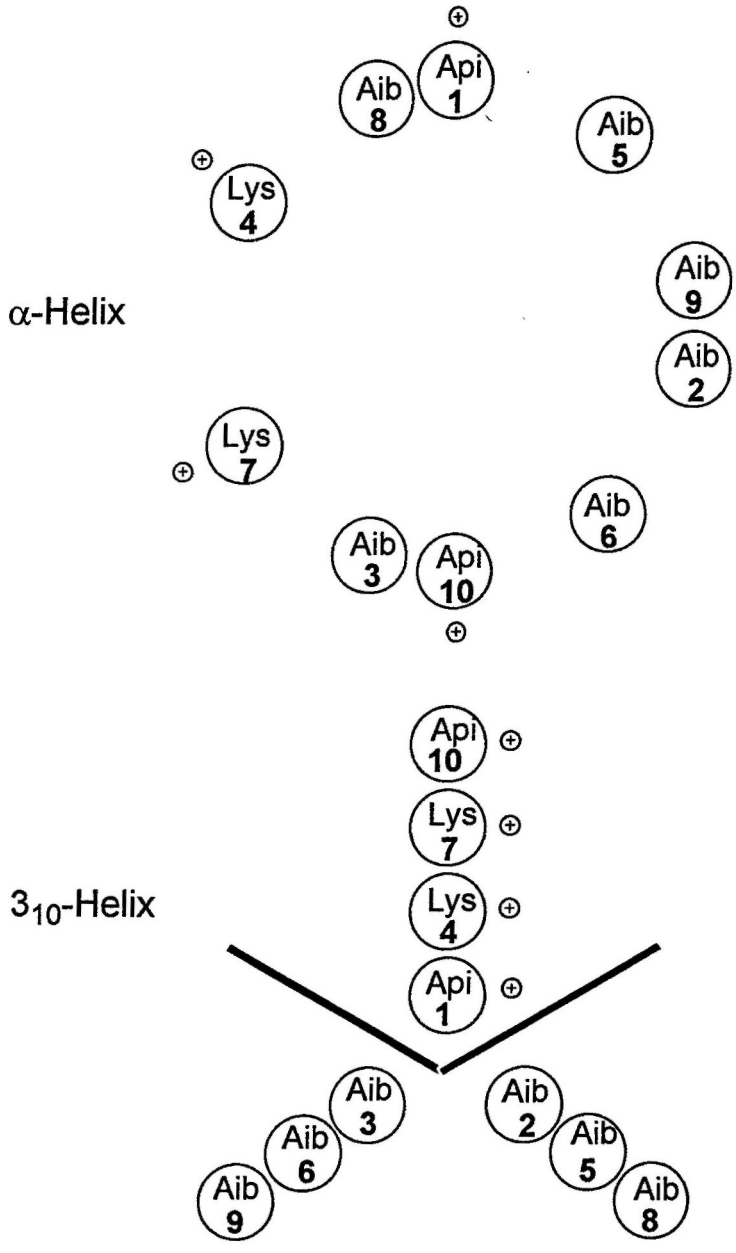

Ipi-10 H-Api-Aib-Aib-Lys-Aib-Aib-Lys-Aib-Aib-Api-NH_2

Figure 4.3. The α- and 3_{10}-helical wheel diagrams and sequence of Ipi-10.

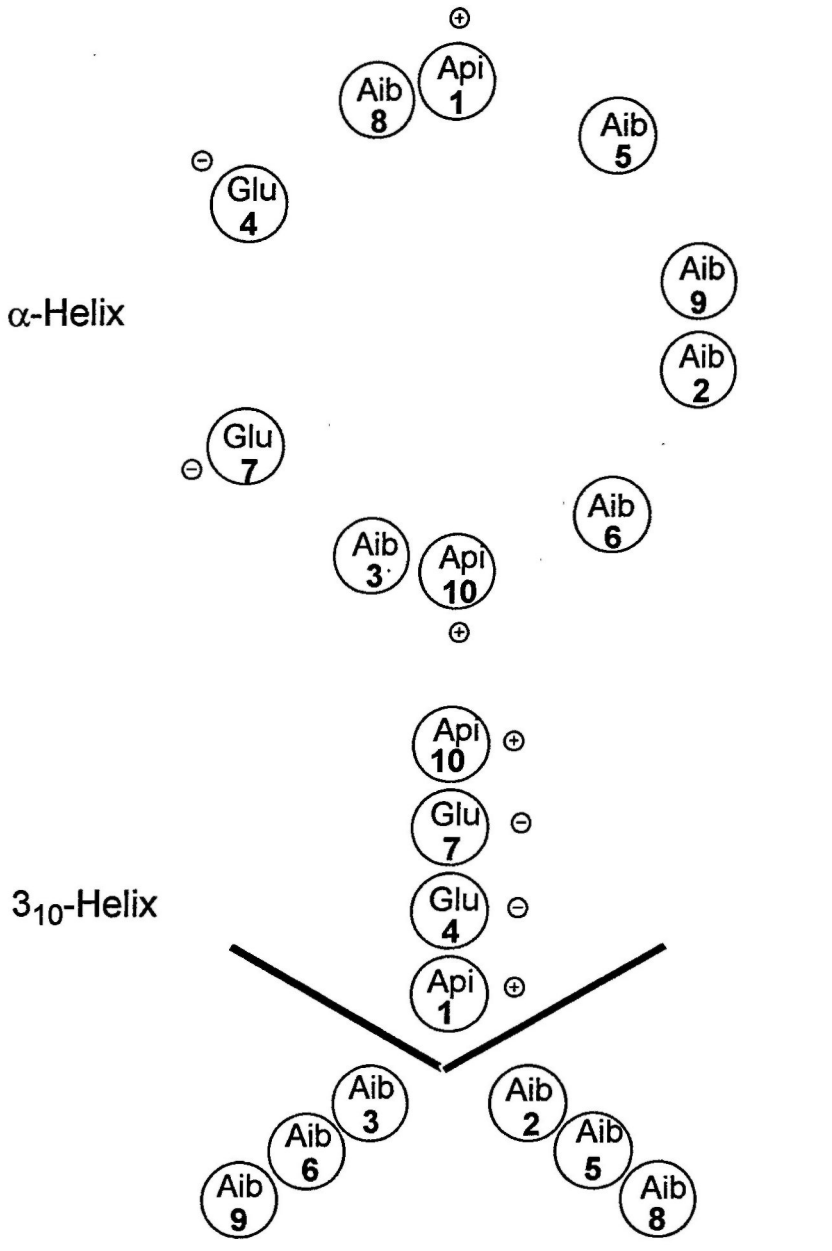

~~Ipi-10~~ H-Api-Aib-Aib-Glu-Aib-Aib-Glu-Aib-Aib-Api-NH_2

Figure 4.4. The α- and 3_{10}-helical wheel diagrams and sequence of Sb-10.

4.2 Results

The peptides are designed to form amphipathic helices with charged residues forming a hydrophilic face and non-polar residues forming a hydrophobic face when viewed along the helical axis.[4.28-4.29] Pi-10 is designed to form an amphipathic α-helix and Sb-10 and Ipi-10 are designed to form amphipathic 3_{10}-helices; all three peptides are less amphipathic in the alternative helical forms (Figures 4.2-4.4). High percentages of ααAAs are incorporated to promote helicity, while only amphipathy is used to influence the preference of the 3_{10}- or α-helical conformations in Pi-10 and Ipi-10. Alternatively, Sb-10 utilizes amphipathy along with two designed salt-bridges for helix type determination and stabilization. The salt-bridges occur between glutamic acid 4 and 4-aminopiperidine-4-carboxylic acid (Api) (Figure 4.5) 1 and between glutamic acid 7 and Api 10. The oppositely charged amino acids are placed in the *i* and *i* + 3 positions to provide the additional stability in the 3_{10}-helical conformation.[4.25]

Peptides Pi-10 and Ipi-10 were synthesized as previously reported.[4.30,4.31] Sb-10 was synthesized via a combination of manual and automated solid-phase synthesis using a procedure developed for Ipi-10. The first three residues were coupled to PAL-PEG-PS by refluxing the 9-fluorenylmethyloxycarbonyl (Fmoc)-amino acid fluoride (8 equivalents) and diisopropylethylamine (3 equivalents) in methylene chloride. The coupling reactions were monitored by quantitative Fmoc cleavage tests.[4.32] After the first three residues were successfully coupled, the

remainder of the peptide was synthesized on a Milligen 9050 peptide synthesizer using preformed Fmoc-acid fluorides. The peptide was purified by reverse-phase HPLC and the molecular weight verified by matrix assisted laser desorption ionization mass spectrometry.

Helical peptides, either 3_{10}- or α-helical, display two minima in a CD spectrum. The CD $n\rightarrow\pi^*$ minimum is centered around 222 nm and the $\pi\rightarrow\pi^*$ minimum is centered around 207 nm.[4.33] The ratio R, where $R = [\theta]_{n\rightarrow\pi^*}/[\theta]_{\pi\rightarrow\pi^*}$, has been suggested as a parameter to distinguish α-helical and 3_{10}-helical secondary structure.[4.33-4.36] For a 3_{10}-helix $R \leq 0.4$, whereas $R \approx 1$ for the α-helix.[4.34-4.36] Tables 4.1, 4.2, and 4.3 show the % α-helicity and R for Pi-10 , the % 3_{10}-helicity/ α-helicity and R for Ipi-10, and the % 3_{10}/ α-helicity and R for Sb-10 in SDS micelles and in aqueous/organic solvent mixtures, respectively. The amphipathic design predetermined the helical conformation of the isomeric peptides in SDS micelles; Pi-10 shows a typical α-helical CD spectrum and Ipi-10 shows a CD spectrum indicative of a 3_{10}-helix (Figure 4.6). In contrast, Sb-10, a designed amphipathic 3_{10}-helix, exhibits a spectra indicative of an α-helix in micellular media (Figure 4.6). Pi-10 displays CD spectra and R values characteristic of α-helices in the organic and aqueous/organic solvent mixtures (Table 4.1 and Figure 4.7). The CD spectra and R values for Ipi-10 and Sb-10 indicate an α-helix to 3_{10}-helix transition as aqueous/organic solvent composition decreases from 50 to 0 % water (Tables 4.2, 4.3 and Figures 4.8, 4.9). The CD spectra of Sb-10 also indicate a transition from an

α-helix to a 3_{10}-helix upon titration with tetramethylammonium trifluoroacetate (TMAT) in 9:1 acetonitrile-TFE from 0.1 M to pure 9:1 acetonitrile-TFE (Figure 4.10 and Table 4.3). A highly organic soluble salt, such as TMAT, is required for titration of the Sb-10 side-chains because strong 3_{10}-helix character is only present in 100 % organic media.

The % α-helix was estimated using the equation: % α-helix = $-100([\theta]_{n\rightarrow\pi^*}+ 3000) / 33000$, where the minimum for the $[\theta]_{n\rightarrow\pi^*}$ is observed from 222-225 nm.[4.29] No methods have been suggested in the literature for the calculation of % 3_{10}-helicity, so we have used as a model 3_{10}-helix, the CD spectra of H-(Leu-Arg-Leu)$_8$ -OH in diphosphatidylcholine liposomes, where $[\theta]_{\pi\rightarrow\pi^*}$ = -21,500 deg cm^2 dmol^{-1} is defined as 100% 3_{10}-helix.[4.34] Therefore, the % 3_{10}-helix can be estimated using the equation: % 3_{10}-helix = $(100)[[\theta]_{\pi\rightarrow\pi^*}/-21{,}500]$.

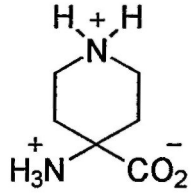

Figure 4.5. Structure of Api.

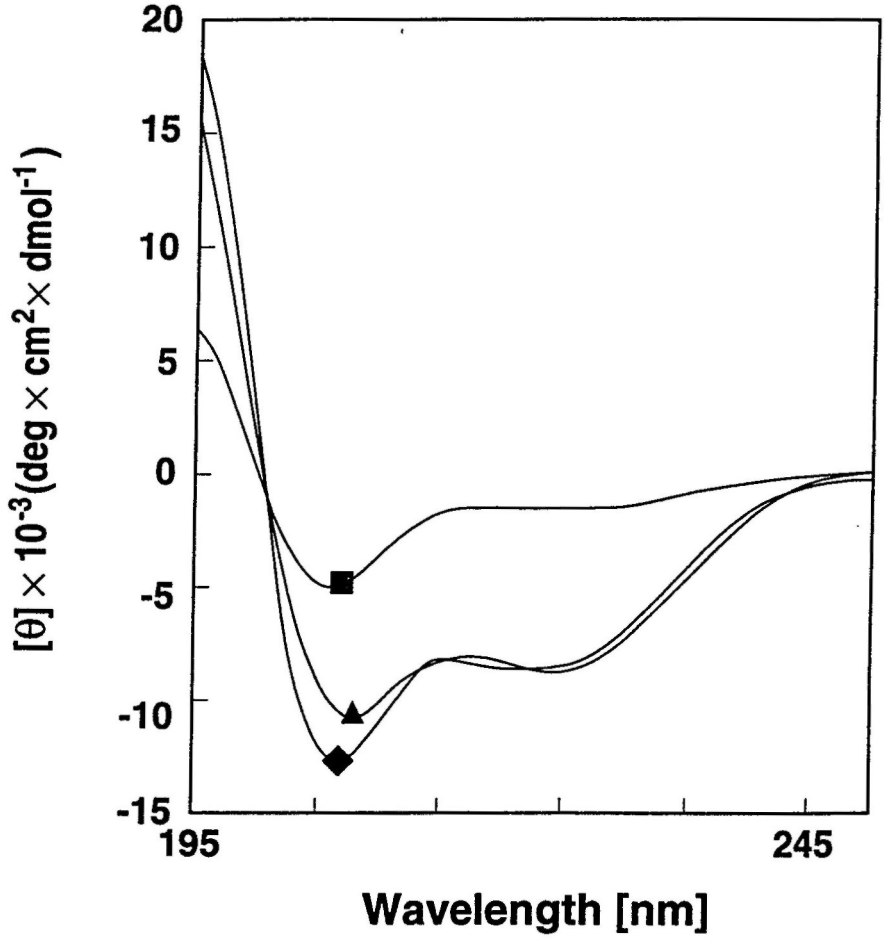

Figure 4.6. CD spectra of Pi-10 (▲),Ipi-10 (■), and Sb-10 (◆) in SDS.

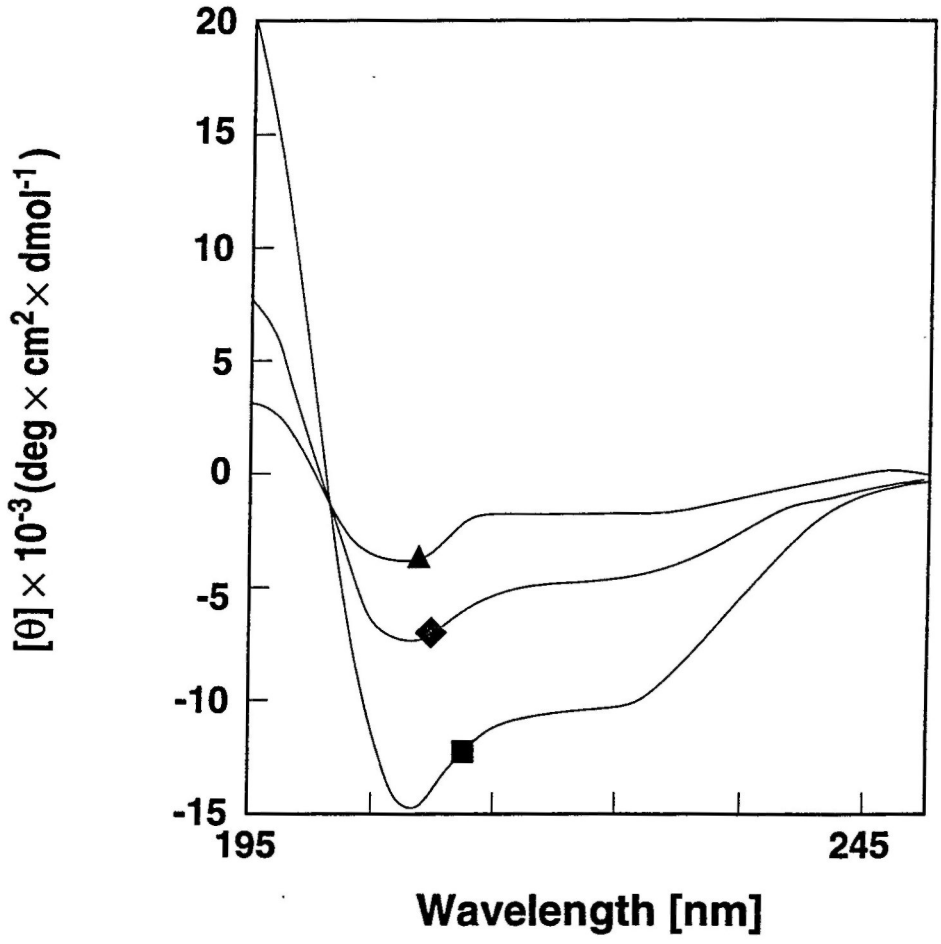

Figure 4.7. CD spectra of Pi-10 in 1:1 CH_3CN-H_2O(▲), 9:1 CH_3CN-H_2O (◆), and 9:1 CH_3CN-TFE(■).

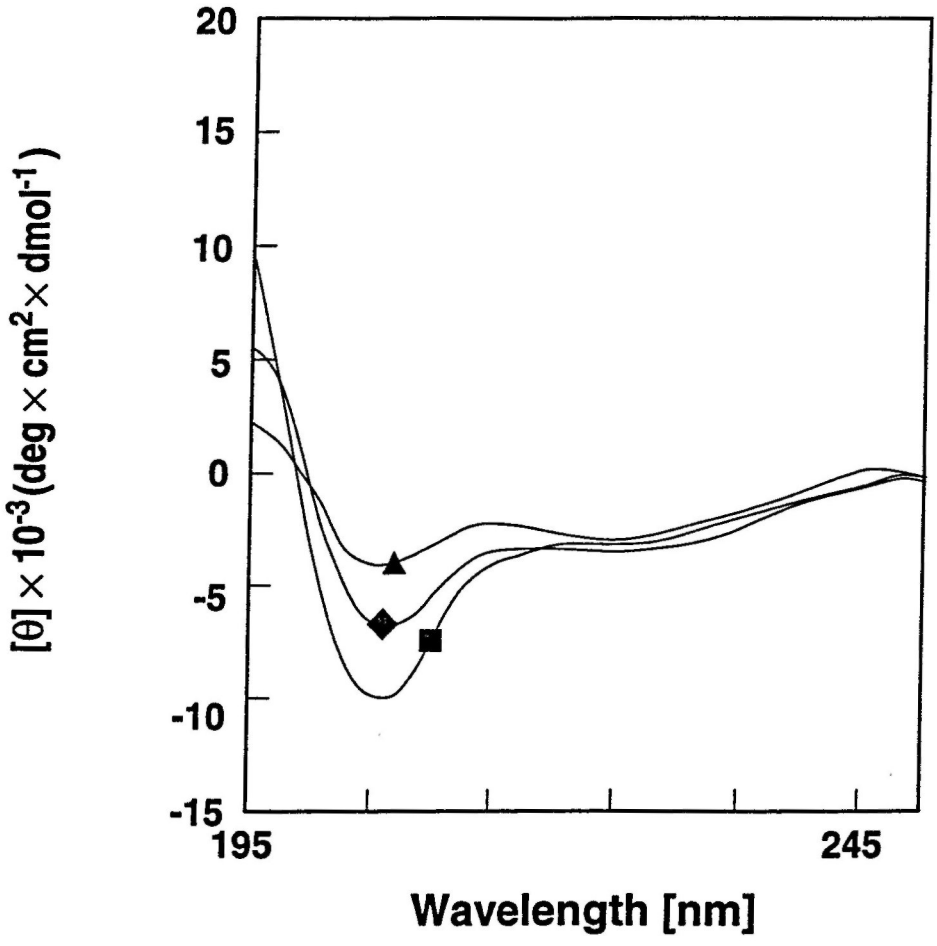

Figure 4.8. CD spectra of Ipi-10 in 1:1 CH_3CN-H_2O(▲), 9:1 CH_3CN-H_2O (◆), and 9:1 CH_3CN-TFE(■).

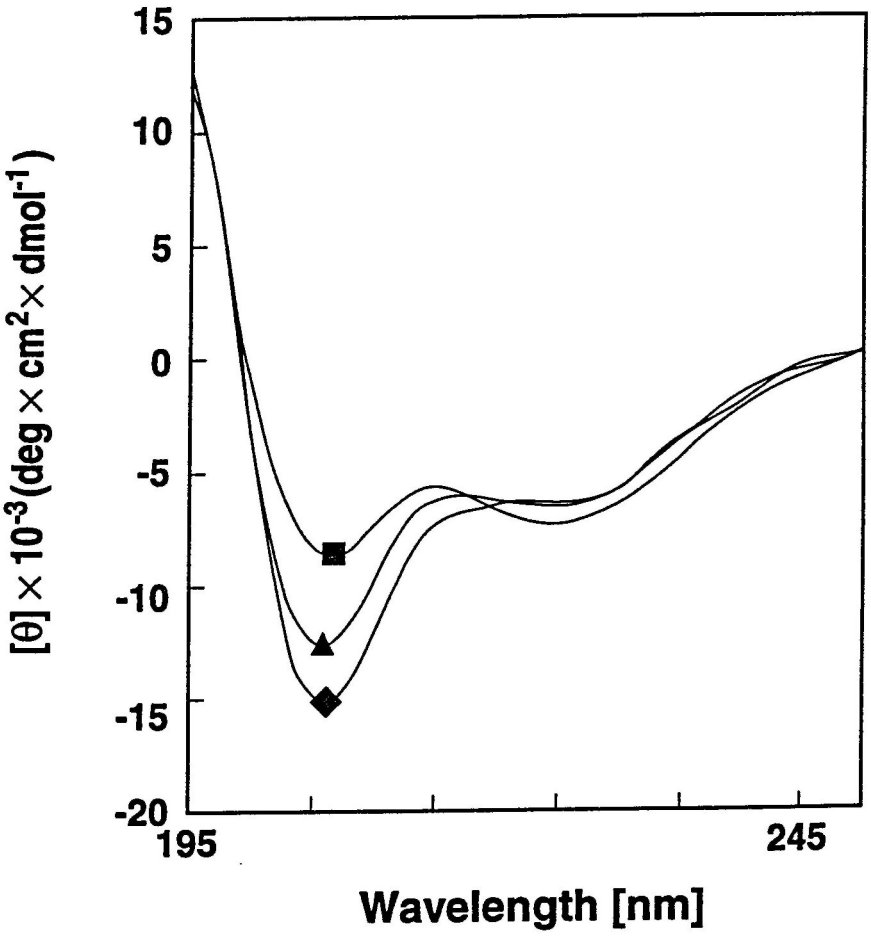

Figure 4.9. CD spectra of Sb-10 in 1:1 CH_3CN-H_2O(■), 9:1 CH_3CN-H_2O (▲), and 9:1 CH_3CN-TFE(◆).

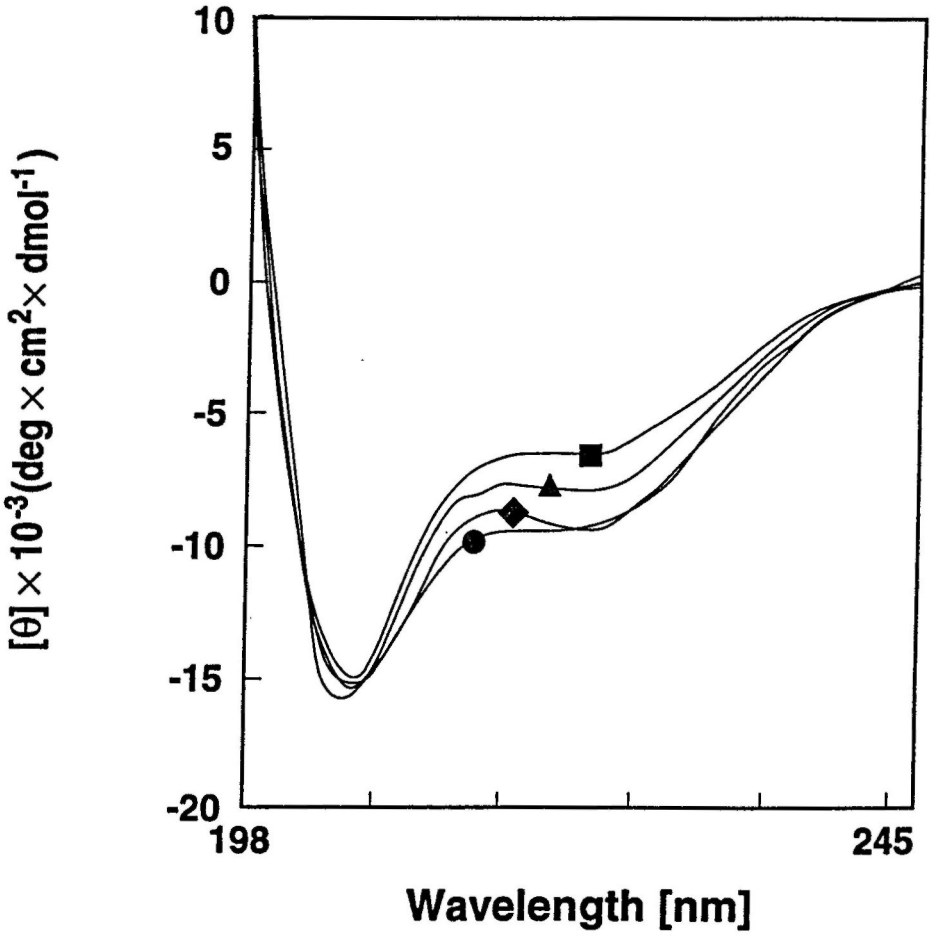

Figure 4.10. CD spectra of Sb-10 with 0.1 M TMAT in 9:1 CH_3CN-TFE(●),0.01 M TMAT in 9:1 CH_3CN-TFE(◆),0.01 M TMAT in 9:1 CH_3CN-TFE(▲) and 9:1 CH_3CN-TFE(■).

Table 4.1

CD data and derived structural parameters for Pi-10.

Solvent	$[\theta]_{\pi\rightarrow\pi^*}$ [a,b]	$[\theta]_{n\rightarrow\pi^*}$ [b,c]	*R*	% Helicity
25 mM SDS	-11860	-9605	0.81	38 (α)
9:1 CH_3CN-TFE	-14647	-10299	0.72	40 (α)
9:1 CH_3CN-H_2O	-7382	-4785	0.65	23 (α)
1:1 CH_3CN-H_2O	-3818	-1899	0.50	15 (α)

[a] Units for [θ] are deg cm^2 $dmol^{-1}$.
[b] The minimum for the $[\theta]_{\pi\rightarrow\pi^*}$ band is observed in the range from 205-209 nm.
[c] The minimum for the $[\theta]_{n\rightarrow\pi^*}$ band is observed in the range from 222-225 nm.

Table 4.2

CD data and derived structural parameters for Ipi-10.

Solvent	$[\theta]_{\pi\rightarrow\pi^*}$ [a,b]	$[\theta]_{n\rightarrow\pi^*}$ [b,c]	*R*	% Helicity
25 mM SDS	-5516	-1750	0.32	25 (3_{10})
9:1 CH_3CN-TFE	-9916	-3145	0.33	45 (3_{10})
9:1 CH_3CN-H_2O	-6740	-3605	0.54	*d*
1:1 CH_3CN-H_2O	-4204	-3118	0.74	19 (α)

[a] Units for [θ] are deg cm^2 $dmol^{-1}$.
[b] The minimum for the $[\theta]_{\pi\rightarrow\pi^*}$ band is observed in the range from 205-209 nm.
[c] The minimum for the $[\theta]_{n\rightarrow\pi^*}$ band is observed in the range from 222-225 nm.
[d] This peptide is likely a mixture of α-helical, 3_{10}-helical, and coil structures. The % α-helix is estimated at 20%; and the % 3_{10}-helix is estimated at 31%.

Table 4.3

CD data and derived structural parameters for Sb-10.

Solvent	$[\theta]_{\pi\rightarrow\pi^*}$ [a,b]	$[\theta]_{n\rightarrow\pi^*}$ [b,c]	*R*	% Helicity
25 mM SDS	-12695	-8813	0.69	36 (α)
9:1 CH_3CN-TFE	-15230	-6579	0.43	71 (3_{10})
9:1 CH_3CN-H_2O	-12749	-6461	0.50	*d*
1:1 CH_3CN-H_2O	-8673	-7433	0.85	31 (α)
0.1 M TMAT in 9:1 CH_3CN-TFE	-15774	-9576	0.61	*e*
0.01 M TMAT in 9:1 CH_3CN-TFE	-15038	-9235	0.61	*f*
0.001 M TMAT in 9:1 CH_3CN-TFE	-15333	-6531	0.43	71 (3_{10})

a Units for [θ] are deg cm^2 $dmol^{-1}$.

b The minimum for the $[\theta]_{\pi\rightarrow\pi^*}$ band is observed in the range from 205-209 nm.

c The minimum for the $[\theta]_{n\rightarrow\pi^*}$ band is observed in the range from 222-225 nm.

d This peptide is likely a mixture of α-helical, 3_{10}-helical, and coil structures. The % α-helix is estimated at 29%; and the % 3_{10}-helix is estimated at 59%.

e This peptide is likely a mixture of α-helical, 3_{10}-helical, and coil structures. The % α-helix is estimated at 57%; and the % 3_{10}-helix is estimated at 73%.

f This peptide is likely a mixture of α-helical, 3_{10}-helical, and coil structures. The % α-helix is estimated at 54%; and the % 3_{10}-helix is estimated at 70%.

4.3 Discussion

The wealth of information on short α-helical peptides in aqueous and aqueous/organic media has been critical to our current understanding of factors stabilizing such helices.[4.37-4.39] For monomeric α-helices, the α-helix/coil equilibrium shifts toward helix as organic composition increases.[4.40] The same phenomenon has been predicted from explicit solvent calculations on the 3_{10}-helix/coil equilibrium.[4.12] Peptides containing ααAAs are also known to favor helix over random coil which arises from the high helix propensities of the disubstituted residues.[4.17-4.24] As a result, ααAAs like the prototypical Aib are popular replacements for the natural amino acids in designed, helical peptides. In general, ≥ 50% ααAAs composition favors the 3_{10}-helix for short peptides.[4.17-4.24] However, the studies deriving this trend have been confined to organic media due to the lack of polar ααAAs. The lysine-like ααAA, Api, can now be readily incorporated into peptides by solid-phase methods.[4.30,4.31] The cationic ααAA acts as a helix-promoting, water-solubilizing, and amphipathic design element in the peptide sequences. As a result, spectroscopic studies on peptides containing Api and high percentages of ααAAs can be performed in aqueous milieu. The ability to study the peptides in aqueous media should provide further experimental insights into the relative stability of 3_{10}- and α-helical structures in water, which is currently a hotly debated issue.[4.9-4.13]

There has been some confusion as to the best methods of defining the secondary structures of α- and 3_{10}-helices. More than a decade ago, Balaram and co-workers concluded there was no definitive difference in the CD spectra for the helix types.[4.36] The laboratories of Millhauser and Marshall have reported contradictory assignments on similar peptides using ESR double-labeling with different spin-labeled amino acids as probes.[4.6-4.8,4.12] Also, differentiation between α- and 3_{10}-helices in ααAA rich peptides is difficult via NMR because of the lack of α-hydrogens on the ααAAs and the repetitive nature of the Aib rich peptides.[4.41] Recently, Toniolo and co-workers concluded that CD spectroscopy can reliably differentiate the helix types in organic solution.[4.35] The 3_{10}-helix shows an R value ≤ 0.4 while the R value is approximately 1 for the α-helix. Also, the positive CD band centered near 195 nm is much weaker in the 3_{10}-helix relative to the α-helix. Toniolo's results support CD spectral assignments reported for putative amphipathic 3_{10}-helices in phospholipid vesicles and simulations of the 3_{10}-helix CD spectra.[4.33,4.34]

Sb-10 and the sequence permutation isomers, Pi-10 and Ipi-10, contain only two chiral amino acids: the L-glutamic acids and the L-lysines, respectively. The remainder of the peptide is composed of eight ααAAs: six Aibs and two Apis. The high percentage of ααAAs are incorporated to promote helicity in the resulting peptides. The proteinogenic residues are included to induce a right-handed helix (detectable by CD) and are well separated and near the middle of the sequences to

have maximal effect.[4.42,4.43] A peptide devoid of chiral amino acids would have no preference for the formation of a right or left-handed helix and as a result, would not be detectable by CD.

Pi-10 and Ipi-10 are designed to be cationic, α-helical and 3_{10}-helical peptides, respectively. Amphipathy is the only design feature incorporated to influence the formation of the desired helix type in Pi-10 and Ipi-10. Sb-10 is designed identical to Ipi-10 with the exception of glutamic acids replacing the two lysines. This design results in an amphipathic 3_{10}-helix and places the two Api residues and the two glutamic acids "on top" (i, $i + 3$) of each other in the 3_{10}-helical conformation. The i, $i + 3$ placement of the glutamic acids and Apis introduces ionic interactions to provide additional helix stability. Baldwin reported the first utilization of ion-pairing for α-helix stabilization in designed peptides.[4.25] Oppositely charged residues (Glu and Lys) with i, $i + 4$ positioning exhibited helix stabilizing characteristics while i, $i + 3$ positioning did not increase α-helix stability. Later studies confirmed these results and found that combinations of various cationic and anionic residues (i, $i + 4$) may also be used for α-helical stabilization.[4.44] The i, $i + 3$ spacing of the oppositely charged residues in Sb-10 should add stability to the 3_{10}-helix while not stabilizing the α-helix.

The peptides showed minimal secondary structure in *p*H 7.1, 2.5 mM phosphate buffer or after addition of up to 10% acetonitrile (see experimental). The random coil conformation of these peptides shows little CD spectra due to the high

percentage of achiral amino acids. Treatment of Pi-10 peptide with 25 mM SDS micelles induces transition to a typical α-helix CD spectra with R = 0.81 and % α-helix = 38% (Table 4.1 and Figure 4.6). The CD spectra of Ipi-10 in the presence of SDS micelles has an R = 0.32 indicating a 3_{10}-helical structure (Table 4.2 and Figure 4.6). The 3_{10}-helicity of Ipi-10 is estimated at 25%. Additionally, the positive CD band centered near 195 nm is much weaker for Ipi-10 than for the α-helical Pi-10, which has been noted in other studies of 3_{10}-helical peptides and is predicted by theory.[4.33-4.35]

In contrast, SDS forces Sb-10 in to an α-helical conformation even though it is designed to form a 3_{10}-helix. The R value for Sb-10 in micelles is 0.74 and the percent α-helicity is estimated at 36% (Table 4.3 and Figure 4.6). The α-helical structure in SDS may be due to a host of factors such as incomplete micelle binding and ion pairing of the charged side-chains with the SDS sulfonates. Sb-10 contains only a + 1 overall charge and therefore is expected to bind much less than Ipi-10 (+ 5 overall charge). Also, a significant degree of ion pairing with the SDS may screen the effective strength of the intra-peptide salt-bridge. It has been previously shown that the helix stability of salt-bridged α-helical peptides decreases with increasing salt concentrations.[4.25] The formation of an α-helical structure in SDS is consistent with the titration of Sb-10 with TMAT where 3_{10}-helix stability decreases as the salt concentration is increased.

The incomplete binding and ion pairing may cause the solvent environment of Sb-10 to have greater aqueous solvent characteristics. In an aqueous medium, the α-helix is energetically favored over the 3_{10}-helix.[4.5] This has been suggested by theoretical calculations and evidenced in the organic/water titration experiment by the transition of Sb-10 from a 3_{10}-helix to an α-helix as the percent water is increased.[4.5] Even though these factors induce an α-helix, SDS still promotes some structure because Sb-10 exhibits a higher degree of helicity in this media as compared to 100% buffer.

CD spectra of Pi-10, Ipi-10, and Sb-10 were taken in 50-100% aqueous-organic solvent mixtures (Tables 4.1-4.3 and Figures 4.7-4.9). In the aqueous/organic solvent mixtures (1:1 CH_3CN/H_2O, 9:1 CH_3CN/H_2O, 9:1 CH_3CN/TFE[4.45]), Pi-10 behaves as a normal α-helical peptide, exhibiting a clear cooperative helix/coil transition. An isodichroic point appears at 201 nm and helicity decreases with decreasing organic solvent composition. The shift of the α-helix/coil equilibrium toward helix as organic composition increases agrees with what is known for monomeric α-helices.[4.28] However, as Pi-10 contains 80% ααAAs and has no two α-amino acids together, both Karle and Balaram and Kuki would have predicted this sequence to be 3_{10}-helical.[4.21,4.42] Karle and Balaram reported that short peptides with ≥ 50% ααAAs will form a 3_{10}-helices and Kuki reported that peptides containing high percentages of ααAAs with no two monosubstituted amino acids together will form 3_{10}-helices.[4.21,4.42] Also, according to calculations, Pi-10 should

have been increasingly 3_{10}-helical as organic solvent content increased.[4.5] Thus, amphipathic design is more important than the mere percentage of ααAAs or order of α-amino acids and ααAAs in the sequence. In contrast, Ipi-10 shows a transition from an α-helix to a 3_{10}-helix as the percent organic is increased. Ipi-10 displays a weak α-helical structure in 1:1 CH_3CN/H_2O, significant 3_{10}-helical character in 9:1 CH_3CN/H_2O and strong 3_{10}-helical character in 9:1 CH_3CN/TFE (45% 3_{10}-helicity). Similar trends have been noted for the *N*-terminal acetylated peptides, Pi-10-ac and Ipi-10-ac (see experimental).

The series of CD spectra taken of Sb-10 in 50% to 100% organic solution indicate a transition from an α-helix to a 3_{10}-helix. Sb-10 exhibits moderate α-helicity in 1:1 CH_3CN/H_2O and begins to show 3_{10}-helical character in 9:1 CH_3CN/H_2O. When treated with 9:1 CH_3CN/TFE, Sb-10 displays very strong 3_{10}-helical character in the CD spectra (71% 3_{10}-helicity). The percent 3_{10}-helicity of Sb-10 is much higher than that of Ipi-10 (71% vs. 45%) suggesting that the two salt-bridges significantly stabilize the 3_{10}-helical conformation with multiple factors considered (i.e. identical peptide length, percent ααAAs, type ααAAs, placement of ααAAs, and similar helix propensities of Lys and Glu). The transition of Sb-10 from an α-helix to a 3_{10}-helix as the TMAT concentration is decreased also suggests that the ionic interactions stabilize the 3_{10}-helical conformation. The trend of decreasing 3_{10}-helix stability as the salt concentration is increased parallels what has been observed for salt-bridge containing α-helical peptides.[4.25]

The transition of Sb-10 and Ipi-10 from an α-helix to a 3_{10}-helix as the percent organic is increased agrees with the theoretical calculations of the solvent effects on the 3_{10}-/α-helix equilibrium. Marshall's calculations revealed that Aib rich peptides favor the α-helix in water while the 3_{10}-helix is favored in less polar media.[4.5] The stability of the 3_{10}-helix in non-polar media arises from the additional hydrogen bond formed as compared to the α-helix.[4.5] Aqueous environments favor the α-helix because of the more favorable interactions of the additional exposed carbonyl and amide with water.[4.5]

The relatively low absolute helicities of the peptides can be accounted for in part by helix end effects and by incomplete micelle binding.[4.29,4.46,4.47] For the 10-mer peptide, Pi-10, in a totally α-helical conformation, a maximum number of 7 hydrogen bonds are possible. This leaves the three *N*-terminal amides and the two *C*-terminal carbonyls without internal hydrogen bonding partners. For Ipi-10 in a totally 3_{10}-helical conformation, a maximum number of 8 hydrogen bonds are possible. This leaves the two *N*-terminal amides and the two *C*-terminal carbonyls without internal hydrogen bonding partners. In either peptide both termini may achieve non-ideal structures at the termini to interact with solvent.[4.48]

Currently, there are no accepted models for estimation of the % 3_{10}-helix by CD. This is due to the lack of a large structural database as is available for α-helix and β-sheet. Also, theoretical calculations suggest that the absolute intensity of CD bands of 3_{10}-helical peptides will be highly dependent on the ϕ and ψ torsion angles

in the peptide backbone. It is known that 3_{10}-helical, ααAA-containing peptides have different ϕ and ψ angles than 3_{10}-helical peptides having only proteinogenic amino acids.[4.21-4.24,4.33] In light of this, the peptide Ac-(αMeVal)$_8$-O*t*Bu, recently prepared and studied by Toniolo and coworkers, may be a better 3_{10}-helical model for Sb-10 and Ipi-10 than H-(Leu-Arg-Leu)$_8$-OH we used for the % 3_{10}- helix calculation (%3_{10}-helix = (100)[$[\theta]_{\pi\rightarrow\pi^*}$/-21,500]).[4.34,4.35] Assuming Ac-(αMeVal)$_8$-O*t*Bu is 100% helical in TFE with $[\theta]_{\pi\rightarrow\pi^*}$ = -9000 deg cm^2 dmol^{-1}, the calculated 3_{10}-helicity for Ipi-10 in SDS micelles and 9:1 CH_3CN/TFE would be 60% and 110% respectively. Clearly, more work is needed on the correlation of solid-state structure with solution structure (circular dichroism and nuclear magnetic resonance) of 3_{10}-helical peptides before helical content of such peptides can be accurately estimated.

4.4 Conclusions

These results show that amphipathy is a design tool for both α-helical and 3_{10}-helical structures, even in very short peptides rich in ααAAs. Additionally, the amphipathic design is primary in controlling secondary structure, overriding other factors such as the number of ααAA residues and the order of α-amino acids and ααAAs in the sequence, which are often thought to be key in controlling the 3_{10}/α-helix equilibrium.[4.21,4.42] We have been able to confirm experimentally what had previously been calculated, *viz.* that at least some peptides rich in ααAAs are more stable as 3_{10}-helices in organic solvents than in aqueous environments.[4.5] Also, we

have been able to show the first example of 3_{10}-helical peptide stabilization via salt-bridges. Utilization of the positively charged ααAA, Api, as a helix-promoting, amphipathic design element in Pi-10, Ipi-10, and Sb-10 was key to these findings. We are currently exploring other structural features such as self-aggregation and side chain bridging to stabilize 3_{10}-helices in water to gain further experimental insights into factors controlling the 3_{10}/α-helix equilibrium.

4.5 Experimental

4.5.1 Peptide Synthesis

Pi-10, Pi-10-ac, Ipi-10, and Ipi-10-ac were synthesized as previously reported.[4.30,4.31] Sb-10 was synthesized by manually coupling the first 3 residues onto a PAL-PEG-PS solid support. The couplings were done by refluxing 8 equivalents of the Fmoc-acid fluoride, 3 equivalents of DIEA, and the resin in methylene chloride. The couplings were allowed to reflux until an acceptable yield was determined by a quantitative Fmoc test.[4.32] After the first three residues were coupled to the resin, the remainder of the peptide was synthesized using a Milligen 9050 peptide synthesizer on the PAL-PEG-PS solid support using 8 equivalents of preformed Fmoc-acid fluorides, 3 equivalents of DIEA and a 1.5 h recycling time. Residues were double coupled when they were third in a series of α,α-disubstituted amino acids. A solution of 20% piperidine/2% 1,8-diazobicyclo[4.5.0]undec-7-ene (DBU) in DMF was used for Fmoc removal.

Sb-10 was simultaneously cleaved from the resin and side-chain deprotected using reagent B (8.8 : 0.2 : 0.5 : 0.5, trifluoroacetic acid (TFA) : triisopropylsilane : water : phenol).[4.49] The resulting acidic solution was diluted with 30% acetic acid, washed with ethyl ether (4 x 50 mL), and lyophilized. The crude peptide was purified by preparative reverse-phase HPLC on a Waters 15 μm Deltapak C_4 column using a water (0.05% TFA) and acetonitrile (0.05% TFA) gradient system. The gradient was run from 10% to 50% organic and the absorption monitored at 222 nm. Purity of the peptide was checked on a Vydac 5 μm C_{18} column using the same conditions. Matrix assisted laser desorption ionization (MALDI) mass spectrometry was used to verify peptide mass. Sb-10, 1039.6 $(M + H)^+$.

4.5.2 Acid Fluoride Synthesis

Under argon, Fmoc-glutamic acid (γ-*tert*-butyl ester) (3.0 g 7.05 mmol) was dissolved in 100 mL of methylene chloride followed by the addition of pyridine (0.623 mL 7.76 mmol) and cyanuric fluoride (1.19 mL 14.1 mmol). The reaction was allowed to stir for 4 h at room temperature. The reaction mixture was diluted with an additional 150 mL of methylene chloride, poured onto ice water, and filtered. The organic layer was washed with ice water (2 x 150 mL), dried over $MgSO_4$, and evaporated *in vacuo* to yield the acid fluoride as a white solid. For best results, the acid fluorides must be prepared fresh (within 24 h of use). Fmoc-glutamic acid (γ-*tert*-butyl ester) (82 % yield) ^{1}H NMR (250 MHz DMSO-d_6) δ 7.95 (d, 2H), 7.89 (m, 3H), 7.42 (m, 4H), 4.32 (m, 3H), 4.06 (m, 1H), 2.37 (m, 2H), 1.90 (m 2H), 1.43 (s,

9H). For Fmoc-Api-(Boc) and Fmoc-Aib acid fluoride synthesis, see chapter 2 experimental.

4.5.3 Circular Dichroism

Circular dichroism measurements were taken on a (+)-camphor sulfonic acid calibrated Aviv 60DS spectropolarimeter at 25 °C. The measurements were recorded over 250-195 nm using a 0.1 cm pathlength quartz cell, 1.2 nm bandwidth, 10 nm/min scan speed, and a 5 second time constant. Background spectra were acquired prior to each sample spectra and the two subtracted. Three repetitive scans were recorded and averaged to improve resolution. The reported mean residue elipticity, [θ] (deg cm^2 $dmol^{-1}$) is derived from the observed elipticity, $[\theta]_{obs}$ (millidegrees), using the formula $[\theta] = [\theta]_{obs}$ (MRW/10*lc*). MRW is the mean residue molecular weight of the peptide (molecular weight of the peptide divided by the number of peptide bonds), *l* is the pathlength (cm), and *c* is the peptide concentration (mg/mL).

0.2 mM final peptide concentrations were used for all experiments. The peptides were dissolved in: trifluoroethanol for spectra taken in 9:1 CH_3CN:TFE and 9:1 CH_3CN:TFE with varying concentrations of TMAT; pH 7.1, 5.0 mM phosphate buffer for spectra taken is SDS; and doubly distilled water for the aqueous/organic spectra. For representative aqueous/organic experiments, pH 7.1, 2.5 mM buffer was also used as the aqueous component and the resulting spectra were nearly identical to the pure H_2O/CH_3CN spectra.

R values and percent helicity for the 9:1 H_2O:CH_3CN and buffer experiments. Ipi-10: (9:1 H_2O:CH_3CN), R = 0.64, % α-helicity = 15%; (buffer), R = 0.85, % α-helicity = 15%.

Pi-10: (9:1 H_2O:CH_3CN), R = 0.30, % α-helicity = 11%; (buffer), R = 0.68, % α-helicity = 16%. Sb-10: (9:1 H_2O:CH_3CN), R = 1.2, % α-helicity = 30%; (buffer), R = 1.3, %, α-helicity = 29%

R values and percent helicity for Ipi-10-ac and Pi-10-ac for the SDS, buffer, aqueous/organic, and organic experiments.

Ipi-10-ac: (SDS), R = 0.40, % 3_{10}-helicity = 34%; (buffer), R = 0.94, % α-helicity = 20%; (9:1 H_2O:CH_3CN), R = 0.93, % α-helicity = 20%; (1:1 H_2O:CH_3CN), R = 0.83, % α-helicity = 24%; (9:1 CH_3CN:H_2O), R = 0.61, % α-helicity = 20%, % 3_{10}-helicity = 41%; (9:1 CH_3CN:TFE), R = 0.28, % 3_{10}-helicity = 36%. Pi-10-ac: (SDS), R = 0.86, % α-helicity = 45%; (buffer), R = 0.72, % α-helicity = 18%; (9:1 H_2O:CH_3CN), R = 0.50, % α-helicity = 14%; (1:1 H_2O:CH_3CN), R = 0.53, % α-helicity = 17%; (9:1 CH_3CN:H_2O), R = 0.41, % α-helicity = 17%; (9:1 CH_3CN:TFE), R = 0.56, % α-helicity = 28%.

4.6 References

4.1 Scholtz, J. M.; Baldwin, R. L. *Annu. Rev. Biophys. Biomol. Struct.* **1992**, *21*, 95-118.

4.2 Hecht, M. H. *Proc. Natl. Acad. Sci. USA* **1994**, *91*, 8729-8730.

4.3 Betz, S. F.; Raleigh, D. P.; DeGrado, W. F. *Curr. Opin. Struct. Biol.* **1993**, *3*, 601-610.

4.4 Barlow, D. J.; Thornton, J. M. *J. Mol. Biol.* **1988**, *201*, 601-619.

4.5 Smythe, M. L.; Huston, S. E.; Marshall, G. R. *J. Am. Chem. Soc.* **1995**, *117*, 5445-5452.

4.6 Millhauser, G. L. *Biochemistry* **1995**, *34*, 3874-3877.

4.7 Miick, S. M.; Martinez, G. V.; Fioro, W. R.; Todd, A. P.; Millhauser, G. L. *Nature* **1992**, *359*, 653-655.

4.8 Hanson, P.; Martinez, G.; Millhauser, G.; Formaggio, F.; Crisma, M.; Toniolo, C.; Vita, C. *J. Am. Chem. Soc.* **1996**, *118*, 271-272.

4.9 Basu, G.; Kitao, A.; Hirata, F.; Go, N. *J. Am. Chem. Soc.* **1994**, *116*, 6307-6316.

4.10 Otoda, K.; Kitagawa, Y.; Kimura, S.; Imanishi, Y. *Biopolymers* **1993**, *33*, 1337-1345.

4.11 Tirado-Rives, J.; Maxwell, D. S.; Jorgensen, W. L. *J. Am. Chem. Soc.* **1993**, *115*, 11590-11593.

4.12 Smythe, M. L.; Nakaie, C. R.; Marshall, G. R. *J. Am. Chem. Soc.* **1995**, *117*, 10555-10562.

4.13 Smythe, M. L.; Huston, S. E.; Marshall, G. R. *J. Am. Chem. Soc.* **1993**, *115*, 11594-11595.

4.14 Toniolo, C.; Benedetti, E. *Trends Biochem. Sci.* **1991**, *16*, 350-353.

4.15 Gerstein, M.; Chothia, C. *J. Mol. Biol.* **1991**, *220*, 133-149.

4.16 McPhalen, C. A.; Vincent, M. G.; Picot, D.; Jansonius, J. N.; Lesk, A. M.; Chothia, C. *J. Mol. Biol.* **1992**, *227*, 197-213.

4.17 Prasad, B. V. V.; Balaram, P. *CRC Crit. Rev. Biochem.* **1984**, *16*, 307-348.

4.18 Balaram, P. *Curr. Opin. Struct. Biol.* **1992**, *2*, 845-851.

4.19 Marshall, G. R.; Hodgkin, E. E.; Langs, D. A. Smith, G. D., Zabrocki, J.; Leplawy, M. T. *Proc. Natl. Acad. Sci. U.S.A.* **1990**, *87*, 487-491.

4.20 Augspurger, J. D.; Bindra, V. A.; Scheraga, H. A.; Kuki, A. *Biochemistry* **1995**, *34*, 2566-2576.

4.21 Karle, I. L.; Balaram, P. *Biochemistry* **1990**, *29*, 6747-6756.

4.22 Karle, I. L. *Acta Crystallogr. B* **1992**, *48*, 341-356.

4.23 Karle, I. L.; Flippen-Anderson, J. L.; Gurunath, R.; Balaram, P. *Biopolymers (Protein Sci.)* **1994**, *4*, 1547-1555.

4.24 Kennedy, D. F.; Crisma, M.; Toniolo, C.; Chapman, D. *Biochemistry* **1991**, *30*, 6541-6548.

4.25 Marqusee, S.; Baldwin, R. L. *Proc. Natl. Acad. Sci. U.S.A.* **1987**, *84*, 8898-8902.

4.26 Marqusee, S.; Robbins, V. H.; Baldwin, R. L. *Proc. Natl. Acad. Sci. U.S.A.* **1989**, *86*, 5286-5290.

4.27 Scholtz, J. M.; Marqusee, S.; Baldwin, R. L.; York, E. J.; Stewart, J. M.; Santoro, M.; Bolen, D. W. *Proc. Natl. Acad. Sci. U.S.A.* **1991**, *88*, 2854-2858.

4.28 For a review of the use of amphipathic design to induce α-helicity and its use in protein design see: Stewart, J. M. in *The Amphipathic Helix*, Epand, R. M., Ed., CRC Press, Boca Raton, FL. 1993; pp. 21-37.

4.29 Javadpour, M. M.; Juban, M. M.; Lo, W.-C. J.; Bishop, S. M.; Alberty, J. B.; Cowell, S. M.; Becker, C. L.; McLaughlin, M. L. *J. Med. Chem.* **1996**, *39*, 3107-3113.

4.30 Wysong, C. L.; Yokum, T. S.; Morales, G. A.; Gundry, R. L.; McLaughlin, M. L.; Hammer, R. P. *J. Org. Chem.* **1996**, *61*, 7650-7651.

4.31 Yokum, T. S.; Elzer, P. H.; McLaughlin, M. L. *J. Med. Chem.* **1996**, *39*, 3603-3605.

4.32 Fields, G. B.; Tian, Z.; Barany, G.. In *Synthetic Peptides: A User's Guide*; Grant, G. A., Ed.; W. H. Freeman and Co.: USA, 1992.

4.33 Manning, M.; Woody, R. W. *Biopolymers* **1991**, *31*, 569-586.

4.34 Iwata, T.; Lee, S.; Oishi, O.; Aoyagi, H.; Ohno, M.; Anzai, K.; Kirino, Y.; Sugihara, G. *J. Biol. Chem.* **1994**, *269*, 4928-4933.

4.35 Toniolo, C.; Polese, A.; Formaggio, F.; Crisma, M.; Kamphuis, J. *J. Am. Chem. Soc.* **1996**, *118*, 2744-2745.

4.36 Sudha, T. S.; Vijayakumar, E. K. S.; Balaram, P. *Int. J. Pept. Protein Res.* **1983**, *22*, 464-468.

4.37 Lau, S. Y. M.; Taneja, A. K.; Hodges, R. S. *J. Biol. Chem.* **1984**, *259*, 13253-13261.

4.38 Hu, J. C.; O'Shea, E. K.; Kim, P. S.; Sauer, R. T. *Science* **1990**, *250*, 1400-1403.

4.39 DeGrado, W. F.; Wasserman, Z.. R.; Lear, J. D. *Science* **1989**, *243*, 622-628.

4.40 Nelson, J. W.; Kallenbach, N. R. *Proteins* **1986**, *1*, 211-217.

4.41 Millhauser, G. L.; Stenland, C. J.; Hanson, P.; Bolin, K. A.; van de Ven, F. J. M. *J. Mol. Biol.* **1997**, *267*, 963-974.

4.42 Basu, G.; Bagchi, K.; Kuki, A. *Biopolymers* **1991**, *31*, 1763-1774.

4.43 Basu, G.; Kuki, A. *Biopolymers* **1993**, *33*, 995-1000.

4.44 Merutka, G.; Stellwagen, E. *Biochemistry* **1991**, *30*, 1591-1594.

4.45 The 9:1 acetonitrile/TFE was used because the the peptides were not soluble in pure acetonitrile.

4.46 Vijayakumar, E. K. S.; Sudha, T. S.; Balaram, P. *Biopolymers* **1984**, *23*, 877-886.

4.47 Shalongo, W.; Dugad, L.; Stellwagen, E. *J. Am. Chem. Soc.* **1994**, *116*, 8288-8293.

4.48 Bindra, V. A.; Kuki, A. *Int. J. Peptide Prot. Res.* **1994**, *44*, 539-548

4.49 Van Abel, R. J.; Tang, Y.; Rao, V. S. V.; Dobbs, C. H.; Tran, D.; Barany, G.; Selsted, M. E. *Int. J. Pept. Protein Res.* **1995**, *45*, 401-409.

Chapter 5

Benz[*f*]tryptophan, a Bathochromic Analog of Tryptophan, Synthesis of its N^{α}-Boc Derivative*

5.1 Introduction

The 3_{10}-/α-helix equilibrium is currently being intensely investigated.[5.1-5.4] This interest arises because the 3_{10}-helix is postulated to be a protein folding intermediate and may also participate in receptor binding.[5.5-5.6] However, there is not a large arsenal of methods available for the solution phase characterization of the 3_{10}-helix. Circular dichroism has only recently been shown as an effective method to characterize the 3_{10}-helix, while NMR and ESR have been applied in a limited number of systems.[5.7-5.11]

Fluorescence spectroscopy has exhibited the capability of effectively detecting the transition between a 3_{10}-helix and an α-helix using a fluorescence lifetime system (donor and acceptor system).[5.12] However, the donor incorporated into the system is an extrinsic probe which may perturb the desired peptide conformation when applied

*Reprinted in part from *Tetrahedron Letters, Volume 38*, T. Scott Yokum, Parithosh K. Tungaturthi, Mark L. McLaughlin, Benz[*f*]tryptophan, a Bathochromic Analog of Tryptophan, Synthesis of its N^{α}-*t*-Boc Derivative, Copyright 1997, pages 5111-5114, with kind permission from Elsevier Science Ltd. The Boulevard, Langford Lane, Kidlington, OX5 1GB, UK.

to other systems. The naphthalene based donor may also suffer from spectral overlap if tryptophan is present in the peptide or in a complex protein environment. A red-shifted intrinsic probe, which does not alter native peptide conformation, would be an ideal candidate for incorporation into this system.

Tryptophan is the most red-shifted of the natural amino acid fluorophores, thus its fluorescence can be studied even in complex protein environments containing tyrosine and phenylalanine residues.[5.13,5.14] Tryptophan's effectiveness may be limited when other tryptophans are present in the peptide or in the environment due to spectral overlap. To address this difficulty, we have designed a benzannulated tryptophan analog with absorbance and emission expected to be red-shifted from the natural amino acids and some extrinsic probes while minimally perturbing the peptide structure. Herein, we report the synthesis of N^{α}-*tert*-butyloxycarbonyl-benz[*f*]tryptophan, **5.1**, a fluorescent amino acid probe suitably protected for incorporation via solid-phase peptide synthesis (Figure 5.1).

As compared to the other benzannulated tryptophan derivatives: benz[*g*]tryptophan and benz[*e*]tryptophan, benz[*f*]tryptophan best mimics the structure of tryptophan and should be the least perturbing of native peptide structure. Unfortunately, the electronic directing effects of the naphthalene moiety makes the synthesis of the benz[*f*]tryptophan the most difficult of the benzannulated tryptophans.[5.15] Benz[*g*]tryptophan and benz[*e*]tryptophan are conveniently synthesized via a Fisher indole synthesis with α- or β-naphthyl hydrazones and the

Michael adduct of acrylaldehyde and acetamidomalonic ester followed by hydrolysis and decarboxylation.[5.15] Since the Fisher indole route is not available for the synthesis of benz[*f*]tryptophan, the most obvious route is construction from benz[*f*]indole. However, very few methods have been reported for the synthesis of benz[*f*]indole and the syntheses have been long and low yielding.[5.16-5.19] Synthetic routes via 3-methylbenz[*f*]indole have been futile because of the instability of the intermediates.[5.15] Therefore, we have chosen a synthetic route which constructs the amino acid through a protected benz[*f*]indoline moiety.

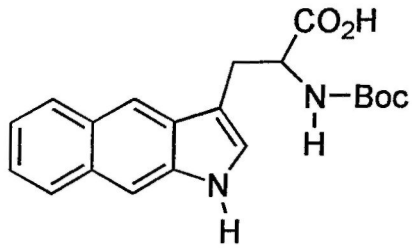

5.1

Figure 5.1. Structure of N^{α}-*tert*-butyloxycarbonyl-benz[*f*]tryptophan.

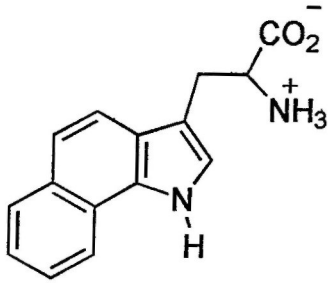

5.2

Benz[*g*]tryptophan

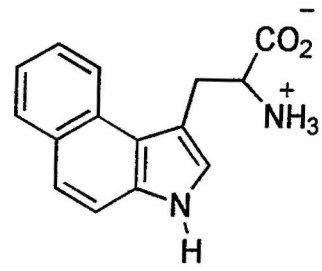

5.3

Benz[*e*]tryptophan

Figure 5.2. Structures of benz[*g*]tryptophan and benz[*e*]tryptophan.

5.2 Results and Discussion

The *N,N*-diallyl derivative of 3-bromo-2-aminonaphthalene, **5.4**, is generated by refluxing 3-bromo-2-aminonaphthalene with 8 equivalents of allyl bromide and excess sodium carbonate in *N,N*-dimethylformamide (DMF) to yield **5.5** (Figure 5.3).[5.20,5.21] A convenient route to pure 3-bromo-2-aminonaphthalene involves nitrating commercially available 2-bromonaphthalene-bis(hexachlorocyclopentadiene)

adduct followed by a retro-Diels-Alder and reduction of the nitro to yield 3-bromo-2-aminonaphthalene.[5.22]

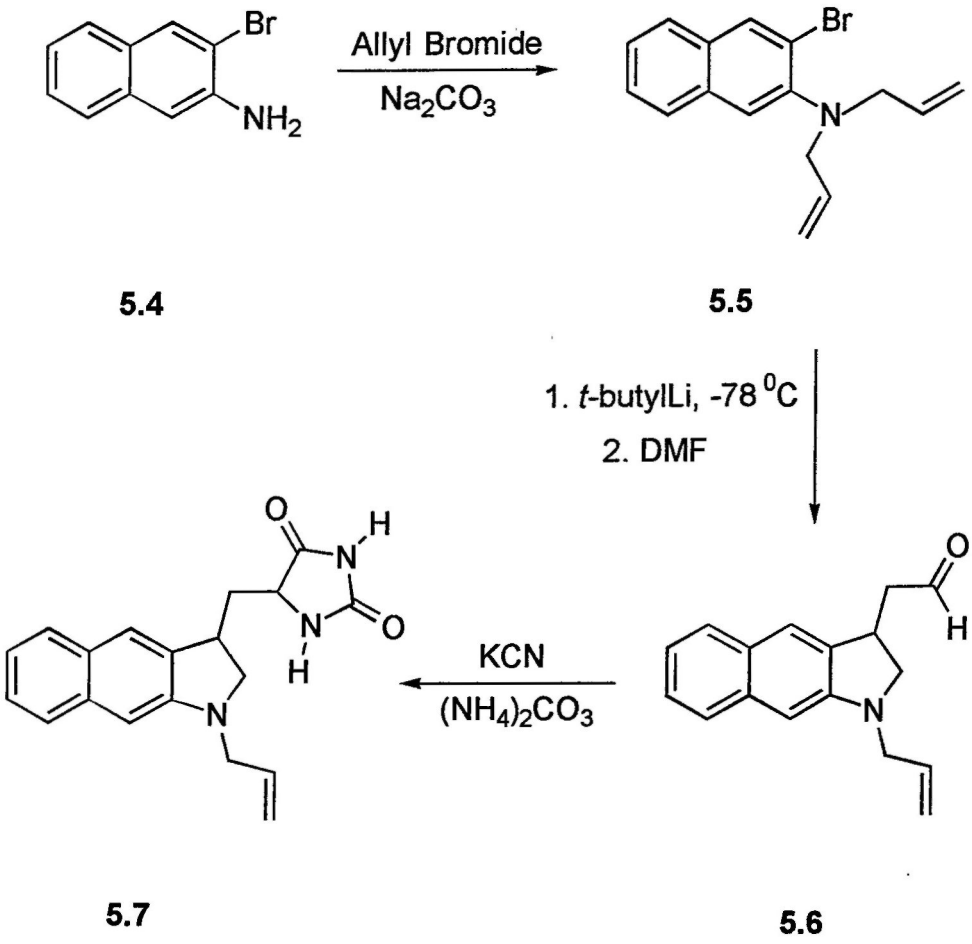

Figure 5.3. Synthesis of indoline **5.7**.

The indoline backbone is formed via an anionic cyclization of **5.5**. The cyclization is done by treating the diallyl derivative, **5.5**, with 2.2 equivalents of *tert*-butyllithium at -78° C in *tert*-butyl methyl ether (TBME) for 1 hour and warming to room temperature for 15 minutes.[5.20] The solution is cooled back to -78° C, 3 equivalents of DMF are added, and the resulting mixture is allowed to warm to room temperature.[5.21] The organic solution is washed with 10% NH_4Cl solution and the aldehyde, **5.6**, is isolated (Figure 5.3). As expected, the anionic cyclization failed to take place unless the temperature is raised.[5.20,5.21] This is evidenced by taking a small aliquot of the solution before warming to room temperature (after *tert*-butyllithium treatment), reacting with excess DMF and quenching with water. GC/MS analysis reveals almost quantitative formation of an isomeric product which is presumably the naphthaldehyde derivative.

The aldehyde, **5.6**, is converted to its corresponding hydantoin, **5.7**, using modified Bucherer-Bergs conditions; 3 equivalents of KCN, 3 equivalents of $(NH_4)_2CO_3$ in a 1:1:1 mixture of methanol:tetrahydrofuran (THF):water with heating to 60° C for 4 days (Figure 5.3).[5.23-5.25] The aldehyde, **5.6**, was not soluble in the traditional methanol-water mixtures used for the Bucherer-Bergs procedure. As a result, THF was incorporated into the solvent mixture to increase the solubility of the hydrophobic molecule. Purification over silica gel (7:3 ethyl acetate:hexanes) yields pure hydantoin, **5.7**, as a mixture of diastereomers confirmed by NMR (49% from 2-bromo-3-aminonaphthalene).

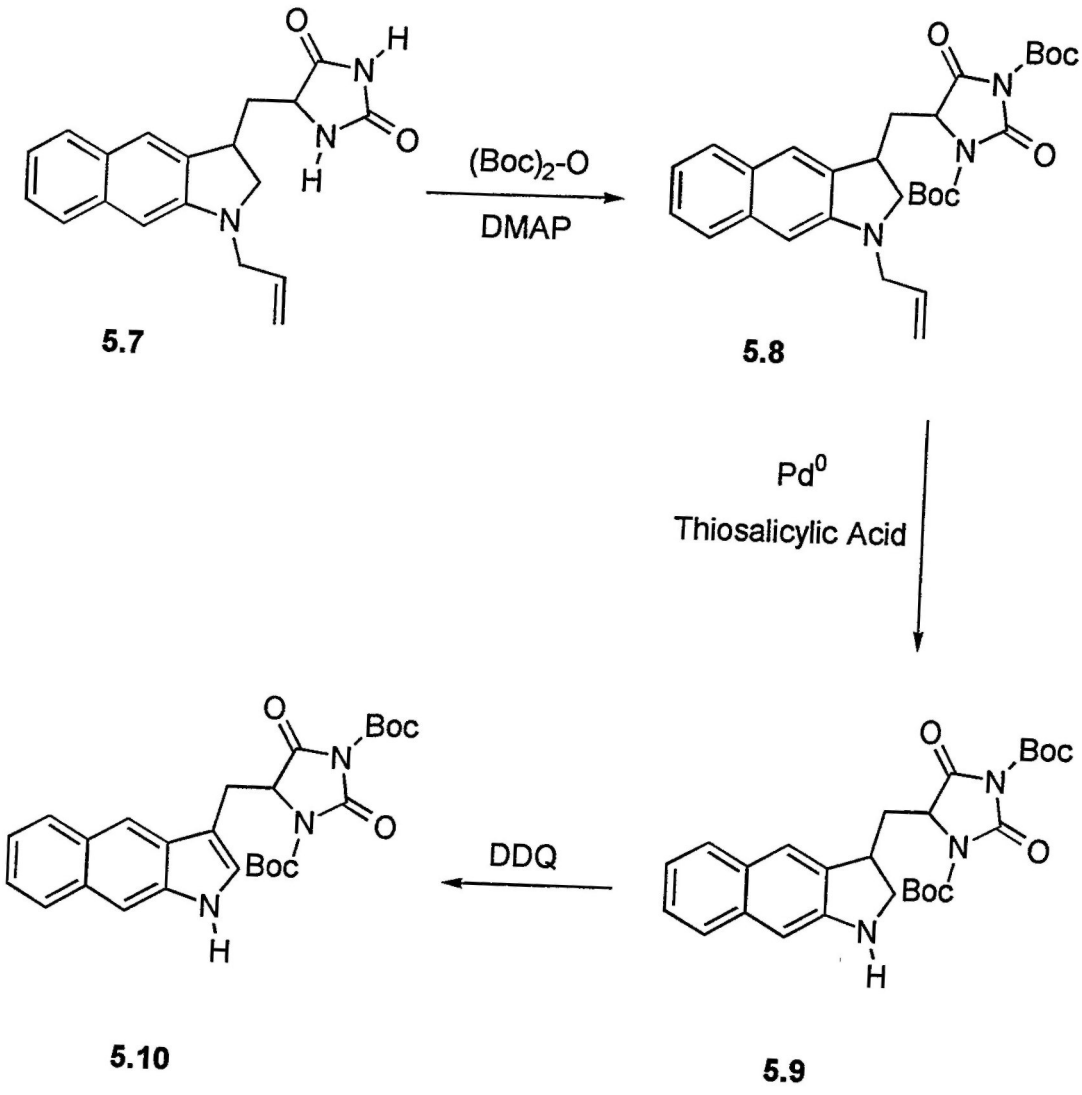

5.7 **5.8** **5.9** **5.10**

Figure 5.4. Synthesis of indole **5.10**.

The next logical step in the synthesis would be the removal of the allyl protecting group followed by oxidation to the indole. We found that after removal of the allyl group, the resulting hydantoin is only sparingly soluble in organic media. Therefore, we activate the hydantoin nitrogens with *tert*-butyloxycarbonyl (Boc) to allow mild hydrolysis of the hydantoin (discussed later) and to alleviate the solubility problem. Hydantoin **5.7** is treated with 3 equivalents of $(Boc)_2$-O and a catalytic amount of 4-*N,N*-dimethylaminopyridine (DMAP) in acetonitrile at room temperature to yield protected hydantoin, **5.8** (89%) (Figure 5.4).[5.23,5.24]

The allyl protection on the indoline nitrogen of hydantoin **5.8** is removed by refluxing with Pd^0 (tris(dibenzylideneacetone)-dipalladium(0)), 1,4-bis(diphenylphosphino)butane and thiosalicylic acid (used as a proton source and a cation scavenger) in dry THF according to the procedure of Genêt and coworkers (54%) (Figure 5.4).[5.27] The air sensitive indoline, **5.9**, is purified over silica gel ($CHCl_3$:hexanes:THF, 6:3:1) and immediately oxidized. The oxidation of the indoline is done by treating **5.7** with 1 equivalent of 2,3-dichloro-5,6-dicyano-1,4-benzoquinone (DDQ) in a TBME-methylene chloride mixture (24:1) for 1 hour to give indole, **5.10** (51%) (Figure 5.4).

Hydrolysis of hydantoins normally requires harsh conditions which may effect other functionalities in the molecule. We adapted a procedure developed by Rebek and co-workers for the mild hydrolysis of hydantoins by first activating the hydantoin nitrogens with the Boc groups followed by treatment with mild base to hydrolyze the

hydantoin.[5.28] The Boc protected hydantoin, **5.10**, is treated with 8 equivalents of 1N LiOH and THF as a co-solvent for 24 hours to give the N^{α}-*tert*-butyloxycarbonyl-benz[*f*]tryptophan, **5.1**, after work-up (50%) (Figure 5.5).[5.22,5.23,5.27]

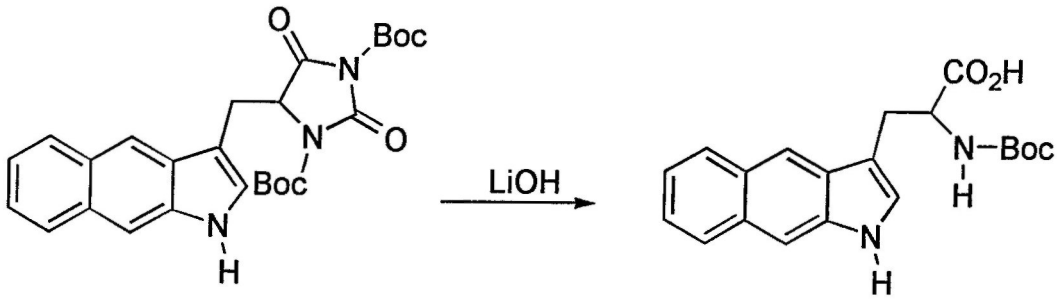

5.10 **5.1**

Figure 5.5. Synthesis of N^{α}-*tert*-butyloxycarbonyl-benz[*f*]tryptophan.

We expected to obtain the free amino acid upon hydrolysis of the protected hydantoin, **5.10**, with LiOH based on previous reports in the literature and results from our laboratory.[5.22,5.23,5.27] However, only α,α-disubstituted hydantoins had

previously been reported to undergo this facile hydrolysis to the free amino acid, while hydantoin **5.10** is only mono-substituted.[5.22,5.23,5.27] This is a fortunate discovery since **5.1** is already suitably protected for incorporation into a peptide via solution or solid-phase peptide synthesis. We postulate that the hydrolysis proceeds via a different mechanism for mono- and α,α-disubstituted hydantoins. Mechanistic studies are currently underway to address this issue and will be reported shortly.

5.3 Conclusions

This synthesis demonstrates that the anionic cyclization of *N,N*-diallylaminobenzene derivatives to indolines independently developed by Liebeskind, Bailey and coworkers is readily extended to the synthesis of a naphthalene derivative. Interestingly, we also observed that the mild hydrolysis of the intermediate mono-substituted, bis-Boc-hydantoin yields the N^{α}-*t*-Boc protected amino acid, whereas the mild hydrolysis of α,α-disubstituted bis-Boc-hydantoins gives the free amino acids. Additionally, we have reported the synthesis of a fluorescent amino acid probe that can be incorporated into a peptide without severely altering peptide backbone conformation. This synthesis gives the racemic amino acid, but it can be incorporated and then separated via HPLC because the resulting peptides will be diastereomers and easily separable. Preliminary fluorescence experiments show that the benzannulation shifts the absorbance and emission ~50 nm to the red from the parent indole chromophore.

5.4 Experimental

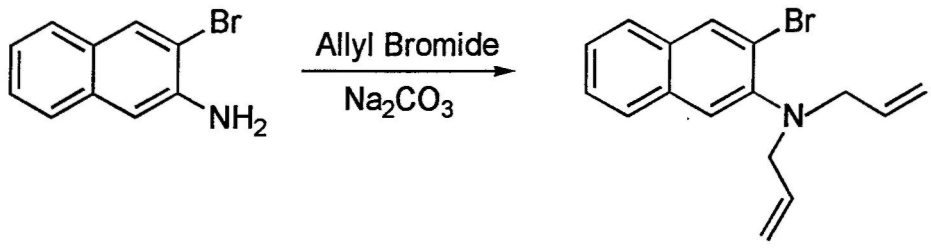

5.4 **5.5**

5.4.1 *N,N*-(bis-2-propenyl)-2-amino-3-bromonaphthalene (5.5)

2-amino-3-bromonaphthalene (**5.4**) (2.5 g, 11.25 mmol) was dissolved in 75 mL of dry DMF followed by the addition of anhydrous sodium carbonate (5.72 g, 54.00 mmol) and allyl bromide (4.28 mL, 49.50 mmol). The solution was heated to reflux for 24 h and an additional 5.72 g, (54.00 mmol) of sodium carbonate and 4.28 mL, (49.50 mmol) of allyl bromide was added. The resulting suspension was allowed to reflux until no starting material or mono-alkylated product was observed by GC-MS (approximately 24 h). The reaction mixture was cooled, diluted with 1000 mL of H_2O, and extracted with ethyl acetate (3 x 150 mL). The organic layers were combined, dried over $MgSO_4$, and evaporated under reduced pressure to give the diallyl derivative (**5.5**) as a yellow oil (2.89 g, 85 %). ^{1}H NMR (200MHz, $CDCl_3$) δ 8.02 (s, 1H), 7.52 (m, 2H), 7.29 (m, 3H), 5.80 (m, 2H), 5.12 (m, 4H), 3.73 (d, 4H). ^{13}C NMR (50 MHz, $CDCl_3$) δ 146.18, 134.50, 132.52, 132.49, 130.88, 126.82, 126.41, 126.26, 125.15, 121.20, 117.66, 55.37. GC/MS 303 $(M)^+$.

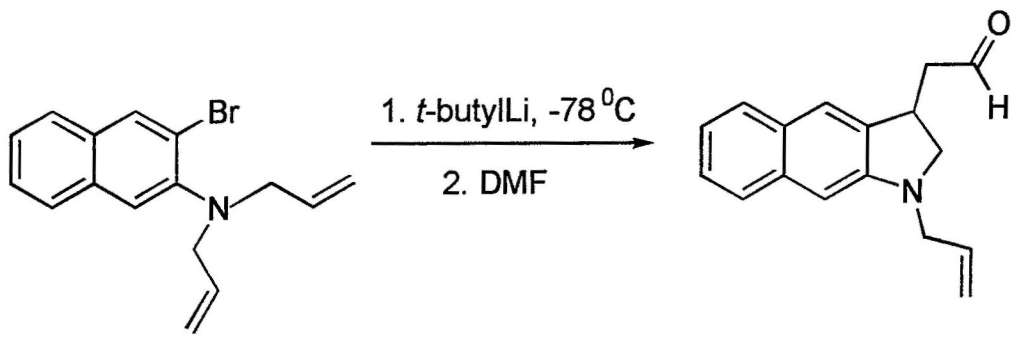

5.5 **5.6**

5.4.2 *rac.* *N*-(2-propenyl)-3-(2-ethanal)-benz[*f*]indoline (5.6)

Under argon, *N,N*-(bis-2-propenyl)-2-amino-3-bromonaphthalene (**5.5**) (1.0 g, 3.31 mmol) was dissolved in 25 mL of *tert*-butyl methyl ether and cooled to -78° C. *tert*-Butyl lithium (3.9 mL of a 1.7 M solution, 6.62 mmol) was added to the cooled solution and the resulting mixture was allowed to stir for 1 h. The solution was removed from the dry ice/acetone bath and allowed to warm to room temperature. After stirring for 15 minutes at room temperature, the solution is re-cooled to -78 °C and DMF (0.513 mL, 6.62 mmol) was added slowly. The resulting solution was stirred at -78 °C for 15 minutes, removed from the bath and allowed to warm to room temperature. The solution was diluted with 150 mL of ethyl ether and poured onto a 10 % NH_4Cl solution and extracted. The organic layer was washed with 10 % NH_4Cl (1 x 150 mL), dried over $MgSO_4$, and evaporated under reduced pressure to give the aldehyde (**5.6**) as a yellow oil (0.749 g, 90%). ^1H NMR (250MHz, $CDCl_3$)

δ 9.87 (s, 1H), 7.65-7.15 (m, 6 H), 5.87 (m, 1H), 5.36 (m, 2H), 3.85 (d, 2H), 3.73 (m, 2H), 3.10-2.73 (m, 3H). ^{13}C NMR (62.5 MHz, $CDCl_3$) δ 200.62, 149.33, 135.06, 134.70, 133.93, 127.93, 125.85, 125.58, 122.08, 121.65, 117.33, 100.05, 58.10, 50.46, 48.22, 33.75. GC/MS 252 $(M)^+$.

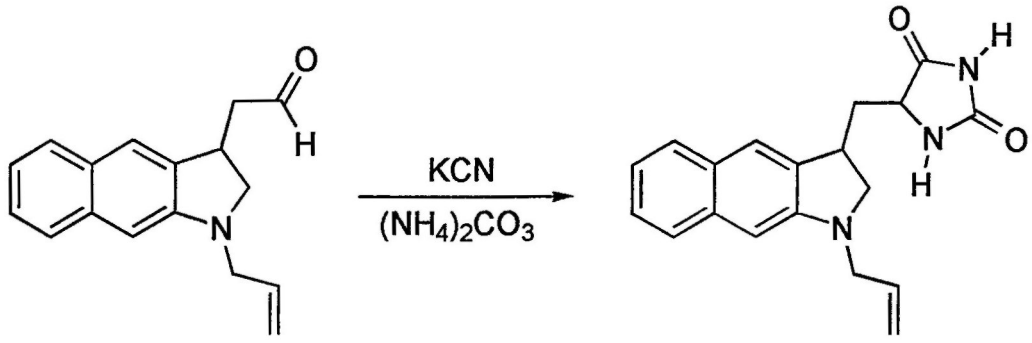

5.6 **5.7**

5.4.3 *rac.* *N*-(2-propenyl)-3-(methano-2,4-diaza-3,5-cyclopentanedione)-benz[*f*]indoline (5.7)

rac. *N*-(2-propenyl)-3-(2-ethanal)-benz[*f*]indoline (**5.6**) (0.492 g, 2.0 mmol) was dissolved in 60 mL of a 1:1 methanol-THF mixture followed by the addition of $(NH_4)_2CO_3$ (0.576 g, 6.0 mmol) in 15 mL of water. To this solution, a solution of KCN (0.391 g, 6.0 mmol) in 15 mL of water was added dropwise with vigorous stirring. The flask was sealed and heated to 50° C for 2 days. The resulting mixture was cooled, poured onto 500 mL of H_2O, and extracted with ethyl acetate (3 x 100mL). The organic layers were combined, dried over $MgSO_4$, and evaporated

under reduced pressure to yield a brown solid. The solid was chromatographed over silica gel using 7:3 ethyl acetate-hexanes to give the hydantoin (**5.7**) (diastereomers) as a light brown solid (0.401 g, 64 %). ^{1}H NMR (400MHz, $CDCl_3$) δ 9.54 (br s, 2H), 7.58-6.60 (m, 6H), 5.85 (m, 1H), 5.21 (m, 2H), 4.13-3.40 (m, 6H), 2.30 (m, 2H). ^{13}C NMR (100 MHz, $CDCl_3$) δ 175.60, (158.52, 158.14), (149.76, 149.71), (135.10, 135.07), 134.96, 133.24, 132.96, 128.64, 128.20, (127.80, 127.75), (126.15, 126.01), (123.09, 122.82), (122.58, 122.23), (118.57, 117.92), (102.03, 101.01), (58.69, 58.52), (56.94, 57.28), (57.28, 56.94), (51.52, 51.07), (36.91, 36.73). MALDI-MS (no matrix) 319.92 $(M)^{+}$.

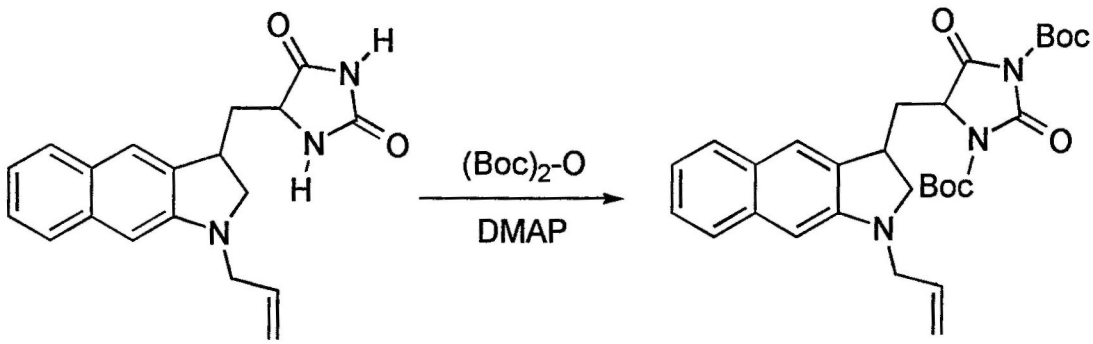

5.7 **5.8**

5.4.4 *rac.* *N*-(2-propenyl)-3-(methano-2,4-diaza-2,4-bis-*tert*-butyloxycarbonyl-3,5-cyclopentanedione)-benz[*f*]indoline (5.8)

In a flask equipped with a mercury bubbler, a solution of *rac.* *N*-(2-propenyl)-3-(methano-2,4-diaza-3,5-cyclopentanedione)-benz[*f*]indoline (**5.7**) (1.0 g, 3.13

mmol) in 50 mL of acetonitrile was sequentially treated with di-*tert*-butyl-dicarbonate (2.05 g, 9.38 mmol), diisopropylethylamine (0.808 g, 6.25 mmol), and DMAP (0.073 g, 0.60 mmol). After 4 h of stirring at room temperature, another 0.073 g (0.60 mmol) of DMAP was added and the reaction was allowed to stir for an additional 20 h. CO_2 evolution was observed after each of the additions of the DMAP. The solvent was removed under reduced pressure and the resulting residue taken up in 100 mL of methylene chloride and washed with 1N HCl (2 x 150 mL) and water (2 x 150 mL). The organic layer was dried over $MgSO_4$ and the solvent removed under reduced pressure to yield a brown solid. The crude material was purified by flash chromatography over silica gel using 7:3 hexanes-ethyl acetate as the mobile phase to give the bis-Boced indoline hydantoin (**5.8**) (diastereomers) as a yellow solid (1.29 g, 79%). ^{1}H NMR (400MHz, $CDCl_3$) δ 7.66-6.73 (m, 6H), 5.90 (m, 1H), 5.27 (m, 2H), 3.83-3.03 (m, 6H), 2.51 (m, 2H), (1.54, 1.53) (s,s 9H), (1.48, 1.39) (s,s 9H). ^{13}C NMR (100 MHz, $CDCl_3$) δ (167.70, 167.73), (149.46, 149.35), (147.97, 147.88), 145.09, 135.72, 135.36, 134.69, 134.62, 133.38, 127.78, 127.70, (127.76, 127.39), 122.34, (121.80, 121.57), (117.60, 117.53), (100.15, 100.04), 85.40, (83.58, 83.46), (58.59, 58.09), (57.41, 57.25), (50.01, 50.04), (35.74, 35.25), 27.53, (27.40, 27.30). MALDI-MS (no matrix) 520.40 $(M)^{+}$.

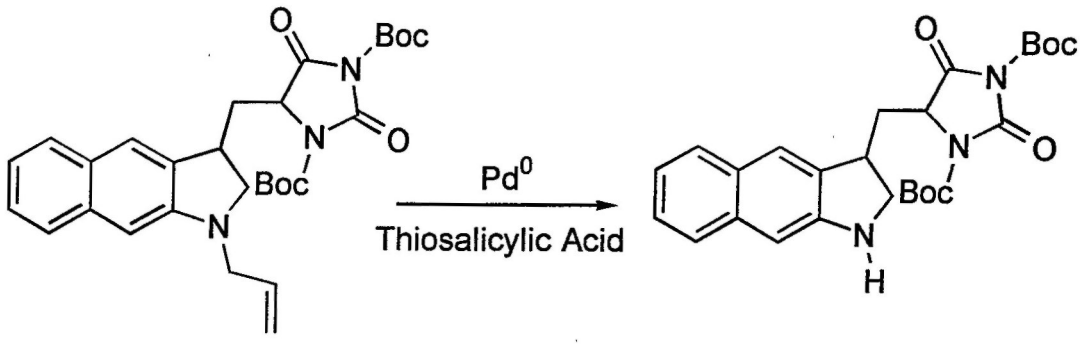

5.8 **5.9**

5.4.5 *rac.* 3-(methano-2,4-diaza-2,4-bis-*tert*-butyloxycarbonyl-3,5-cyclopentanedione)-benz[*f*]indoline (5.9)

Under an inert atmosphere, *rac.* *N*-(2-propenyl)-3-(methano-2,4-diaza-2,4-bis-*tert*-butyloxycarbonyl-3,5-cyclopentanedione)-benz[*f*]indoline (**5.8**) (0.388 g, 0.75 mmol) was dissolved in dry THF (40 mL) and the solution was bubbled with argon for 1 h. This solution was added onto solid tris(dibenzylideneacetone)-dipalladium(0) (0.017 g, 0.019 mmol), 1,4-bis(diphenylphosphino)butane (0.032 g, 0.075 mmol) and thiosalicylic acid (0.126 g, 0.82 mmol). The resulting solution was bubbled with argon for 1 h. The solution was heated to reflux for 24 h when tris(dibenzylideneacetone)-dipalladium(0) (0.017 g, 0.019 mmol), and 1,4-bis(diphenylphosphino)butane (0.032 g, 0.075 mmol) were added and the solution refluxed for an additional 24 h. The solution was cooled and the solvent removed *in vacuo* to give a brown oil. The residue was taken up in ethyl acetate, washed with 10% Na_2CO_3 solution (2 x 100 mL), and water (1 x 100 mL). The organic layer was

dried over $MgSO_4$ and the solvent removed *in vacuo* to give a yellow solid. The crude material (air sensitive) was purified by flash chromatography over silica gel using chloroform-hexanes-THF (6:3:1) under nitrogen pressure. The pure indoline (**5.9**) (0.201 g, 56 %), which quickly decomposes, was immediately carried onto the next step. MALDI-MS (no matrix) 479.77 $(M)^+$.

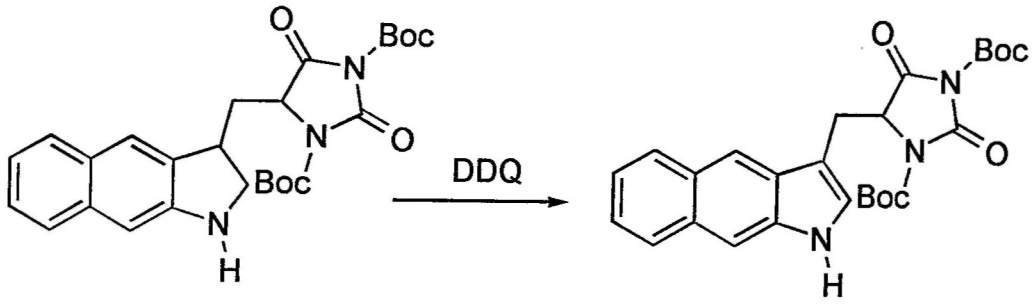

5.9 **5.10**

5.4.6 *rac.* 3-(methano-2,4-diaza-2,4-bis-*tert*-butyloxycarbonyl-3,5-cyclopentanedione)-benz[*f*]indole (5.10)

Under argon, *rac.* 3-(methano-2,4-diaza-2,4-bis-*tert*-butyloxycarbonyl-3,5-cyclopentanedione)-benz[*f*]indoline (**5.9**) (0.080 g, 0.017 mmol) was dissolved in 25 mL of a dry *tert*-butyl methyl ether-methylene chloride mixture (24:1) and solid 2,3-dichloro-5,6-dicyano-1,4-benzoquinone (DDQ) (0.038 g, 0.017 mmol) was added.

The resulting mixture was allowed to stir at room temperature for 2 h. The reaction mixture was immediately filtered through an alumina plug to remove the reacted DDQ. The solvent was removed under reduced pressure to give the indole (**5.10**) as a brown residue (0.041 g, 51 %). ^{1}H NMR (400MHz, DMSO d_6) δ 9.90 (s, 1H), 8.05-7.76 (m, 4H), 7.39-7.20 (m, 3H), 3.94 (m, 1H), 3.32 (dd, 1H), 3.05 (dd, 1H), 1.70 (s, 9H), 1.31 (s, 9H). ^{13}C NMR (100 MHz, $CDCl_3$) δ 167.20, 150.04, 149.75, 148.31, 135.01, 130.04, 129.70, 128.10, 128.00, 127.05, 126.62, 123.21, 122.08, 115.91, 110.41, 108.34, 76.18, 76.07, 53.20, 28.97, 27.20, 26.14. MALDI-MS (no matrix) 477.84 $(M)^{+}$.

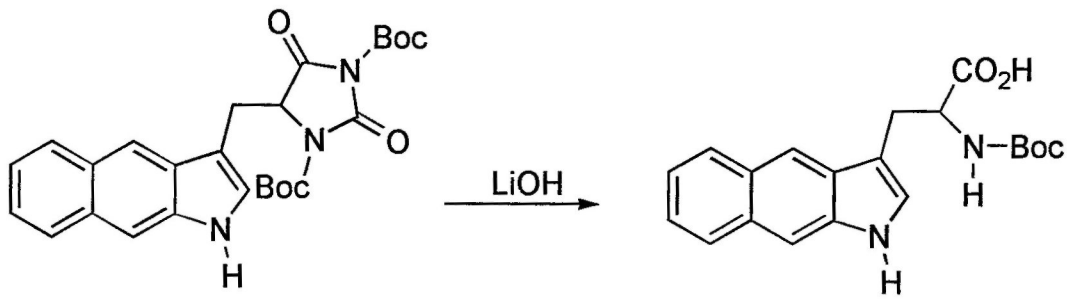

5.10 **5.1**

5.4.7 *rac.* N^{α}-*tert*-butyloxycarbonyl-benz[*f*]tryptophan (5.1)

Under argon, *rac.* 3-(methano-2,4-diaza-2,4-bis-*tert*-butyloxycarbonyl-3,5-cyclopentanedione)-benz[*f*]indole (**5.10**) (0.475, 0.99 mmol) was dissolved in 88 mL

of THF and 8 mL of 1N LiOH was added. The mixture was allowed to stir vigorously overnight at room temperature. The resulting solution was diluted with 15 mL of 1N LiOH and the THF removed under reduced pressure at 25° C. The aqueous solution was washed with ether (4 x 50 mL). The pH of the aqueous layer was adjusted to 3 with the addition of 1N HCl and washed with ethyl acetate (3 x 25 mL). The organic layers were combined, dried over $MgSO_4$, and evaporated *in vacuo* to yield the crude material as a brown solid. The crude material was purified by flash chromatography over silica gel using chloroform-hexanes-THF (6:3:1) to yield the title molecule (**5.1**) as a solid.(0.238 g, 50 %). ^{1}H NMR (400MHz, DMSO d_6) δ 10.88 (s, 1H), 8.06 (s,1H), 7.89 (m, 2H), 7.81 (s, 1H), 7.41 (s, 1H), 7.30 (m, 2H), 4.24 (dd, 1H), 3.29 (dd, 1H), 3.10 (dd, 1H), 1.31 (s, 9H). ^{13}C NMR (100 MHz, $CDCl_3$) δ 174.07, 155.23, 136.98, 129.81, 129.43, 128.18, 127.89, 127.50, 127.19, 122.94, 121.87, 115.27, 109.69, 106.13, 77.75, 54.76, 28.20, 27.15. FAB-MS (glycerol) 354.3 $(M)^+$; HRMS (*m*-nitrobenzyl alcohol) 354.1552 (calcd. for $C_{20}H_{22}N_2O_4$, 354.1579).

5.5 References

5.1 Basu, G.; Kitao, A.; Hirata, F.; Go, N. *J. Am. Chem. Soc.* **1994**, *116*, 6307-6316.

5.2 Otoda, K.; Kitagawa, Y.; Kimura, S.; Imanishi, Y. *Biopolymers* **1993**, *33*, 1337-1345.

5.3 Smythe, M. L.; Huston, S. E.; Marshall, G. R. *J. Am. Chem. Soc.* **1995**, *117*, 5445-5452.

5.4 Toniolo, C.; Benedetti, E. *Trends Biochem. Sci.* **1991**, *16*, 350-353.

5.5 Gerstein, M.; Chothia, C. *J. Mol. Biol.* **1991**, *220*, 133-149.

5.6 McPhalen, C. A.; Vincent, M. G.; Picot, D.; Jansonius, J. N.; Lesk, A. M.; Chothia, C. *J. Mol. Biol.* **1992**, *227*, 197-213.

5.7 Toniolo, C.; Polese, A.; Formaggio, F.; Crisma, M.; Kamphuis, J. *J. Am. Chem. Soc.* **1996**, *118*, 2744-2745.

5.8 Yokum, T.S.; Gauthier, T. J.; Hammer, R. P.; McLaughlin, M. L. *J. Am. Chem. Soc.* **1997**, *119*, 1167-1168.

5.9 Smythe, M. L.; Nakaie, C. R.; Marshall, G. R. *J. Am. Chem. Soc.* **1995**, *117*, 10555-10562.

5.10 Millhauser, G. L.; Stenland, C. J.; Hanson, P.; Bolin, K. A.; van de Ven, F. J. M. *J. Mol. Biol.* **1997**, *267*, 963-974.

5.11 Basu, G.; Kuki, A. *Biopolymers* **1993**, *33*, 995-1000.

5.12 Hungerford, G.; Martinez-Insua, M.; Birch, D. J. S.; Moore, B. D. *Agnew. Chem. Int. Ed. Engl.* **1996**, *35*, 326-329.

5.13 Creighton, T. E. *Proteins: Structure and Molecular Properties*, 2nd ed.; W. H. Freeman and Co.: New York, 1993.

5.14 McLaughlin, M. L.; Barkley, M. D. *Methods in Enzymology*, **1997**, *278*, 190-202.

5.15 Rydon, H. N.; Siddappa, S. *J. Chem. Soc.* **1951**, 2462-2467.

5.16 Morales, G. A. Louisiana State University, Ph. D. Dissertation, 1995.

5.17 Süs, V. O.; Glos, M.; Möller, K.; Eberhardt, H.-D. *Liebigs Ann. Chem.* **1953**, *583*, 150-160.

5.18 Watanabe, T.; Miyagi, C.; Murakami, Y. *J. Heterocyclic Chem.* **1993**, *30*, 217-224.

5.19 Sakamoto, T.; Yoshinori, K.; Yamanaka, H. *Heterocycles* **1986**, *24*, 1845-1847.

5.20 Zhang, D.; Liebeskind, L. S. *J. Org. Chem.* **1996**, *61*, 2594-2595.

5.21 Bailey, W. F.; Jiang, X. L. *J. Org. Chem.* **1996**, *61*, 2596-2597.

5.22 Fenyes, J. G. *J. Org. Chem.* **1962**, *27*, 2614-2618.

5.23 Wysong, C. L.; Yokum, T. S.; Morales, G. A.; Gundry, R. L.; McLaughlin, M. L.; Hammer, R. P. *J. Org. Chem.* **1996**, *61*, 7650-7651.

5.24 Yokum, T. S.; Bursavich, M. G.; Piha-Paul, S. A.; Hall, D. A.; McLaughlin, M. L. *Tetrahedron Lett.* **1997**, *38*, 4013-4016.

5.25 Bergs, H. German Patent 566,094 (May 26, 1929); Chem. Abst. **1933**, *27*, 1001.

5.26 Bucherer, H. T.; Steiner, W. *J. Prakt. Chem.* **1934**, *140*, 291-316.

5.27 Lemaire-Audoire, S.; Savignac, M.; Genêt, J.P.; Bernard, J.M. *Tetrahedron Lett.* **1995**, *36*, 1267-1270.

5.28 Kubik, S.; Meissner, R. S.; Rebek, J. *Tetrahedron Lett.* **1994***Lett.* **1994**, *35*, 6635-6638.

Chapter 6

Summary and Future Studies

6.1 Summary and Future Studies

This dissertation focused on the synthesis and studies of helical peptides and the synthesis of novel amino acids for the construction and characterization of helical peptides. The helical peptides synthesized were short, amphipathic peptides composed of high percentages of α,α-disubstituted amino acids (ααAAs). The peptides were studied for their antimicrobial activities and their helix preference in different solvent environments. Four structurally related amino acids were synthesized to serve as a helix promoting, water solubilizing peptide design tools while another amino acid was synthesized as a fluorescent probe to examine the 3_{10}/α-helix equilibrium.

Chapter 2 described the synthesis of short, highly helical peptides, the percent helicity determination of these peptides via circular dichroism (CD), and their *in vivo* and *in vitro* antimicrobial activities. The peptides were synthesized to test the hypothesis that short, helical peptides would retain the biological activity of the longer antimicrobial peptides while becoming increasingly selective for bacterial destruction over mammalian cell destruction. The hypothesis arose form correlations observed between length and selectivity and also helicity and activity.[6.1-6.4] The correlations

being the shorter the peptide, the more selective and the more helical the peptide, the more active.[6.1-6.4]

Based on these correlations and the fact that ααAAs promote helicity, a series of short (10-14 residues), amphipathic α-helical and 3_{10}-helical peptides with high percentages of ααAAs were synthesized.[6.5-6.7] The peptides incorporated α-aminoisobutyric acid (Aib), 1-aminocyclohexane carboxylic acid (Ch), and the novel 4-aminopiperidine-4-carboxylic acid (Api) using preformed acid fluorides for the difficult couplings.[6.8,6.9] The Api amino acid, synthesized by our group and optimized in Dr. Robert Hammer's group, was important because, as of the time of the work, it was the only polar ααAA that promoted helicity and was suitable for incorporation via solid-phase peptide synthesis.[6.10,6.11] Api was also significant because it permitted the use of Api on the polar face of the amphipathic helix, thus allowing a higher percentage of ααAAs to be incorporated. The peptides were evaluated *in vitro* for direct antimicrobial activity against representative Gram-positive and Gram-negative bacteria and *in vivo* and *in vitro* for biological activity against *B. abortus*. Almost all of the ααAAs rich α-helical peptides showed good *in vitro* antimicrobial activity against *S. aureus* and *E. coli*. Also, the 3_{10}-helical peptides unexpectedly exhibited direct antibacterial activity against *E. coli*. This was unanticipated because no other water soluble 3_{10}-helical peptides have exhibited antimicrobial activity. While none of the peptides were directly active *in vitro* against *B. abortus*, many significantly reduced the *B. abortus* load in BALB/c mice. Ai-11,

Ai-14 and Pi-10 showed significant *B. abortus* reduction where Pi-10 was the most effective with a 90 % reduction upon a single dose (500μg). The more hydrophobic peptides, Ch-10 and Ch-13, showed little selectivity where they were toxic upon injection. A 3_{10}-helical peptide, Ipi-10, also showed some *in vivo* activity, which was also unexpected. The exploration of hybrid Ch-Aib peptides may produce a peptide with better *in vivo* activity while retaining good selectivity. Also, the investigation of shorter 3_{10}-helical peptides as antimicrobial agents is a promising area given the initial results and the length of the 3_{10}-helix as compared to the α-helix.

Chapter 3 described the synthesis of a series of polar, orthogonally protected, ααAAs. From the previous studies, the importance of polar ααAAs in the synthesis of highly helical, short, water soluble peptides was obvious. Therefore, a series of orthogonally protected ααAAs with varying hydrophobicity of the side chains was synthesized. The side-chains introduced onto the cyclohexanone backbone were: ethylamine, butylamine, benzylamine, and 2-naphthylmethylamine. The synthesis began with a reductive amination with the desired amine on 1,4-cyclohexanedione monoethylene ketal.[6.12] Sodium triacetoxyborohdride was employed as the reducing agent after it was found to be more effective than the traditional sodium cyanoborohydride.[6.12] The reductive amination was followed by ketal removal, protection of the nitrogen with *tert*-butyloxycarbonyl, hydantoin formation, and activation of the hydantoin nitrogens.[6.10,6.11,6.13] The hydantoin was hydrolyzed using a mild hydrolysis procedure to leave the side chain nitrogen unchanged which

allowed the orthogonal protection of the two amino groups.[6.10,6.11,6.14] After hydrolysis, the free amino acid was protected with 9-fluorenylmethyloxycarbonyl to give the fully protected amino acids.[6.15] The synthesis was moderately high yielding and convenient because no intermediates needed to be isolated. Potential future studies include the incorporation of the amino acids into peptides and the study of their effects on antimicrobial activity and helicity.

The studies of the solvent effects on the helical preference of short, designed 3_{10}-helical and α-helical peptides are reported in Chapter 4. Three peptides were studied: an amphipathic α-helical peptide (Pi-10), an amphipathic 3_{10}-helical peptide (Ipi-10), and an amphipathic 3_{10}-helical peptide with two side-chain salt-bridges (Sb-10). The peptides all contained 80 % ααAAs, therefore the peptides were expected to be very helical based on the helix promoting abilities of ααAAs.[6.5-6.7]

Pi-10 formed an α-helix in the amphipathic environment of SDS micelles according to circular dichroism (CD) spectroscopy. However, a 3_{10}-helix would have been predicted according to the literature due to its high ααAAs content and the placement of the proteinogenic residues.[6.16,6.17] The isomeric peptide, Ipi-10, displayed the expected 3_{10}-helical structure in the SDS micelles. In contrast, Sb-10, a designed 3_{10}-helix, showed a spectra indicative of an α-helix in SDS micelles. The formation of an α-helix may have been due to incomplete micelle binding and ion pairing.

CD spectra of all three peptides were taken in organic and aqueous/organic solvent mixtures. Pi-10 displayed an α-helix in 100% organic solvent, and aqueous/organic mixtures. In contrast, Ipi-10 and Sb-10 displayed a 3_{10}-helices in 100% organic solvent but made a transitions to α-helices as the percent water was increased. The % 3_{10}-helicity in 100% organic solution was significantly greater for Sb-10 as compared to Ipi-10 which indicated that the salt-bridges stabilized the 3_{10}-helix conformation. Titration experiments of Sb-10 with tetramethylammonium trifluoroacetate (TMAT) from 0.1 M TMAT in 100 % organic to solely organic media also indicate that the ionic interactions stabilized the 3_{10}-helical conformation. Sb-10 makes a transition from an α-helix to a 3_{10}-helix as the salt concentrations were increased.

The Sb-10 and Ipi-10 aqueous-organic and organic studies experimentally confirmed theoretical calculations of solvent effects on the 3_{10}-/α-helix equilibrium.[6.18] Also, the work showed that amphipathy is a significant factor in the design of peptides which can override the placement or percentage of ααAAs. The studies additionally demonstrated that side-chain salt-bridges, which have previously been shown to stabilize α-helices, may also be used for the stabilization of 3_{10}-helices.[6.19] The investigation of other methods for the stabilization of 3_{10}-helices such as other salt-bridges and covalently linked side-chains is a potentially fruitful area of future investigation.

The final research chapter, chapter 5, described the synthesis of N^{α}-*tert*-butyloxycarbonyl-benz[*f*]tryptophan, a red-shifted fluorescent tryptophan derivative. The amino acid was synthesized as a fluorescent probe to be incorporated into a donor/acceptor system for the study of the 3_{10}-/α-helix equilibrium. Fischer indole synthesis routes are not available for the synthesis of benz[*f*]tryptophan, therefore the amino acid was constructed via a protected indoline backbone. The amino acid was synthesized in seven steps from 3-bromo-2-aminonaphthalene. The key synthetic steps in the synthesis were: anionic cyclization, hydantoin formation, hydantoin activation, dehydrogenation, and mild hydrolysis.[6.10,6.11,6.13,6.14,6.19,6.20]

The final step of the synthesis was the mild hydrolysis of the bis-Boc hydantoin with 1N LiOH. The hydrolysis produced the N^{α}-Boc derivative while it was expected to form the free amino acid based on previous results of the hydrolysis of α,α-disubstituted, bis-Boc hydantoins.[6.10,6.11,6.14] Though unexpected, this finding was fortunate because the amino acid is suitably protected for incorporation into peptides via solid-phase or solution-phase peptide synthesis. Mechanistic studies of the hydrolysis of mono-substituted, bis-Boc hydantoins and α,α-disubstituted, bis-Boc hydantoins is a potential area for future investigation. Also, the incorporation of benz[*f*]tryptophan into helical peptides and investigating the 3_{10}-/α-helix equilibrium with a fluorescent lifetime system is the obvious application of this amino acid.

6.2 References

6.1 Javadpour, M. M.; Juban, M. M.; Lo, W. J.; Bishop, S. M.; Alberty, J. B.; Cowell, S. M.; Becker, C. L.; McLaughlin, M. L. *J. Med. Chem.* **1996**, *39*, 3107-3113.

6.2 Bessalle, R.; Gorea, A.; Shalit, I.; Metzger, J. W.; Dass, C.; Desiderio, D. M.; Fridkin, M. *J. Med. Chem.* **1993**, *36*, 1203-1209.

6.3 Andreu, D.; Ubach, J.; Boman, A.; Wåhlin, B.; Wade, D.; Merrifield, R. B.; Boman, H. G. *FEBS Lett.* **1992**, *296*, 190-193.

6.4 Blondelle, S. E.; Houghten, R. A. *Biochemistry* **1992**, *31*, 12688-12694.

6.5 Karle, I. L.; Balaram, P. *Biochemistry* **1990**, *29*, 6747-6756.

6.6 Benedetti, E. *Biopolymers (Peptide Sci.)*, **1996**, *40*, 3-44.

6.7 Balaram, P. *Curr. Opin. Struct. Biol.* **1992**, *2*, 845-851.

6.8 Wenschuh, H.; Beyermann, M., Krause, E.; Brudel, M.; Winter, R.; Schumann, M.; Carpino, L.; Bienert, M. *J. Org. Chem.* **1994**, *59*, 3275-3280.

6.9 Wenschuh, H.; Beyermann, M., Haber, H.; Seydel, J. K.; Krause, E.; Bienert, M.; Carpino, L.; El-Faham, A.; Albericio, F. *J. Org. Chem.* **1995**, *60*, 405-410.

6.10 Wysong, C. L.; Yokum, T. S.; Morales, G. A.; Gundry, R. L.; McLaughlin, M. L.; Hammer, R. P. *J. Org. Chem.* **1996**, *61*, 7650-7651.

6.11 Yokum, T. S.; Elzer, P. H.; McLaughlin, M. L. *J. Med. Chem.* **1996**, *39*, 3603-3605.

6.12 Abdel-Magid, A. F.; Maryanoff, C. A.; Carson, K. G.; *Tetrahedron Lett.* **1990**, *31*, 5595-5598.

6.13 Edward, J. T.; Jitrangsri, C. *Can. J. Chem.* **1975**, *53*, 3339-3350.

6.14 Kubik, S.; Meissner, R. S.; Rebek, J. *Tetrahedron Lett.* **1994**, *35*, 6635-6638.

6.15 Bolin, D. R.; Sytwu, I.-I.; Humiec, F.; Meienhofer, J. *Int. J. Pept. Protein Res.* **1989**, 353-359.

6.16 Karle, I. L.; Balaram, P. *Biochemistry* **1990**, *29*, 6747-6756.

6.17 Basu, G.; Bagchi, K.; Kuki, A. *Biopolymers* **1991**, *31*, 1763-1774.

6.18 Smythe, M. L.; Huston, S. E.; Marshall, G. R. *J. Am. Chem. Soc.* **1995**, *117*, 5445-5452.

6.19 Marqusee, S.; Baldwin, R. L. *Proc. Natl. Acad. Sci. U.S.A.* **1987**, *84*, 8898-8902.

6.20 Zhang, D.; Liebeskind, L. S. *J. Org. Chem.* **1996**, *61*, 2594-2595.

6.21 Bailey, W. F.; Jiang, X. L. *J. Org. Chem.* **1996**, *61*, 2596-2597.

Appendix:
Letters of Permission

LOUISIANA STATE UNIVERSITY
AND AGRICULTURAL AND MECHANICAL COLLEGE
Department of Chemistry

August 10, 1997

American Chemical Society
1155 16th St., N.W.
Washington, DC 20036

To whom it may concern:

I am writing to obtain permission for the use of an article published in the Journal of Medicinal Chemistry. I am a graduate student in the Department of Chemistry at Louisiana State University. I am first author on the article and would like to include the article in my doctoral dissertation. The article is "Antimicrobial α,α-Dialkylated Amino Acid Rich Peptides with *In-Vivo* Activity against an Intracellular Pathogen", Vol. 39, No. 19, pp. 3603-3605.

Thank you for your consideration of this request.

Sincerely,

J. Scott Yokum

T. Scott Yokum

voice: 504-388-2338
FAX: 504-388-3458

email: syokum@chrs1.chem.lsu.edu

Baton Rouge • Louisiana • 70803-1804 • 504/388-3161 • Fax 504/388-3458 • Fax 504/388-3463

American Chemical Society

PUBLICATIONS DIVISION
COPYRIGHT OFFICE

1155 SIXTEENTH STREET, N.W.
WASHINGTON, D.C. 20036
Phone (202) 872-4367 or -4368
Fax (202) 872-6060

FAX NUMBER: 504/388-3458

DATE: August 26, 1997

MEMORANDUM

TO: T. Scott Yokum, Louisiana State University
Department of Chemistry
Baton Rouge LA 70803-1804

FROM: C. Arleen Courtney *C. Arleen Courtney*
Assistant Copyright Administrator

RE: Your letters dated August 10 and 20, 1997

Thank you for your recent letters, regarding your request for permission to include your paper(s) or portions of your paper(s), per your attached letter, in your thesis. Please note the following:

* If your paper has already been published by ACS, I would be happy to grant you this permission royalty free provided that you print the required ACS copyright credit line on the first page of your article: "Reprinted (or 'Reprinted in part') with permission from FULL REFERENCE CITATION. Copyright YEAR American Chemical Society."

  Note: If you plan to submit your thesis to UMI or to another dissertation publisher, please inform them that permission to include your already published ACS article as part of your thesis is granted for paper and microform copies only; the ACS copyright notice (see above) must appear on the first page of the ACS article.

* If your paper has not already been published by ACS, you may include it in your thesis provided that you print the following ACS copyright credit line on the first page of your article: "Reprinted (or 'Reprinted in part') with permission from JOURNAL NAME, in press (or 'submitted for publication'). Unpublished work copyright CURRENT YEAR American Chemical Society."

  Note: If you plan to submit your thesis to UMI or to another dissertation publisher, you may NOT include the ACS paper in the version that you submit to UMI or to another dissertation publisher until ACS has published your paper.

* Other: ______________________________

Thank you for writing. If you have any questions, please call me at 202/872-4368.

4/17/97

SENT BY:Xerox Telecopier 7020 ; 8-26-97 ; 6:23PM ; 2→ 504 388 3458:# 2

LOUISIANA STATE UNIVERSITY
AND AGRICULTURAL AND MECHANICAL COLLEGE
Department of Chemistry

August 10, 1997

American Chemical Society
1155 16th St., N.W.
Washington, DC 20036

To whom it may concern:

I am writing to obtain permission for the use of an article published in the Journal of the American Chemical Society. I am a graduate student in the Department of Chemistry at Louisiana State University. I am first author on the article and would like to include the article in my doctoral dissertation. The article is "Solvent Effects on the 3_{10}-/α-Helix Equilibrium in Short Amphipathic Peptides Rich in α,α-Disubstituted Amino Acids", Vol. 119, No. 5, pp. 1167-1168.

Thank you for your consideration of this request.

Sincerely,

T. Scott Yokum

voice: 504-388-2338
FAX: 504-388-3458

email: syokum@chrs1.chem.lsu.edu

American Chemical Society

PUBLICATIONS DIVISION
COPYRIGHT OFFICE
FAX NUMBER: 504/388-3458

1155 SIXTEENTH STREET, N.W.
WASHINGTON, D.C. 20036
Phone (202) 872-4367 or -4368
Fax (202) 872-6060

DATE: August 26, 1997

MEMORANDUM

TO: T. Scott Yokum, Louisiana State University
Department of Chemistry
Baton Rouge LA 70803-1804

FROM: C. Arleen Courtney C. Arleen Courtney
Assistant Copyright Administrator

RE: Your letters dated August 10 and 20, 1997

Thank you for your recent letters, regarding your request for permission to include your paper(s) or portions of your paper(s), per your attached letter, in your thesis. Please note the following:

* If your paper has already been published by ACS, I would be happy to grant you this permission royalty free provided that you print the required ACS copyright credit line on the first page of your article: "Reprinted (or 'Reprinted in part') with permission from FULL REFERENCE CITATION. Copyright YEAR American Chemical Society."

  Note: If you plan to submit your thesis to UMI or to another dissertation publisher, please inform them that permission to include your already published ACS article as part of your thesis is granted for paper and microform copies only; the ACS copyright notice (see above) must appear on the first page of the ACS article.

* If your paper has not already been published by ACS, you may include it in your thesis provided that you print the following ACS copyright credit line on the first page of your article: "Reprinted (or 'Reprinted in part') with permission from JOURNAL NAME, in press (or 'submitted for publication'). Unpublished work copyright CURRENT YEAR American Chemical Society."

  Note: If you plan to submit your thesis to UMI or to another dissertation publisher, you may NOT include the ACS paper in the version that you submit to UMI or to another dissertation publisher until ACS has published your paper.

* Other: _____

Thank you for writing. If you have any questions, please call me at 202/872-4368.

4/17/97

LOUISIANA STATE UNIVERSITY
AND AGRICULTURAL AND MECHANICAL COLLEGE
Department of Chemistry

August 10, 1997

Elsevier Science Ltd.
The Boulevard
Langford Lane
Kidlington
Oxford
OX5 1GB

To whom it may concern:

I am writing to obtain permission for the use of an article published in Tetrahedron Letters. I am a graduate student in the Department of Chemistry at Louisiana State University. I am first author on the article and would like to include the article in my doctoral dissertation. The article is "Benz[*f*]tryptophan, a Bathochromic Analog of Tryptophan, Synthesis of its N-α-*t*-Boc Derivative" Vol. 38, No. 29, pp. 5111-5114, 1997.

Thank you for your consideration of this request.

Sincerely,

J. Scott Yokum

T. Scott Yokum

voice: 504-388-2338
FAX: 504-388-3458

email: syokum@chrs1.chem.lsu.edu

PLEASE TURN OVER

18 AUG 1997

Baton Rouge • Louisiana • 70803-1804 • 504/388-3361 • Fax 504/388-3458 • Fax 504/388-3463

We hereby grant you permission to reprint the material specified in your letter (see recto) for the purpose you have indicated therein, at no charge, provided that:

1. The material to be used has appeared in our publication without credit or acknowledgement to another source.

2. Suitable acknowledgement to the source is given as follows:

For Books: "Reprinted from (Author/Title), Copyright (Year), Pages No., with kind permission from Elsevier Science Ltd. The Boulevard. Langford Lane. Kidlington 0X5 1GB, UK"

For Journals: "Reprinted from Journal title, Volume number, Author(s), Title of article, Pages No.,Copyright (Year), with kind permission from Elsevier Science Ltd, The Boulevard, Langford Lane, Kidlington 0X5 1GB, UK"

3. Reproduction of this material is confined to the purpose for which permission is hereby given.

For future permissions, please contact:
Frances Rothwell (Mrs)
Subsidiary Rights Manager
Elsevier Science Ltd
The Boulevard, Langford Lane
Kidlington 0X5 1GB, U.K.

Frances Rothwell

Should your thesis be published commercially, please reapply for permission.

LOUISIANA STATE UNIVERSITY
AND AGRICULTURAL AND MECHANICAL COLLEGE
Department of Chemistry

August 10, 1997

Elsevier Science Ltd.
The Boulevard
Langford Lane
Kidlington
Oxford
OX5 1GB

To whom it may concern:

I am writing to obtain permission for the use of an article published in Tetrahedron Letters. I am a graduate student in the Department of Chemistry at Louisiana State University. I am first author on the article and would like to include the article in my doctoral dissertation. The article is "Synthesis of a Series of Polar, Orthogonally Protected, α,α-Disubstituted Amino Acids" Vol. 38, No. 23, pp. 4013-4016, 1997.

Thank you for your consideration of this request.

Sincerely,

J. Scott Yokum

T. Scott Yokum

voice: 504-388-2338
FAX: 504-388-3458

email: syokum@chrs1.chem.lsu.edu

PLEASE TURN OVER

18 AUG 1997

Baton Rouge • Louisiana • 70803-1804 • 504/388-3361 • Fax 504/388-3458 • Fax 504/388-3463

We hereby grant you permission to reprint the material specified in your letter (see recto) for the purpose you have indicated therein, at no charge, provided that:

1. The material to be used has appeared in our publication without credit or acknowledgement to another source.

2. Suitable acknowledgement to the source is given as follows:

For Books: "Reprinted from (Author/Title), Copyright (Year), Pages No., with kind permission from Elsevier Science Ltd. The Boulevard. Langford Lane. Kidlington 0X5 1GB, UK"

For Journals: "Reprinted from Journal title, Volume number, Author(s), Title of article, Pages No.,Copyright (Year), with kind permission from Elsevier Science Ltd, The Boulevard, Langford Lane, Kidlington 0X5 1GB, UK"

3. Reproduction of this material is confined to the purpose for which permission is hereby given.

For future permissions, please contact:
Frances Rothwell (Mrs)
Subsidiary Rights Manager
Elsevier Science Ltd
The Boulevard, Langford Lane
Kidlington 0X5 1GB, U.K.

Frances Rothwell

Should your thesis be published commercially, please reapply for permission.

Vita

Thomas Scott Yokum graduated from Marietta College, Marietta, Ohio, in December 1992, where he received his bachelor of science degree in Chemistry. In 1993 he began graduate school at Louisiana State University under the direction of Dr. Mark L. McLaughlin. Currently, he is a candidate for the degree of Doctor of Philosophy in the Department of Chemistry, which will be awarded at Spring Commencement, 1998.

DOCTORAL EXAMINATION AND DISSERTATION REPORT

Candidate: Thomas Scott Yokum

Major Field: Chemistry

Title of Dissertation: Synthesis of Novel Amino Acids and 3_{10}- and Alpha-Helical Alpha, Alpha-Disubstituted Amino Acid Rich Antimicrobial Peptides

Approved:

Mark L. McLaughlin
Major Professor and Chairman

Dean of the Graduate School

EXAMINING COMMITTEE:

Robert P. Hammer

Thomas N. Fiscella

Date of Examination:

January 30, 1998